ALMA MATER STUDIORUM - UNIVERSITÀ DI BOLOGNA

DEPARTMENT OF STATISTICAL SCIENCES

Second Cycle Degree

In

QUANTITATIVE FINANCE

HEDGING ENERGY AND EU ALLOWANCES PRICE RISK: SWING CONTRACT ON A QUANTO OPTION

DEFENDED BY:

LUCA RUSTICELLI

0000991770

SUPERVISOR:

Prof. SILVIA ROMAGNOLI

Third Graduation Session - March 2023

Academic Year 2021/2022

Abstract

The purpose of this thesis is to present a new financial derivative which permits to hedge risk linked to energy and EU Allowances prices increase.
The proposed financial instrument is a swing contract, heavily utilized in the commodity sector, where the underlying option is a Quanto, therefore it is based on two assets that are the Italian Unitary Energy (PUN) and the EU Allowances prices.
The valuation problem is analyzed both from a theoretical and practical point of view, for which a Least Squares approach is applied to Monte Carlo simulations to obtain the final price. The possible outcome is investigated both through parameters modification and utilizing a scenario-based approach. These procedures permit to conclude that the derivative isn't useful in situation of low price level for one of the two assets, while it brings a cost saving in case of combined higher prices.

Contents

Chapter 1

Introduction

Climate change is an urgent and threatening matter; if global temperature increases more than $1.5°C$ above pre-industrial levels, there will be irreversible effects such as droughts and extreme weather events that already started in some part of the world. One of the main causes of temperatures increase is the pollution in the atmosphere which is mostly due to the release on air of damaging molecules where the most famous is the CO^2. The latter, with many other substances, vaporizes during actions at the base of our current life; the ones that emit the most are for example driving a non-electric car, create energy in non renewable-based power plants like burning fossil fuel.
With the aim of limit CO^2 (and other molecules under the name of Green House Gasses) emissions, in 1997 the international treaty under the name of Kyoto Protocol was signed by 192 countries to reduce their global emissions. This step forward in the fight against climate change brings a new climate related risk, more implicit than the intuitive physical one, that regards the additional costs that a company incur in the transition to a more green and environmental friendly economy. It is the "transition risk" and it could be caused by any of the company stakeholders in many ways: customers start shifting their habits due to the environmental strategy of the company or to its products, suppliers apply an additional margin due to regulations or supply chain frictions, regulators charge the firm with fees and additional costs if it isn't in line with the green policies framework. In this thesis the transition risk is linked to CO^2 emissions and for this reason can be named "Carbon Risk". In particular, it is caused by European Union regulations set in response to Kyoto Protocol to limit the pollution of a group of around $11,000$ European companies which have an high degree of CO^2 emissions due to their core business. They are regulated by the European Trading Scheme mechanism that, without considering some exceptions presented in section 2.3.1, imposes firms to have certificates that allow them to pollute for a given tonne amount. These certificates, that we call EUAs, are exchanged between companies and bought in the market. If we consider this market efficient we can see their price as an indicator of the current European transition costs. To explain the last sentence consider that the EUAs' market isn't in equilibrium and the cost companies will incur to pollute 1 CO^2 tonne less than before is higher than the EUAs price, then they will prefer buy certificates. This will bring a increase in their demand and an higher price until costs are equal. The same argumentation can be done in the opposite side where EUAs price exceeds the costs incurred for the sector to lower their emissions. The impact that ETS has on companies isn't straightly

clear but it affects their business model both from a monetary and strategical point of view since they know the regulator is pushing in that direction and could impose new rules to restrict their pollution. Therefore, the transition to a lower CO^2 emissions business isn't simple and may bring financial instability to firms under the ETS as the ones from the most energy-intensive sectors. In fact, companies in the manufacturing industry are the ones which requires more eletricity to run their daily operations, this aspect permits to introduce the second risk source: the energy price risk.

Another main cost item in the manufacturing industry is the electricity bills since machinery and production lines require high level of energy to work. The energy price is a great source of risk and it is heavily related to the GHG emissions since higher the utilized energy, higher the production and higher the pollution linked to those processes.

To deal with these two risk sources a new financial derivative is presented named Swing contract on a Quanto option. The theory and practical implementation's literature is provided in a well but summarized way by Lempa J. in Chapter 4 of [5]. The Swing contract, widely called Swing option, takes the name from the fact that usually it consists in two different parts: the forward and the swing. Where the "forward" part is a conventional contract, which guarantees a fixed delivery for a given period, while the "swing" one regards the derivative object of this thesis. It is a group of American options which can be exercised in a given delivery period under some contractual rules and restrictions. Its features and functioning will be deeply analyze in section 2.1.1.
As stated before, the general derivative was quite utilized in last decades, while the distinguishable feature is the quanto option utilized as inner contingent claim. The Quanto is an option on two different underlying assets which could concur in many ways to the payoff function. It will be deeply analyzed in section 2.4 and for the moment it is worth knowing that its characteristic permits to consider both energy and EUAs prices, allowing to hedge itself on both risks. This contract can be considered useful for a European firm under the ETS whose business is deeply affected by electricity bills. Since these companies are many and they are central for Europe's economical growth as well as for its shift to a lower carbon economy, this contract can help to permit a more balanced change. Therefore, the aim of this thesis is going deep on Quanto Option, investigating its utility to solve the situation of a raise of energy prices and low-GHG-economy transition costs. It starts from the swing option's basic foundation to the presentation of its practical implementation procedure, whose results are assessed under either theoretical, statistical and economically valuable point of view.

Chapter 2

Theoretical Framework

In the following chapter we focus our attention on the theory behind the swing contract cited in the introductory pages, as well as the explanation behind the procedure applied in the empirical part.
The theory behind a swing contract starts from the most famous financial derivative, the option, passing through the Least Square estimation and Monte Carlo simulation methods, introduced in section 2.1. It is presented also the reason why the just cited procedures are utilized and their inner assumptions and properties.
Furthermore, in order to run the simulation in the proper way, sections 2.2 and 2.3 present the stochastic modeling of our two underlying prices (energy and EU allowances). With this aim, the two assets and their corresponding markets are previously presented to give a complete view on their characteristics and possible outcomes. In the case of EUAs, a new theoretical approach is introduced in subsection 2.3.3, the scenario based analysis, that permits us to create different scenarios that deviate from the pattern modelled through stochastic theory. It is the starting point to assess the swing contract utility in different cases.
In section 2.4 it is presented the customized quanto option, which is utilized as underlying derivative for the swing contract. Since this option payoff is affected by two assets behaviors, their dependence must be taken into account to run the simulation. For this reason the last section (2.5) regards the introduction of Copula functions theory with the aim to find the right class to model their joint probability distribution.

2.1 Swing contract theory and pricing

2.1.1 Swing Contract Theory

A swing contract, usually named "swing option", is a strip of American or Bermudan options with a series of additional constraints on the exercise policies [5]. The name "swing contract" is preferable since usually its underlying instruments are named "options" too. Nevertheless, the two names are interchangeable and will be utilized to refer to the same financial instrument in this chapter.

Swing contracts were born in the last 90^{th}'s with the deregulation and the energy market opening to private sector, when its price stops to be set by governmental bodies but it starts to be the results of trades in open and regional markets.

To sake of clarity we present a brief introduction on options, passing to a wider swing contract definition from a notional point of view.

Options

It is worth mention the definition of a plain vanilla option, which is a financial instrument where the holder has the option to exercise the contract in the future. The exercise terms vary among its types, for example, an European option can be exercised at the contract's maturity date while an American one at any time up to the exercise date. The exercise consists in the exchange of the underlying asset that defines the option (like a stock), where in case of a "call" option the holder has the right to buy the asset at a given pre-defined price (named "strike") while in case of a "put" option he has the possibility to sell it at a given strike. The just presented mechanism is the most typical and it is considered the "physical delivery" of the underlying asset, even thought sometimes an option can be "cash-settled". The latter term means that in place of the asset it is exchanged only cash given by the option payoff defined as $\max(S_t - K; 0)$ for the call and $\max(K - S_t; 0)$ for the put case, where K is the strike price and S_t the underlying price at/during the maturity date/period [22].

The two delivery methods (physical and cash) can be considered equal if we ignore transition and other subsidiary costs, however the second type can be more suitable for a market full of frictions as the energy one, where sometimes it is complex deliver physically energy power along the grid network. This difference is assessed later in this chapter and for now on we consider both methods identical.

Swing Contract

Once that the base concepts of options are presented, we can introduce a wider definition for the swing contract. It gives to the holder the option to exercise a number N of American options in a given time interval, called "delivery period", at a given strike price K for a set of exercise rules. These latter are linked to the maximum quantity of options to be exercised at the same time and the time that must pass before the next possible exercise t_r ("recovery time"). Here, it can be identified two versions of the swing contract: the more basic one is when there isn't a relationship between the number of exercise options in a single date and the recovery time, while in the more complex one they are linked to each other. The latter statement means that either the maximum number $N(t)$ is in function of the time passed

from the last exercise, or the recovery time $t_r(n)$ is in function of the last number of option rights exercised together. Our analysis will focus on the easier mechanism since we are more interested in its inner utility and in construction of a two underlyings based swing contract rather than add complexity without a significant reason.

We present the contract in its plain vanilla form, considering a normal call American option as the inner contingent claim; while the selected Quanto option will be soon investigated later in this chapter together with its requirements and properties.

The financial theory behind the swing contract can be approached mainly from two different points of view named by [5] in *Martingale* and *Markovian* approaches. The first is focused on a maximization problem based on the probabilistic properties, while the second is linked to stochastic control theory. They have usually two different practical price estimations since the first one is often translated in a Monte Carlo method while the second one brings to the definition of a (non-) linear partial differential equation to be approximated with finite differences and Trees models. We will look at them deeply in the next subsections, where, for sake of simplicity, we consider the discount rate equal to zero.

Martingale Method

The martingale methodology starts from the base theory utilized also for plain vanilla American options, where the definition of *Snell Envelope* V_t^* for the process $\{Z_T\}$ is utilized as follow:

$$Y_t^* = \text{ess sup}_{t\leq\tau\leq T}\ E\Big[Z_\tau \mid \mathcal{F}_t\Big] \tag{2.1}$$

Where the essential superior is the smallest value greater or equal of a function in all the points for which the function has measure different from zero. In our case this leads to define the term Y_t^* as the smallest super-martingale that dominates the process $\{Z_t\}$. We can consider Z_t our payoff process for a single exercise option ($N = 1$). In case of a strip of options the formula become in function of more stopping time processes $\{\tau_N, ..., \tau_1\}$, where a τ_i represents the time when the remaining i-option is exercised. If we assume we can exercise more than one option at that time their relation is $\tau_N \leq ... \leq \tau_1$ i or $<$ otherwise. For this case on, for sake of simplicity, we consider the number of exercises in the same period capped to 1 in order to have more plain formulas which could help us to make the problem more understandable. Coming back to $\{Z_t\}$, we could assume it independent from N and integrable ($E[\max|Z_t|] < \infty$).

To formalize, the definition of stopping time for a single American option is the following:

$$\tau_t^* = \inf\{j \geq t\ ;\ Y_j^* = Z_j\} \tag{2.2}$$

where t is today price while Y_t^* is the Snell Envelope of Z_T.The stopping definition can be expanded for our financial instrument, given n-option to be exercised, in this way:

$$\tau_t^{n,*} = \inf\{j = t, ...T\ ;\ Z^{[\tau_1^*(i),...,\tau_{n-1}^*(i)]}(j) \geq Y^*(j; Z^{[\tau_1^*(i),...,\tau_{n-1}^*(i)]})\ \} \tag{2.3}$$

Where the new modified process has definition with respect the total number of N options:

$$Z_j^{[\tau_1,...,\tau_n]} = \begin{cases} Z_j & \sum_i^n \mathbf{1}_{\tau_i=j} < N; \\ 0 & \text{otherwise.} \end{cases} \tag{2.4}$$

Furthermore, if we define the policy π as a strip of stopping times for a given swing contract, it permits us to give a broad definition of Snell Envelope calling it *Value Function* for a group of n options at time t as:

$$V_t^{*,n}(x) = \sup_\pi E\Big[\sum_{n=1}^{N} Z_{t_n} \mid \mathcal{F}_t\Big] \tag{2.5}$$

Where the optimal policy it is identified as $\pi^* = \{\tau_N^*, ..., \tau_1^*\}$. This formula can be extended in a more practical way defining $V_t^{*,n}(x)$ in function of the fact that time t belongs to the optimal policy π^* or not. If $t \in \pi^*$ it means that the option will be exercised and the number of available exercises will be decreased to $n-1$ rights for the future periods, while in the other case the option isn't exercised therefore the number of possible future exercise remain n. This choice is done at time t utilizing the information given by $\mathcal{F}_t$ filtration, and it is affected by actual expectations on future Snell Envelope functions. The formula that can be derived it's a maximization problem based on conditional expectations presented below.

$$V_t^{*,n}(x) = \max\Big(Z_t(x) + Q_t^{*,n-1}(x)\ ;\ Q_t^{*,n}(x)\Big) \tag{2.6}$$

Where $Q_t^{*,n}(x)$ is named *Continuation Value* which is defined as follow:

$$Q_t^{*,n}(x) = \begin{cases} E\Big[V_{t+1}^{*,n}(x)|\mathcal{F}_t\Big] & \text{for } t < T; \\ 0 & \text{for } t = T. \end{cases} \tag{2.7}$$

After this definition, the optimal stopping time for every $n = \{1, ..., N\}$ can be defined as:

$$\tau_n = \min\{t\ : Z_t > E_t[\Delta V_{t+1}^n]\} \tag{2.8}$$

where $\Delta V_t^n = V_t^n - V_t^{n-1}$ (called *Marginal Value*).

More generalized formulas for multiple exercises in the same period and a different refracting time delta δ, now set to 1, can be found in [11]. That theory goes beyond the scope of this section even though it gives us the possibility to enunciate some basic assumptions for our Snell Envelope. In order to avoid technical problems in Formula 2.6 it is important that the Snell Envelope of continuous processes is continuous. To ensure that it should be assumed two properties for the inner filtration $\mathcal{F}_t$: it should be left continuous and every $\mathcal{F}_t$-adapted martingale should have continuous sample paths.

For what concerns the Continuation value, it is an expectation, meaning we have to estimate it. The employed methods utilized by literature are many but the main are:

- *Basis Expansion methods*: if it can be assumed $Q_t^{*,n}$ is in $\mathbb{L}^2$-space, it can be approximated through partial sums of orthonormal basis functions. This point will be deeply analyzed in the following subsection since this is the approach followed in our estimation.

- *Kernel methods*: in this case the $Q_t^{*,n}(x)$ is approximated through a fraction that contains the Dirac mass at point x. This won't be investigate due to the different approach selected.

As already cited, we utilize this Martingale approach due to its plain probabilistic theory and straight-forward Monte Carlo implementation.

The literature suggest that applying the previous formulas in a practical estimation will lead to a negative biased price since the optimal exercise policy π^* is never reach due to discretization and simulation errors. For these reasons they suggest to find an upper bound in order to create confidence intervals constructed from two different Value Functions formulas. This approach can be named "Dual Formulation" where the Formula 2.6 is employed for the lower price while the Doob-Meyer Decomposition is utilized for a new Snell Envelope representation. That formula isn't reported here since this work regards a different scope even it is useful remark that our result will be negatively biased.

Markovian Method

The second method is briefly presented hereafter. Since its practical implementation is usually a marginal differential equations problem, we don't go deep in the theory but we revise the framework foundations until the definition of the famous *Hamilton-Jacobi-Bellman* equation.

In the dynamic programming framework we should introduce two different spaces linked to control and controlled random variables. In particular, the state controlled process X and the control u can be defined as:

$$X \ : [t,T] \longrightarrow \mathbb{R}^n$$

$$u \ : [t,T] \longrightarrow \mathbb{U} \in \mathbb{R}^n$$

Where u_t is the decision we have to take at time t while the entire strategy Z is defined as $Z_T = \int_t^T u_s ds$. Its value is capped by another constant term N which is an upper constraint for our process such that $Z_T \leq N$. In our case the last term represents the maximum number of exercise options in the whole delivery period [48].
The dynamic formula of X_t can be assumed as general as possible now and then assumptions will be added when necessary. Its dynamic is of the form:

$$dX_t = \mu(t, X_t)dt + \sigma(t, X_t)dW_t$$

where W_t is the usual Brownian Motion term explained in the next sections. Then, consider a general reward function composed both by a L running and Θ final payoffs, of the form:

$$V(t,X,u) = E\Big[\int_t^T L(s, X_s, u_s) + \Theta(T, X_T, u_T) \ |\mathcal{F}_t\Big]$$

Now in our case Θ is equal to zero and L equal to a call option as usual in Swing contract. The value function becomes:

$$V(t,X,u) = E\Big[\int_t^T (X_s - K)u_s \ |\mathcal{F}_t\Big]$$

where K is the strike price and u_s is the decision to exercise the option or not at time s, which our variable to control the system.

The optimal value is the $V(t, X, u^*)$ for the optimal strategy u^* that can be stated as:

$$V(t, X, u)^* = \sup_{u \in \mathbb{U}} E\Big[\int_t^T (X_s - K)u_s \mid \mathcal{F}_t\Big]$$

Assuming that the optimal value exists we can apply the Bellman principle of optimality that employs the optimal control u^* as feedback control[1]. Define a new control formed by a optimal and not optimal part:

$$\hat{u}(s, X) = \begin{cases} u(s, X) & \text{for } s \in [t, t+h); \\ u^*(s, X) & \text{for } s \in [t+h, T]. \end{cases} \tag{2.9}$$

Then we can ensure that $V(t, X, u^*) \geq V(t, X, \hat{u})$, but if we define $V(t, X, \hat{u})$ as:

$$V(t, X, \hat{u}) = \Big[\int_t^{t+h} (X_s - K)u_s + \int_{t+h}^T (X_s - K)\hat{u_s} \mid \mathcal{F}_t\Big] \tag{2.10}$$

utilizng the tower rule and optimality definition we can re-write the inequality seen before as:

$$V(t, X, u^*) \geq E\Big[\int_t^T (X_s - K)u_s + V(t+h, X, u^*) \mid \mathcal{F}_t\Big] \tag{2.11}$$

Then, if we assume that the state process $X \in C^{1,2}$ (two times integrable) we can takes $V(t, X, u^*) = V$ inside the expectation and apply Ito formula to obtain the equation:

$$E\Big[\frac{1}{h}\int_t^{t+h} (X_s - K)u_s + (\zeta V^* + u_s \frac{\partial V}{\partial Z} df + (Y_{t+h} - Y_t) \mid \mathcal{F}_t\Big] \leq 0 \tag{2.12}$$

Where the linear operator ζ is equal to:

$$\zeta V = \frac{\partial V}{\partial t} + \mu(t, X)\frac{\partial V}{\partial X} + \frac{1}{2}\sigma^2(t, X)\frac{\partial^2 V}{\partial^2 X} \tag{2.13}$$

And Y is a local martingale defined as:

$$Y_t = \int_0^t \sigma(s, X)\frac{\partial V}{\partial C} dWs$$

In particular, if σ can be assumed constant (or at least regular to ensure the following property) Y_t is a Martingale and applying the property of limits we can discard the expectation and maximize the resulting function to reach 0 as optimal value. Lastly, we can finally derive the famous Hamilton-Jacobi-Bellman equation customized for our swing option case, as cited by [4] and reported below:

$$V_t + \frac{1}{2}\sigma^2 V_{xx} + \mu V_x + \sup_u\{u(X_t - K + V_z)\} = 0 \tag{2.14}$$

Where V_t, V_x, V_{xx}, V_z are the derivatives with respect that corresponding variable and the term related to the discount factor is not present since it is assumed to be zero.
We conclude this section remarking that the properties stated above are mandatory to find

[1]The feedback control is when an output (or a part of the output) returns to the input side and it is utilized as part of the input system to solve the problem.

a unique solution but in other cases a viscosity solution[2] can be derived.

The theory exposed here it is related to a plain vanilla option as the inner contingent claim of our Swing contract, but, as it will be analyzed in the next sections, in our case the underlyings are two. Also for this reason the choice falls to utilize as basic theory the Martingale framework instead of the current one due to the increase of complexity not only in its practical implementation but even theoretically.

The already presented Martingale Theory is applied to our problem through the Least Squares Monte Carlo method suggested for the first time by Longstaff and Schwartz in 2001 and presented in the next section after a brief introduction on the reasons why the Monte Carlo simulation is been selected.

2.1.2 Least Squares Monte Carlo Method

The derivation of Swing contract price can be done through different methods such as Monte Carlo, Binomial/Trinomial Trees, and Finite Difference methods that bring different levels of precision and adaptability to the underlying characteristics. Our choice is to utilize the Monte Carlo simulation because it is easy to implement, and it is more adaptable to any stochastic process path without increasing complexity since the valuation procedure remains the same and we should change only the process specifications. Tree and Finite Differences methods are usually more complex since more bounds and conditions have to be set to not spread the branches too far from realistic values; these constraints could lead to an over-simplification and weak fit on current data. Furthermore, as stated by [27] and [34], with the increase in dimensions, finite difference methods based on PIDE and PDE bring more time-consuming, and therefore Monte Carlo methods can be the solution. The main problem linked to the Tree method is the presence of scenarios in which downward and upward movements remain usually fixed along all the paths to keep low the complexity and computation efforts.
The Monte Carlo valuation method is a numerical technique which regards the simulation of a real world event employing random sampling techniques with the aim to reach an approximation to the true state [42]. In our case it is utilized to simulate discrete stochastic processes that model our state variables (electricity and allowances price). The aim is to reach a convergence of the algorithm relying on the *Law of Large Number*[3] since we employ independent and identically distributed random samples.
To summarize, on one hand, MC is clear, flexible, and requires a quite simple implementation; on the other hand, the convergence of MC methods is often low and heavily linked to the number of simulations, as stated by [26].

The peculiarity of the swing contract is the presence of a set of American options to

[2]The viscosity solution is the one that solves a partial differential equation problem.

[3]It is given the definition of the "Strong Law of Large Numbers", a simplified version of the WLLN: given a $\{X_n, n \geq 1\}$ sequence i.i.d. (whose random variables are independent from each others and indentically distributed), then their summation divided by n converges almost surely to a constant c if and only if the expectation $E[|X_1|] < \infty$. In that case $c = E[X_1]$ [45].

be exercised during the delivery period, this requires a method to evaluate the expected discounted value of the contract in the future for every time step. The procedure that was employed in this work is the "Least-Squares Monte Carlo" method, utilized for the first time by [32] to price a single American Option and other derivatives. This method is quite straightforward since the conditional expectation of the discounted value function at the next time $t + \Delta t$ is estimated through a linear least squares approach utilizing as regressors basis functions $F(x)$ based only on "in the money" (so positive payoff) paths, where every single input value x represents either the state variable realization S_t or the payoff Z_t in every different ITM simulation path for that moment of time. Through this estimation we can carve out the optimal exercise strategy and initial premium price for each path, then we compute the mean and obtain the final result price in terms of different levels of the strike, number of exercise rights, and waiting period.

Going further in the work of [32], the LSMC method relies on some important assumptions:

- Simulated paths are constructed under the risk-free measure $\mathbb{Q}$. This feature can be easily assumed if we incorporate market risk premium terms in the applied stochastic process.
- The conditional expectation must belong to the $\mathbb{L}^2(\Omega, \mathcal{F}, \mathbb{P})$ space so it can be represented by a linear function of a countable set of $\mathcal{F}_t$-measurable basis functions. This is due to the fact $\mathbb{L}^2$ is Hilbert, therefore the expectation has a countable orthonormal basis and it can be expressed by it [26].
- It is preferable that the underlying asset could be assumed Markovian since then the conditional expectation can be regressed utilizing only the state variable's values at the current time t and not at previous ones, which simplifies the calculations.
- The assumption to have independent and identically distributed paths is important, along with past hypotheses, to state the convergence in mean and probability of the estimated values to the real ones. Furthermore, it is possible to assume that the estimators are the "best linear unbiased" ones as reported in a simplified form in *Proposition 2* in [32].

The $\mathbb{L}^2$ space is the most preferable among the $\mathbb{L}^p$ ones which are heavily used in mathematics and probability theory. Coming back to $p = 2$, its popularity is given by the characteristic to be an Hilbert Space which is "complete" [4] and brings many properties for its inner product and subsets. In particular the one of interest is that functions in Hilbert space are orthogonal [5] to a wide set of orthogonal functions [53], which is the key to the least squares estimation, since it relies on the *Best approximation theorem* [31] which states for the $\mathbb{R}^n$ space:

Theorem 2.1.1 *Let W be a subspace of $\mathbb{R}^n$, let y be a vector in $\mathbb{R}^n$, and let $\hat{y}$ be the orthogonal projection of y onto W. Then $\hat{y}$ is the closest point in W to y (in the sense of norm*

[4] A metric space R is said to be complete if every Cauchy sequence in R converges to an element of R. Where a Cauchy class are sequences that for every $\epsilon > 0$ exists a natural number N such that for every $m, n > N$ the metric distance of x_n and x_m is lower than ϵ [29].

[5] Two vectors are said to be orthogonal if their inner product gives zero as result

distance of the space) such that:

$$\| y - \hat{y} \| < \| y - v \|$$

for all v in W distinct from $\hat{y}$.

Then, thinking to least squares, it concerns to find a vector x which is the solution of $A \cdot x = b$, where A represents the explanatory variables' matrix and b the dependent vector. A real and exact solution usually doesn't exists, therefore the real vector x can be approximated by $\hat{x}$ considering that more the product $A \cdot \hat{x}$ is near b, more is accurate. The best fit is ensured when we select an orthogonal family of basis functions for the reasons stated before.

The Markovian property, instead, means that our process is memory-less, usually due to independence from previous states. The formal definition provided by [30] follows.

Proposition 2.1.1 *A stochastic process X_t is said to satisfy the Markov property, and so be a Markov process, if for any $t_1 < t_2 < ... < t_n < t$ the equality*

$$P(X_t \leq x | X_{t1}, X_{t2} ... X_{tn}) = P(X_t \leq x | X_{tn})$$

holds for any $x, y_1, y_2, ..., y_n \in \mathbb{R}$.

Coming back to the LSMC method, it leads to an approximation of the swing contract price since the process is discretized, therefore options couldn't be exercised at any time; in addition simulations number is limited and it isn't assured that it is enough to reach the convergence together with the uncertainty of the correct number of basis functions. The literature states that higher the complexity of the model, the higher the number of regressors. According to [32], there are different families of functions that can be employed in a proper way to regress the dependent variable[6], while the choice for the paper to utilize only ITM realizations should help to keep low the degree of the utilized polynomial since there is evidence it leads to more accurate estimations and the need of fewer basis functions. The method will be conducted both on ITM and all sample simulations in order to assess the validity of the selected method. However, the regressors selection impacts the numerical implementation caused by scaling problems between explanatory and dependent vectors. In particular, order of magnitude of the Value Function obtained at every point of time must be similar to the one of the underlying price if we want utilize it as independent variable x. Considering also the basis functions transformation $F(x)$, it could require a normalization to reach a convergence in the contract premium price.
Furthermore, we decide to use the Generalized Least Squares together with the usual OLS since we aren't certain about the homoscedasticity and linearity of errors. This point will be analyzed in the empirical part. Another source of risk is the possibility to have a nearly singular cross-moment matrix; this problem could be solved with the proper selection of the estimation algorithm and orthogonal polynomials approximation for which we follow the work of [26].

[6] They are infinite degree polynomials as: Laguerre, Hermite, Legrendre and Jacoby ones.

Coming back to the MC procedure, first K simulations are initialized from the same starting point x_0 for the underlying asset, following that,option payoffs are computed at every time step. Then, the estimation of discounted value function is done backward, starting from $t = T$ until $t = 0$. We employ the method in [34], where the first set of simulations is used to perform estimation while a new MC is applied to the resulted regression parameters to obtain new fitted value functions and derive the swing contract's initial price. Another reason to follow this method is the implied robustness test we are doing on estimation, applying new data to the estimated parameters and then checking the deviation from the data utilizing the RMSE. [34] states that this estimation is negative biased since we are computing the optimal strategy on a given set of possible paths, and that it is preferable identify a likelihood range for the price. Anyway, this goes beyond the scope of our work, therefore the identification of a positive biased estimation together with the confidence interval values is left as suggestion for further works.

2.2 Electricity Modeling

In the following sections, we analyze the electricity market, its features, and peculiarities that distinguish it from all other commodity markets. Based on that, we will introduce the main models' classes, assessing which one is better for our purpose. Furthermore, we present two selected models showing their different levels of complexity and accuracy to reach better simulations.

2.2.1 Electricity Market

Electricity is defined as a "flow" commodity since it lacks in storability: once it is created it must be consumed immediately or scattered out of the network to avoid high-tension and transmission system overcharge. When a market player buys a certain amount of electricity he cannot store it, as can be done for gas, given the fact that batteries which can contain electricity are surprisingly costly and inefficient. One solution could be the ability to store the initial sources as it can be done with gas for gas-fired power stations, coal for coal-fired ones, and water for hydroelectric plants. This strategy is somewhere applied but it is not so convenient in terms of storage costs and it doesn't solve the problem since other power sources cannot be stored as sun and wind, or electricity-generation mechanisms that cannot be stopped without incurring high costs such as for nuclear power plants. Furthermore, the electricity is delivered through a proper transmission system, a complex infrastructure of power grids that links the seller's infrastructure to the buyer's one. It is subjected to access fees, and limited speed and size capacities which can create bottlenecks and energy losses during long distances [50]. In addition, every power method has its own production cost and efficiency during the day. For instance, the peak of production for solar panels is during midday while it is null during the night; the marginal cost of production of a gas-fired power station is much higher than a hydroelectric plant.

Summing up, the price is linked to the current production method, region, and power grid connections. It is now clear another market peculiarity contributing to its complexity: the market is not singular and general but it is fragmented and regional. For example, a MWh of power in the north-east part of Italy doesn't cost the same amount in the north of France, based on the fact that the trade is not cash settled but the electricity is physically sent to the buyer through the transmission system for a determined period stated in standard contracts. The main consequences of these characteristics, as stated by [3], regard the fall of the common cost-of-carry relationship [7] and the impossibility to find an arbitrage opportunity exploiting the differences in prices between regional markets since it is costly (and sometimes even impossible) buy, store and send electricity either in a second moment or to far locations.

Another factor that affects each regional market is the weather condition which is linked with the power demand since in periods characterized by cold and hot temperatures it is required and utilized a bigger amount of energy to heat or cool buildings and products. This should bring prolonged phases of higher prices in summer and winter and it makes markets

[7] The cost-of-carry is the link between the spot and future/forward price of an asset, which measures the storage cost plus the funding cost of the investment minus the income given by the asset in that period of time [22].

more fragmented. For instance, assuming all other factors are identical, the electricity price in Norway during winter will be higher than in Spain, while in summer it is possible to register the opposite situation. Furthermore, in the last decades, the weather became more and more important with the affirmation of renewable power methods since a region with a high time-presence of the sun can produce more solar power than other regions and benefits from the lower marginal cost compared to other power sources. The same reasoning can be done with hydroelectric plants which can benefit from the winter season thanks to the presence of more water. Unfortunately, the increase in power creation linked to summer and winter weather is not enough to mitigate the corresponding growth of power needs in society.

We just presented a yearly seasonality based on temperatures, but the electricity price is also affected by a weekly time-depended component because during the weekend (Saturday and Sunday) factories and offices are usually closed. This factor brings the power demand to decrease in a significant way which reduces a proportional amount of the traded price.

The next feature presented is price jumps, also called "spikes". Although the demand can be viewed as affected by the weather and working calendar it is price-inelastic since electricity consumers cannot store electricity, in which case it would be possible avoiding to pay a higher price if they have bought energy in excess in a previous less costly period. Given this impossibility, market operators buy the required electricity in the moment of necessity at the current price. Even the presence of existing contracts, where the counter-party pays an agreed price, it is not enough to fulfill the needs in some recurring situations, so they have to go on the trading market.

It is clear that in electricity markets short-term prices (i.e. infra-day and spot) are fastly affected by a bottleneck in the power grid, a fall in the supply, or a peak of demand. For instance, imagine the case when in a specific region the supply suddenly decreases due to an unexpected stop of a coal-fired power station. In this case, the inelastic demand remains almost equal and buyers are willing to pay more than before, bringing the local price to increase to new market equilibrium. The new level price is defined by the "marginal pricing" mechanism, where the final price, paid by all the current buyers, is set equal to the highest offered price which represents the highest marginal cost incurred during production among the sellers who participate in the current electricity delivery. The main consequence of such frictions and trade method is the presence of short and medium term spikes in the electricity prices, which make its stochastic modeling more complex as can be viewed later. Extreme spikes could result in negative prices, which are not so common in efficient markets but they are still present due to error estimations and network congestion which could lead to over-supply in one specific region [5].

2.2.2 Stochastic Modeling

In the stochastic modeling of electricity, we must distinguish spot from future prices: the first can be considered under the real probability measure $\mathbb{P}$, while in the second ones, which are necessary if we want model derivatives like options and forward-prices-based contracts, the conditional expectation should stay under the risk-neutral measure $\mathbb{Q}$ since we assume a constant discount risk-free rate $r > 0$.

Analyzing the risk-neutral framework, consider a future $f(t,T)$ (or forward, since r is constant) with delivery at time T and issuance at time t, then the price exchanged in t must be equal to zero, meaning that the expected price at time T is equal to the accorded future price. This relation holds for every period T so the price of the derivative should look as:

$$0 = E_t^{\mathbb{P}}[e^{-r(T-t)}(S(T) - f(t,T))]$$

For the validity of the latter formula, the contingent claim must be a martingale under the expectation measure. From the financial theory, we know we have to shift to the risk-neutral measure for which (under the assumption of constant r) each risk-free-discounted asset is a martingale. So we reach the formula:

$$f(t,T) = E_t^{\mathbb{Q}}[S(T)] \tag{2.15}$$

In the case that (2.15) holds also for the probability measure $\mathbb{P}$ the market is under the *Rational expectation hypothesis* [3] as implicitly assumed by several papers during the pricing of Swing Contract. In this way, it is legitimate to forecast future prices utilizing the model calibrated on spot prices only. Of course, the latter hypothesis is not valid in reality, meaning we should investigate further the difference between $f(t,T)$ seen on the market and our forecast $E_t^{\mathbb{P}}[S(T)]$ based on spot calibration. This discrepancy is named *Forward Premium* by [49] or *Risk Premium* by [3]. In particular, in case it is negative (so $f(t,T) < E_t^{\mathbb{P}}[S(T)]$, named Normal Backwardation), it means buyers of the future are willing to pay a premium in order to hedge the spot price risk, meanwhile inside $E_t^{\mathbb{Q}}[S(T)]$ it is present a positive market risk premium λ which is exploited for the change of numéraire. On the contrary, in case the Forward Premium is positive ($f(t,T) > E_t^{\mathbb{P}}[S(T)]$), λ is negative meaning that sellers are willing to pay a premium (Contango).

Coming back to the selection of a stochastic model for electricity, [6] distinguishes three main model classes: Econometric, Reduced-form and Equilibrium/Structural models.

The Econometric method doesn't concern stochastic processes since it utilizes past data and fundamental variables such as power sources (i.e. gas prices), weather conditions, production volumes, and others. The main downsides are that explanatory variables data are available ex-post, for this reason, we should derive forecasts and simulations for each variable taken into consideration in order to simulate the electricity price. In the short term is possible to forecast a good number of variables but it couldn't properly predict spikes.

The Reduced-form models utilize a tighter number of determinants for spot and futures prices. In particular, they try to capture electricity properties in a theoretical and tractable way and then test their results empirically together with computing simulations. They can present a single stochastic factor or more, increasing the complexity of the model and simulation method. Here, the usual way to predict future prices is to calibrate the model on past spot prices and then apply a market risk premium factor to pass to future ones (see in the next section). The cons are linked to the calibration problems with spikes, and heavy reliance on past expectations which leads to the inability to answer to market changes. In addition, most of the time they couldn't identify the relation with other energy markets and demand.

The last family of models is the structural one, where methods focus on the equilibrium between supply and demand assessing the analysis from a micro and macroeconomic point of view. The simplest models are the ones where the demand curve is assumed inelastic and it is possible to model the price spikes with supply functions. In more complex models it is taken into consideration capacity, margin, and other power sources such as gas and fuel [5]. The downside is mainly the unavailability of data to construct an equilibrium model and the necessity to have a forecast for every single explanatory factor.

Since the goal of this thesis is not to find the best fitting model between the previous ones, but it is enough to select a good and reliable method that could forecast forward prices in a simple and tractable way, we decide to utilize the simplest, which was utilized by almost all the literature on the swing contracts: the reduced-form method.

Stochastic processes can be of two opposite forms: geometric or arithmetic, based on their mathematical construction. A geometric example of the process X_t is the following:

$$\ln(X_t) = \ln(f(t)) + \sum_{n=1}^{m} Z_{t,i} + \sum_{k=1}^{j} Y_{t,i}$$

Where X_t,Y_i,Z_i are a stochastic processes and $f(t)$ is a deterministic function of t.
An arithmetic form example is:

$$X_t = f(t) + \sum_{n=1}^{m} Z_{t,i} + \sum_{k=1}^{j} Y_{t,i}$$

The main difference is that geometric models don't show negative values for the process X_t due to the exponential function while the arithmetic one does. We follow most of the literature selecting two geometric forms since in electricity markets negative prices are so rare and, given the recent macroeconomic and market turmoil, the probability to incur a negative price in the following years tends to zero.

Coming back to the electricity's characteristics, it was already mentioned the presence of random spikes due to supply shortages, demand peaks, and power grid frictions and inefficiencies. Furthermore, the price has a strong yearly and weekly seasonality given by the different temperatures and weekend days. The last main feature of electricity is a mean-reversion behavior in the medium-long term as other commodity prices. This trend is due to its trading mechanism in which when there is an unfulfilled power demand at the current price it will bring higher marginal cost producers to enter the market, which pushes the price upward. But we stated that the demand is inelastic to price, meaning that in next periods it is more probable the demand will come back to its usual requirement amount, pushing the more costly sellers to leave the market. The contrary happens in case of lack of demand, when other producers' prices will be pushed out of the market and the equilibrium price decreases based on the rule of marginal pricing. Here below we introduce two models which try to deal with the electricity features enunciated above.

Exponential Ornstein-Uhlenbeck Process

The first model selected is based on the famous Ornstein-Uhlenbeck Process, where, given a probability space $(\Omega, \mathcal{F}, \mathbb{P})$, the process has the form below:

$$dX_t = \alpha(\kappa - X_t)dt + \sigma dW_t \tag{2.16}$$

Where $X_0 = x_0$, $t \in [0, T]$, κ represents the long mean factor, α the mean-reversion factor, and σ the model volatility. Furthermore, for the validity of the model, the W_t is adaptable in $\mathcal{F}_t$ and it could be assumed to be one of the Levy processes' family since they all have independent and stationary increments and for this reason, even $dX_t = X_{t+\delta t} - X_t$ has the same properties [3]. Note that in (2.16) parameters are assumed to be constant and not time-dependent. This feature is due to two main reasons: the additional complexity that even a single time-dependent parameter will bring to the model (i.e. a process with $\kappa(t)$ will become the famous Hull-White Model) and secondly the time factor is taken into account inside the seasonality term that will be analyzed later in this chapter.
It is worth noticing that the process is a Markov Chain thanks to the independence of increments. Furthermore, the mean reversion is ensured by the stationarity of the process, which holds if $\alpha > 0$. This property will be analyzed during calibration utilizing a t-stats test on the parameter together with a Unit Root Test. In the end, we remark on the uncertainty in the significance level of parameter κ since part of the mean will be captured by the seasonality which is presented below.

The seasonality term has to reflect both yearly and weekly fluctuations based on the different levels of demand. The literature exposes two different approaches: the use of sinusoidal or characteristic functions. We employ the sinusoidal modeling for the yearly seasonality while the characteristic functions for the weekly one, following in part the work of [44] who takes into account yearly pattern with Sine and Cosine functions, but also each weekly day, the Christmas period, holiday effect and a linear trend. We decided to not consider Christmas period, since it represents few days when holidays are already considered, together with the rejection of the linear trend since there is no seasonal market explanation for an increase in prices in Europe year after year. The final selected formula is the following:

$$f(t) = \beta_1 \sin(\frac{2\pi t}{365.25}) + \beta_2 \cos(\frac{2\pi t}{365.25}) + \beta_3 \sin(\frac{4\pi t}{365.25}) \dots \\ + \beta_4 \sin(\frac{4\pi t}{365.25}) + \beta_5 + \beta_6 \mathbb{1}_{WD} \tag{2.17}$$

Where $\mathbb{1}_{WD}$ represents an indicator function for the working days, to be distinguished from weekends and holidays based on the European standard calendar named "Target". As already mentioned, the Cosine and Sine are utilized for the yearly trend.

The model selected for electricity prices is the Exponential Ornstein-Uhlenbeck process with the addition of seasonality at the exponential, with the noise factor inside (2.16) identified by a $\mathcal{F}$-measurable Brownian Motion, which adds the property of normality to increments dX_t. It is presented below:

$$\ln(P_t) = f(t) + X_t \tag{2.18}$$

$$\ln(P_t) = f(t) + +\kappa(1 - e^{-\alpha t}) + x_0 e^{-\alpha t} + \sigma e^{-\alpha t} \int_0^t e^{\alpha u} dW_u \tag{2.19}$$

Given the properties enunciated above the price P_t is Markovian and follows a Log-Normal distribution which permits us to write its expected value as follows:

$$E_0[P_t] = \exp(E_0[\ln P_t] + \frac{1}{2} VAR_0[\ln P_t]) \tag{2.20}$$

Where, given $\ln P_t$, under some calculation, we know:

$$E_0[\ln P_t] = f(t) + \kappa(1 - e^{-\alpha t}) + x_0 e^{-\alpha t} \tag{2.21}$$

$$VAR_0[\ln P_t] = \frac{\sigma^2}{2\alpha}(1 - e^{-2\alpha t}) \tag{2.22}$$

Coming back to the choice to keep parameters α, κ and σ constant, [33] shows that the presence of the seasonality $f(t)$ changes the starting equation of dP_t for a usual Exponential Ornstein-Uhlenbeck process:

$$dP_t = \alpha(\kappa - \ln P_t)P_t dt + \sigma P_t dW_t$$

to the formula of a process characterized by time-dependent long-run mean (given some regularity conditions for $f(t)$):

$$dP_t = \alpha(b(t) - \ln P_t)P_t dt + \sigma P_t dW_t$$

Where $b(t)$ is equal:

$$b(t) = \frac{1}{k}\Big(\frac{df(t)}{dt} + \frac{\sigma^2}{2}\Big) + f(t)$$

For what concerns futures pricing, the market risk premium λ must be introduced inside dX_t which results in a new Brownian motion under the new meaure $\mathbb{Q}$ and κ^* equal to $\kappa - \frac{\lambda\sigma}{\alpha}$ as stated by [43]. The formula for the logarithm of the future price is linked to the spot one but presents the new κ^*:

$$f(t,T) = E_t^{\mathbb{Q}}[P(T)]$$

$$\ln(f(t,T)) = f(T) + \kappa^*(1 - e^{-\alpha(T-t)}) + x_t e^{-\alpha(T-t)} + \frac{\sigma^2}{4\alpha}(1 - e^{-2\alpha(T-t)}) \tag{2.23}$$

Regarding the model fit, it lacks the adaptability to spikes due to the presence of the sole σ factor which accounts for volatility. It is a trade-off between tractability and simplicity against accuracy in spikes predictions. For this reason, a second model which should fit more to data peaks is presented below. The aim is to utilize it in a parallel way and compare results.

Exponential Ornstein Uhlenbeck Process with Jump factor

The model presented below is an extension of the previous one in order to map the jump patterns in electricity prices. In [44] are presented three different types of jumps, where differences are given by their mean reversion behavior. The first is the "single jump" which will mean-reverts in a few periods since the process starting level in the following period is at a higher level than before. The second was named by the authors "Spike" since, if the jump

happens at time t, at time $t+1$ the process is near the level of $t-1$ because it is affected by the spike only in one period. The last type is the "cluster of jumps" where in the case that a jump occurs after a long time it is followed by others in the following periods. The difficulty is to fit all these three jump patterns; the literature shows is not simple and that is better to focus on one/two of them to cover a good part of the noise. In our work, we consider only the first pattern, "single jump", which is the common one. In order to model it, a Poisson process, with constant parameter θ, is inserted inside dX_t, which is multiplied by a gaussian term ξ_j with a mean equal to μ_j and a variance given by σ_j^2. The corresponding formula is presented below:

$$dX_t = \alpha(\kappa - X_t)dt + \sigma dW_t + \xi(\mu_j, \sigma_j^2)dJ_t \tag{2.24}$$

The θ is the intensity of the Poisson process and represents the probability that a jump will occur in a given time, while the jump size is symmetric around the mean since ξ_j is a Gaussian distribution. Important assumptions are the independence between the Brownian process W_t and the Poisson one J_t, together with the absence of specific seasonality for the spikes.

The general model presents the same seasonality showed in (2.17) and it keeps the same form as (2.18), but the log-normality property falls due to the presence of the Poisson process while the Markov Chain property could be assumed in a state space $D \subset \mathbb{R}^n$ as stated by [14].

For what concerns the futures pricing, we couldn't consider one single market risk premium since there are three sources of uncertainty: W_t, J_t which regards jump intensity risk and ξ_t linked to the jump size risk. For sake of simplicity, we assume that the last two risks are incorporated in the single market price of risk of ξ_t ignoring J_t as done in [39]. We can call λ the constant market risk premium related to W_t which leads to the new κ^*, while the new market risk premium, ν_j goes to impact the Poisson process, which becomes J_t^* (measurable under the risk-neutral measure), and on the mean μ_j^*. The pricing formula for the natural logarithm of futures on P_t was derived by [49] within the solution of a more complex process; it is valid for our model and it is presented below:

$$\ln(f(t,T)) = f(T) + \kappa^*(1 - e^{-\alpha(T-t)}) + x_t e^{-\alpha(T-t)} + \frac{\sigma^2}{4\alpha}(1 - e^{-2\alpha(T-t)}) + \dots$$
$$\theta(T-t)\Big[\exp\Big((\mu_j - \nu_j)e^{-\alpha(T-t)} + \frac{1}{2}\sigma_j^2 e^{-2\alpha(T-t)}\Big) - 1\Big] \tag{2.25}$$

The latter formula, as (2.23), will be useful for the market risk premium estimations during the calibration phase.

2.3 European Allowances Modeling

In the following pages, we will present the European Trading Scheme where emission certificates are auctioned and traded. This is the reference market to price the emission cost which is the main part of the transition costs[8] that European companies are currently facing. Furthermore, we introduce the method utilized to model the spot and future prices of these allowances together with the presentation of the Scenario Based Analysis approach and its functioning. The latter will be utilized for a final analysis on the Swing contract utility.

2.3.1 EU Emission Trade Scheme

The European Union Emission Trading Scheme (EU ETS) is a system that permits to limit the greenhouse-gas emissions (GHG) of its participants. It is a "cap and trade" mechanism where certificates of permission are sold and bought among market players in accordance with their pollution needs. These certificates are named "European Union Allowances" (EUA) and correspond to 1 tonne of CO_2 emission; their annual amount is capped by regulators in order to give flexibility to companies (which can decide to emit more CO_2 tonnes acquiring more EUAs) but, on the other side, keeping under control the total number of GHG realized every year. The players subjected to this mechanism are companies in the most GHG-emission intensive sectors concerning power creation and manufacturing [9] and, from 2012 on, even the aviation sector [10].
As already stated breifly in the Introduction, the reason why the European Union introduced the ETS has to be searched in its commitment to the Kyoto protocol agreed in the UN Framework Convention for Climate Change (UNFCCC) in 1997. The ETS would have allowed each member state to meet the Kyoto targets within 2012. Based on that the ETS scheme was divided into four phases:

- Phase 1: it goes from 2005 to 2007 in order to ensure the functioning of the ETS. Here most of EUAs were given for free to participants from each member state whose behavior was assessed and approved at the European level.

- Phase 2: The period lasts until the end of 2012, it was permitted to trade and utilize even its own Kyoto protocol emission units (CERs & ERUs). In this phase, new countries outside the EU entered the scheme (such as Norway and Iceland), which help ETS to become the most important emission market in the world. The total cap was decreased in order to meet Kyoto targets and aviation was introduced.

- Phase 3: It concerns the years from 2013 to the end of 2020. The scheme was extended to new emissions (like N_2O and PFC) and the annual decrease of emission allowances was fixed to a quote 1.74% of the 2010 level.

- Phase 4: This phase starts only in 2021 and will last until 2030. The main changes are higher targets and a reduction quote of 2.2% which is being revised upwards by the

[8]The Transition Cost is the one caused by a disordered transition to a low-carbon economy which leads to drawbacks given by climate policies and regulations, as stated in [18].

[9]The data speak about more than 11,000 companies as power stations and other factories where a thermal rated input greater than 20MW, acid and steel production, oil refineries and many others.

EU Commission these months.

Since the beginning, the market was far been efficient and incurred significant friction and many critics. For example one of the main inefficiency features is the free provision of allowances to some specific sectors which are subject to the "market leakage"[10]. The latter is the risk that companies subject to ETS will shift production outside the EU in order to avoid such costs or, even worse, they will lose competitiveness in favor of competitors located in countries with a lower penalizing policy on GHG emissions. Furthermore, the main consequence would be to make the ETS effort useless since the pollution will simply shift to a new country instead of decreasing over the years. Regulators tried to avoid these scenarios by allowing free certificates allocation during the last years, but with the European Parliament resolution of the 10^{th} march 2021 the situation is going to change soon. That day a new "Carbon border Adjusting mechanism" was approved in order to mitigate carbon leakage and gradually stop the free EUAs provisions. It imposes to EU importers to buy certificates corresponding to the number of carbon allowances needed to produce those goods within the Union. They are exempt only if they prove to have already paid a carbon cost in the country of export [8]. This new rule will be effective from 2023 and will affect almost 94% of the industries responsible for GHG emissions [9].

The EU ETS works in the following way: every year the European Union provides each member state with a fixed number of certificates, and the country conveys EUAs for free to specific sectors approved by the European supervisors. The remained certificates are auctioned by specific exchanges [11] which serve also as houses for their further trading. Then, in April, each company has to surrender in the "Union Registry" a certificates amount equal to the CO^2 emitted the previous year. In the case that they don't fulfill the requirement they incur penalties that go from fines to the surrender of all their EUAs package.
This last point helps us to introduce the last ETS inefficiency which is linked to the number of EUAs available on the market. During the first phases, with the aim to have a gradual and soft transition, the EUAs offered were far more than the needed number. For this reason a high amount of them was simply stored by participants, which brought market inefficiency. The European Union Decision number 1814 of 2015 tried to fix this friction, imposing a new "Market Stability Reserve" mechanism. It concerns the creation of a storage for the allowances in excess at the end of the year and rules on how to manage the market's offer-demand balance in the following years.

It is clear that the EU Allowances market was far to be perfect and the road is still long. This permits us to introduce and legitimate our choices during the EUAs' spot and futures modeling.

[10]In 2013 the percentage of free EUAs was near 50% but it decreases every year (i.e. for the industry sectors it passed from 80% to 30%).

[11]The most important exchange is the EEX. Almost every week these companies sell EUAs on behalf of member states which will collect the main part of revenues and have the duty to invest them in green projects.

2.3.2 EUAs Stochastic Modeling

The EUAs aren't the usual financial asset class that can be bought with the aim to receive a periodic yield or to sell it at a higher price. We can say that for ETS participants exists a sort of convenience yield since they have to surrender a part of them every year. The identification of the right stochastic model is not immediate, in addition, the literature is poor since it is a niche market and its day-life impact isn't directly visible. The price can be seen as the carbon cost companies have to face to run their businesses, cost whose a part is surely transferred to customers along the supply chain.

The selected approach follows the work of [13] where the historical data are modeled with different stochastic processes selecting the one which fits better spot modeling. The models taken into consideration are four:

- The Ornstein-Uhlenbeck process whose main feature, already cited in the last chapter, is the mean reverting behaviour (express by α) around a long mean κ with a costant volatility term represented by σ.

- The so called "squared root" process which is the base of the famous Cox-Ingersoll-Ross model, mostly utilized to parse interest rates. The main feature is the presence in the stochastic part of the square root of the asset, as shown below:

$$dS_t = \alpha\ (\kappa - S_t)\ dt + \sigma\ \sqrt{S_t}\ dW_t$$

  Where the three parameters are constant and W_t represents the usual Brownian Motion. The base condition for its validity is the inequality $\sigma^2 > 2\kappa\alpha$ which permits the price to not be negative, avoiding to incur in calculation error in the case of negative prices under the square root [12]. If the condition is not met it is very problematic for the Monte Carlo method since the higher the number of simulations, the higher the probability of incurring errors. To summarize, the model has the same mean reversion pattern as Ornstein-Uhlenbeck, but it permits to see an increase in volatility in parallel with an upward movement of the price.

- The Geometric-Brownian-Motion process to model EUAs dynamic when we consider log-returns. It has the form:

$$dS_t = \mu\ S_t\ dt + \sigma\ S_t\ dW_t \tag{2.26}$$

  It was usually utilized to model stock returns and other common asset classes. It relies on the assumption of having normal log returns, which is strong for most asset classes like also for allowances. The main difference from the last two models is the incorporation of only two parameters: σ which represents the volatility and μ which represents the deterministic part of its dynamic. These features, as we will see in the next chapters, will give it an advance in the calculation of the BIC measure for the goodness of fit assessment.

- The Exponential Ornstein-Uhlenbeck process, that was already utilized in the modeling of electricity prices and presented in the last chapter.

Following [13], model parameters are estimated through Maximum Likelihood and the best is chosen based on statically accuracy and model parsimony, which is very important during a Monte Carlo simulation.
The stochastic model selection is less important than in the case of electricity price since there is no clear market evidence on the EUAs dynamic. This is also because every few years a new European Regulation goes out changing the ETS framework and bringing the market to change direction. Moreover, every ETS phase is different in some parts, therefore it should be risky to calibrate the model on past phases but the fourth one is short on observation since it starts only in 2021. For these reasons, we decide to apply a scenario-based analysis on EUAs before doing the simulation. This method permits us to apply expert beliefs and forecasts to the model because otherwise it would be based only on past data, which is one of the main downsides of reduced-form models.

2.3.3 Scenario Based Analysis

The scenario-based analysis is a method to forecast future outcomes making projections on different possible situations. It is useful in mid-long time-range situations where both uncertainty and predictability are present in a considerable amount. The approach is imagining different possible scenarios with a certain probability of occurrence and then asking itself the "what if" question to carve out the main consequences. The method shift from asking what is the most likely situation to what are the implications in the case that different circumstances occur [15]. Therefore, the analysis of the likelihood isn't usually considered but the focus is on the consequences of different possible events. We consider this approach valid since the ETS market is regulated by mechanism as the "Stability Reserve" and the EUAs annual cut of available certificates, together with a grade of uncertainty given by the participants' needs and expectations.

Unfortunately, there are no explicit forecasts and scenarios on future EUAs prices; for this reason we decide to utilize carbon emission projections to create allowances price scenarios since the rules and behaviors that affect the ETS market are within the ones which heavily influence gas emissions. In this way we pass from speculative but realistic emissions forecasts, based on the work of sector experts, to different possible outcomes on EUAs prices which are applied to the deterministic part of the stochastic process identified in the last chapter. The utilized method is explained in deep in the following paragraphs after a brief presentation of the input scenarios.

For what concerns the CO_2 emission (CO_2e) scenarios we have two different data sources: EEA and IPCC studies. The first one is the European Environmental Agency, a body of the European Union whose task is to produce independent, relevant, and reliable information on the environment to direct the work of policymakers. It checks and reports information submitted by each member state on realized GHG emissions and future projections required by the "Governance of Energy Union and Climate Action" (EU 2018/1999) to be prepared every two years. These forecasts go from 2020 to 2040, they are split by gas type as well as by sector, and they consider at least two different scenarios, the WAM and WEM, while the WOM is submitted by a few countries. WEM makes projections on future GHG emissions levels

based on "existing measures", therefore, it considers effects from currently adopted policies and measures; while the WAM is the acronym for "with additional measures" meaning that the member state takes into consideration even planned and expected relevant policies and events which affect future emissions. Lastly, the WOM scenario is based on the absence of climate change measures as ETS itself, meaning probably a price for the EUAs equal to zero. Its likelihood is too low that only four countries out of 27 report the emissions forecast and for this reason it's not considered in our work.

The Intergovernmental Panel on Climate Change (IPCC) is instead an international body under the United Nations whose task is to do a periodical and reliable assessment of expert-based researches on climate change, utilizing a sound scientific basis that makes it trustworthy. Therefore, it doesn't conduct its investigations but it checks the work of other climate experts with the aim to guide governments' climate and energetic policies. IPCC is divided into three different working groups: the first assesses scientific works on climate change, the second focuses on impacts and vulnerability and the third one identifies researches on mitigation responses. From 1988 onwards, within the Working Group I (WGI) task there is the composition of an Assessment Report, the latest is the sixth one (AR6), that identifies climate changes and their causes both anthropogenic (inducted by human behaviors) and naturally forced. The AR6 contains the CO_2e scenarios employed by us, but also additional gas emissions like CH4, N2O and others.
The construction process concerns the work of every working group since climate effects have an impact on human beings which, in turn, define socio-economic pathways that affect the drivers of future effects. In our case, the IPCC creates five main different scenarios extracted from an analysis of socio-economic drivers (i.e. population growth, energy and land usage) and mitigation assumptions, from which future outcomes were extracted. These scenarios are of the form $SSP\,X - Y$, where SSP means "shared socio-economic pathway" whose resulting level X goes from 1 to 5 based on population growth, urbanization, technological development projections For what concerns Y, it is a measure of the approximate radiative forcing level [12] in 2100 which goes from 1 to 8.5. These two processes are developed separately and then utilized together to create the main five different scenarios from which are derived gas emissions forecasts. Following [23], they are:

- SPP1-1.9: it describes the situation where the atmosphere warming is capped at 1.5° above the pre-industrial level in the year 2100, and where net zero CO_2 emissions is achieved around 2050. For our purpose is important to notice that it involves a peak-and-decline pathway in the following years, which is the first one assumed in the history of IPCC.

- SPP1-2.6: it concerns a final global temperature increase of 2° relative to $1850 - 1900$ while the net zero CO_2 is reached in the second half of the century.

- SPP2-4.5: this scenario is slightly better than the "no-additional-climate-policy" one, leading to an increase of 2.7° from pre-industrial levels at the end of the century. In

[12]The radiative forcing is the difference in energy that the Earth absorbs and reflects back to the space. It is measured in radiation since energy comes from the sun in such form. The mechanism is important since space is colder than the planet so during the day-night cycle the Earth receives and unleashes energy, but less energy is radiated back out, warmer is the Earth' atmosphere that brings an increase in global temperatures.

the short-medium term, CO_2 emissions are assumed to be in line with current levels until 2050 even though more countries adopt mitigation policies in line with the Paris Agreement goals [13].

- SPP3-7.0: it is related to the "no-additional-climate-policy" scenario whose main effect is a double increase in CO_2 emissions until the end of the century, leading to a radiant forcing level between 6.0 and the maximum of 8.5.

- SPP5-8.5: it presents an indefinite temperature increase caused by a double growth of gas emission before 2050, leading to the highest level of radiative forcing. It is due to a socio-economic development highly supported by fossil fuel utilization and dirty energy. It is the worst-case scenario, on the opposite side from the best one represented by SPP1-1.9.

The presented scenarios concern CO_2 emissions while we are interested in the ETS market's possible future pathways. For this reason the aim is to link every IPCC and EEA forecast to a EUAs price scenario based on the relationship between them. Past years showed a negative EUA-CO_2 relation since ETS pushes companies to decrease their emissions, as happened worldwide, while in the meantime the certificates price rises. In a traditional market, lower gas emissions would bring a lower allowances demand and therefore a decline in their prices, but, thanks to the Stability Reserve Mechanism and other restrictions, the European Union controls the supply of allowances, without permitting to have a decreasing demand for a long time. In this framework, a fast decline in CO_2 emissions represents the aim of the EU, therefore a decreased CO_2e scenario brings the assumption of intensified pressure from regulators for a shift to a green economy, whose translation is a higher transition risk and emission costs represented by the price of EUAs. On the other side, a CO_2e increase shows that companies prefer to emit more than before, meaning that transition costs are affordable with respect to the costs they would incur the shift to a greener business. This can be due to an increase in the CO_2e-related product demand or a relaxation in the ETS regulation or both.
The just explained relation between CO_2e and allowances price is confirmed by their historical path and, more importantly, by the EU behavior since when the Kyoto protocol's objectives were reached, higher green standards were settled for future years by regulators, pushing companies under ETS to respond to these changes in an effective and fast way. To sum up we can link an increase in CO_2e to a decline in EUAs price and vice-versa.

The method that will be utilized, links the worldwide CO_2e to the solely European emission certificates price. This means it relies on the big assumption that global forecast can be applied to a sub-continental area such as European Union. It is a strong assumption which could bring EUAs' price forecasts to be underestimate since the EU is the leading entity in the green transition compared to other countries. Therefore, a CO_2e decrease worldwide could represent a greater fall in the European ones. To check this fact, we can utilize the two EEA scenarios on CO_2e that regards only the 27 member states. We expect to see an lower

[13]The Paris Agreement is a legally binding international treaty whose main goal is to limit the temperature increase far below 2.0° Celsius relative to pre-industrial levels. The primary course of action is decreasing CO_2 emissions to limit radiant forcing and other climate effects.

CO_2 emissions amount in EEA rather than the ones derived from IPCC. We can also do the opposite analysis: check if the EEA forecasts are too optimistic with respect to the world-wide ones. In particular is remarkable to notice that, while the IPCC output is based on the assessment of sound, reliable and mostly independent scientific works, the EEA scenarios are the result of an aggregation of forecasts estimated by every single member state following general guidelines provided by European regulators, meaning that the emissions reduction can be overestimated due to countries' benefit. For this reason, we decide to consider valid IPCC results and then do a cross-check with the EEA ones in order to highlight differences.

Coming back to the estimation of EUAs scenarios, we utilize an OLS regression to link the CO_2e values with the EUAs, assuming a linear relation between them. This is another strong assumption since the ETS market is conditioned by many causes even though the main point is the regulatory work that implicitly fixes the path that market participants should follow, and that is closely related to the GHG emission reduction targets fixed at the EU level.
The practical part and details are left for the following chapters where, due to the lack of daily data and the not clear link between European and worldwide frameworks, interpolation and transformation methods will be used.

The scenario based analysis just presented concludes this chapter on EUAs price modeling, which allow us to pass to the definition of the Quanto Option.

2.4 Quanto Option

The underlying derivative of a swing contract is usually a call or a put American option which can be exercised a number N of times during its delivery period. In our case, we introduce a new derivative named in the literature Quanto Option. It is an exotic instrument based on two different underlings: the first one determines the payoff (which is the one of a plain vanilla option) while the other one is outside multiplying it.
The most famous Quanto option is a cross-currency option where the payoff is defined in one country and is converted to the other one thanks to the exchange rate which represents the second stochastic part [46]. It can be either American or European and is utilized by practitioners to be exposed to a foreign asset without incurring the exchange risk: when the value of one currency moves up or down when compared to the other. The form of the final payoff is the following:

$$\text{Payoff}^{d}_{\text{Quanto}} = \text{Payoff}_{\text{Put/Call}}(S^f, K^f) \cdot X^d$$

Where ^{d} represents the domestic market, ^{f} the foreign one, S_t is the underlying process, K the strike and X_t the exchange rate.

Another type of Quanto option is the one presented in [7] on two underlings: the weather temperature and the energy price. In this case, the payoff has the following form:

$$\max\Big((E - K_1) \cdot \tau \cdot (DD - K_2)\ ;\ \ 0\Big)$$

Where DD represents the HDD, Heating Degree Day index, or the CDD, Cooling Degree Day,or both. They measure the temperature exposure given a threshold as shown in the formulas below:

$$HDD = \max(65°F - \text{average daily temperature}\ \ ,\ 0)$$

$$CDD = \max(\text{average daily temperature} - 65°F\ \ ,\ 0)$$

Therefore, when degrees are lower than 65° the measure is positive for HDD and zero for CDD, vice versa. The E is the power price, τ is the tick value that transforms the HDD points into an economic amount, and K_1 and K_2 are their respective strike prices. It is usually utilized to cover buyers from colder winters and hotter summers than expected when they are accompanied by a high level of power prices, a situation that is realistic since an increase in the need for heating or cooling will bring an increase in power demand. The correlation between the two underlings is its point of strength (when they do an upward movement the option goes deep ITM) but also its weakness. This is because they are inside the same payoff, therefore their product becomes negative when one is ITM and the other one not leading to an out-the-money situation. On the opposite when both are ITM or OTM the option can be exercised, so it permits to protect against colder winters and hotter summers (it has the feature of a Straddle). This type of option isn't useful for our scope since our underlings assets are the electricity price and carbon emission allowances auctioned on the market. Most companies ruled by EU ETS are exposed to the risk of an increase in both prices, as can be investigated in the following pages, while nobody is affected by a

downward movement of both of them since lower EUAs price is every-time hoped by market participants. Even in the remote case that investment and credit institutions, authorized and regulated by European financial law, buy allowances during the auction process to sell them to the EU ETS participants, their businesses aren't exposed to an increase in electricity prices to legitimate their interest in this swing contract.

To sum up, the last showed quanto option doesn't fit our purposes while the first one does because its payoff is mainly linked to the first security only, while the second one propagates its effect through multiplication. Thinking about it, the probability that the exchange rate goes to zero is almost null in a short term, considering the fact that probably the quanto is utilized in countries with a less powerful currency whose market participants would like be exposed to assets in the most robust currencies (like Dollar and Euro) but doesn't want be penalized by exchange rate fluctuations. The situation of the exchange rate is analog to our one since the EUAs price could go to zero only in case of EU ETS removal by the European Union, a situation very unlikely to occur in the following years before 2030.

The quanto option, selected by us and presented in the following lines, is a call American type of the form:

$$\text{Payoff} = \max(S_t - K_1 \ ; \ 0) \ \frac{A_t}{D_{\text{EUA}}} \tag{2.27}$$

S_t is the electricity price at time $t \in [\text{T}_1, T_2]$ delivery period, K_1 is its strike, A_t the carbon allowances price in t while D_{EUA} is a fixed quantity for all the contract's options. The latter is a new feature added to limit the value of the derivative since the current emission allowances prices are near 100 which will bring the option to have a too-high payoff. Introducing D_{EUA} brings the fraction outside the Maximum to be around 1 therefore the electricity payoff will be increased in a short amount.

It comes time to present which are the possible counterparts of a swing contract based on this quanto option. The first hypothetical buyer is a company that belonged to the energy-intensive sector which is ruled by EU Emission Trading Scheme. It has to surrender a variable number of emission certificates every year and it is certainly affected by an upper movement of allowances price. In the meantime, it utilizes a high amount of electricity to run its business which usually is predictable during the year. For this type of company it is useful to have a swing contract with a fixed number of exercised rights per day since it doesn't need too much flexibility in the energy purchase.
A second buyers category is the national and European players which produce, buy and sell energy. They are certainly under the ETS mechanism since they represents the biggest energy producers in Europe; moreover, they supply electricity to enterprises, households and other smaller utility companies; usually they don't produce all the energy amount but they purchase it from other small players as local power plants. In the case that they incur a higher purchase price, it is unrealistic that they could pass it completely to clients due to the high competition. For this reason they could be interested in such contract. In Italy we have firms that produce and operate trading business, they are for sure Enel, Eni, Edison, A2A and Eon. This is clear when we look at the energy amount produced and supplied

for example by the main operator, Enel, which in past years has an energy market quote near 61% while it controls the production of not more than the 25%. Therefore they are the perfect long holder of this contract but also a possible seller since the energy-intensive company presented before could be interested to modulate the supply with both traditional contracts and swing ones. Due to the complex value chain of their business, they could be interested in more flexible swing contracts where the amount of options that can be exercised in a single day isn't fixed but linked to the waiting period of time that has to pass before being able to exercise again the option.
Coming back to the possible buyers, players that consume high energy amounts but are not subjected to EU ETS aren't interested in this contract since it is inefficient to buy a derivative on two underlings which costs more than a plain vanilla swing on electricity only. It could make sense if the allowances price would be recognized as representing the transition risk, giving them the possibility to hedge their business on fluctuations of this type of risk which will involve soon every traditional sector.
The last possible buyer of the swing contract, even though its needs aren't straightforward, is the medium-small producer of energy based on non-renewable sources, such as a coal plant, which stays under the ETS and sell energy to big market players or directly to final consumers. It benefits from a situation of higher energy prices and suffers when electricity price is low and the "marginal pricing" mechanism pushes it out of the market. For these reasons, it is interested in a swing contract based on put-quanto option that goes ITM when energy price decreases and its effect is propagated by an increasing emission allowances price. The main downside is the presence of a high correlation between the two prices, leading to a weakened product in case of a put quanto, which calls into question its usefulness.

The next characteristic to define is the settlement type of our quanto option which is related to the definition of possible sellers. The two possibilities are "cash" and "physical", where the first means that positive payoffs are paid with money by the seller to the option holder, while in the physical case the underlying asset is exchanged between them based on rules set in the contract.
In both quanto options presented previously it is clear that the option is cash settled:

- The cross-currency quanto option couldn't have a physical settlement since if the underlying, which is in foreign currency, is exchanged there is no meaning for the presence of the rate.

- In the straddle, in the case of an option deep ITM, the buyer could be forced to acquire an amount of electricity higher than needed that couldn't be utilized, which could lead to grid network and pipeline problems.

This last point is significant even in our quanto option since the fraction between A_t and D_{EUA} isn't upper bounded, therefore the settled electricity could be impossible to be managed. On one hand, Energy-intensive firms will benefit from physical delivery as well as companies like Enel which can take advantage of market opportunities. On the other hand, a cash settlement will result in low risks linked to the electricity delivery through the network and fast negotiations which could support the usage of the swing contract. A solution could be to settle a part of the energy physically and the other to be paid in cash, for example,

the amount related to the multiplication factor resulting from allowances, if present, which can have the form $\Big((A_t \ / \ D_{\text{EUA}} - 1) \cdot \text{Payoff}\Big)$. Anyway, for sake of simplicity and usage, it is preferable set it cash deliverable.

For what concerns the employment of the Least Squares Monte Carlo method (LSMC), we already saw the maximization procedure. In order to evaluate the future discounted possible payoffs we estimate the discounted value function for a different number of remaining exercise rights. In the case of constant recovery time equal to one period, fixed risk-free rate, the estimation formula is the following:

$$E_t[V_{t+1}^n e^{-r}] = F(x_t)$$

Where the $F(x)$ represents the selected basis functions while the value function V_{t+1}^n is given by the Formula 2.6 and Z_t represents the quanto payoff shown in Formula 2.27. This implies that the conditional expectation is based on both the underlying processes of electricity S_t and emission allowances A_t.
In the previous chapter it was stated the conditional expectation must belong to $\mathbb{L}^2(\Omega, \mathscr{F}, \mathbb{P})$ to be allowed to utilize the Least Squares Monte Carlo method. To fulfill this property is enough that the resulting stochastic process is square-integrable. A function f is square-integrable if it satisfies the condition:

$$\int_{-\infty}^{\infty} |f(x)|^2 dx < \infty$$

In our case, since all PDEs' parameters are constant and their random parts are Levy's processes (in particular Brownian motions), we could assume the $\mathbb{L}^2$ property if the Monte Carlo simulation reaches a convergence.

Another property that helps us during the least squares regression, is the Markov one. It allows us to consider only state variables at the current time t and not at previous periods, since for a Markovian process the information accessible up to time t brings the same result of using information given at time t. In the case of emission allowances, it is ensured since the process selected is the Geometric-Brownian-Motion, whose stochastic part is a Brownian which is Markovian. An analogous case is the Ornstein–Uhlenbeck process selected for the electricity for which stationarity is proven as stated by [43]. For the jump part, instead, the assurance isn't straightforward but it is assumed by [14]. In any case, the least squares validity under a single time period will be tested in comparison to the regression with lags of the state variable during the algorithm implementation.

While the relation between the the Brownian and Poisson part of the electricity dynamic can be assumed independent due to the randomness of jumps, the same idea couldn't be assumed for the stochastic parts of the two underlings utilized in the Quanto option. In particular, we have to focus on their correlated paths due to the generation of random numbers during the Monte Carlo simulation. Their independence couldn't be proved either theoretically or empirically, due to the fact that companies under ETS come usually from energy-intensive sectors, therefore it is quite possible that energy market has an influence on EUAs prices.

If we look at the stochastic processes identified to represent our two underlings dynamics, they presents a Brownian noise. This leads us to assume their dependence is incorporated in the bivariate normal distribution, where it is defined by the linear Pearson correlation among the two samples. To test this hypothesis, in the practical part, it is utilized the Henze-Zirkler multivariate normality test which results in a strong refuse of the null hypothesis, leaving the necessity to find a new method to model their dependence. Due to the high linear correlation in the last period of time, and the promising scatter plot (showed in the next chapter), we decide to utilize the Copula functions to model their dependence. These latters are the topic of the next section.

2.5 Copula Theory

The Copula is a cumulative distribution function with some recognizable characteristics. Every copula is defined by a d-dimensional unit since it is a joint CDF with mapping that goes from d-th $[0,1]$-uniform random variables to the usual interval: $[0,1]^d \to [0,1]$. More in detail, [21] helps us to define the identification properties of a Copula. It means that every Copula fulfils them, meanwhile every function for which they hold can be considered of this family.

Proposition 2.5.1 *If we consider a copula function of d-order, defined as $C(U_1, U_2, ...U_d)$ then:*

- *C is non-decreasing for each component U_i;*
- *The i^{th} marginal distribution is equal to u_i due to the fact that u_i is $[0,1]$-uniform distributed. In fact to obtain a marginal we should integrate for the other random variables, meaning:*

$$C(1, 1, ..., u_i..., 1, 1) = F_i(u_i) = \frac{u_i - 0}{1 - 0} = u_i$$

- *The rectangle inequality is fulfilled due to the fact that $P(U_1, U_2, ..., U_d)$ is non-negative.*

Coming back to our purpose, the Copula function helps to separate the marginal distributions from their dependency structure incorporated in their joint distribution. This permits us to model independently the dynamics of every single asset and then analyze their relation through Copula functions relying on the following theorem.

Theorem 2.5.1 (Sklar's Theorem) *Consider a d-dimensional CDF, F, with marginal distribution functions $F_1, ...F_d$. Then it exists a copula function C, such that the copula of marginals is equal to the joint function F. In mathematical terms is:*

$$F(x_1, ..., x_d) = C(F_1(x_1), ..., F_d(x_d))$$

Moreover, if marginals F_i are continuous, then the C function is unique. Otherwise, it can be determined uniquely by the range of the marginals.

The opposite direction is possible, meaning that given a Copula function and a set of marginals it is possible define one or more multivariate CDF.

The last theorem permits us to utilize a Copula function to model the generation of random numbers during our Monte Carlo simulation after have calibrated it on our sample data. It requires only few assumptions on which Copulas' family is the best to model our inner processes.

Copulas classes are many, the most famous are:

- the Gaussian Copula, which assumes a multivariate normal distirbution function as CDF and univariate gaussian for marginals,
- the t Copula that is of the same form of the Gaussian but with the t-distribution,

Copula	$\phi(t)$	C(u,v)
Clayton	$t^{-\theta}-1$	$(u^{-\theta}+v^{-\theta}-1)^{-\frac{1}{\theta}}$
Frank	$-\ln\left(\frac{e^{-\theta t}-1}{e^{-\theta}-1}\right)$	$-\frac{1}{\theta}\ln\left(1+\frac{(e^{-\theta u}-1)(e^{-\theta v}-1)}{e^{-\theta}-1}\right)$
Gumbel	$(-\ln(t))^{\theta}$; $\theta \geq 1$	$\exp\{-[(-\ln u)^{\theta}+(-\ln v)^{\theta}]^{\frac{1}{\theta}}\}$; $0 \leq u,v \leq 1$

Table 2.1: Generator ϕ and Copula function for the Archimedean family

- Archimedean family, that will intrduced later on in this section.

We don't consider these first two classes appropriate for our underlyings for the reasons stated in the last section on the rejection of the Normality property's assumption.

Passing to the famous Archimedean family, it is composed by three different main copula functions: Clayton, Frank and Gumbel. This family can be utilized only in case of a bivariate copula as in our case, and it is characterized by the following definition [19] which allows us to derive well-defined equations.

Proposition 2.5.2 *Given a uniform random variables X, Y whose dependence function is of the form:*

$$\phi^{-1}\{\phi(x)+\phi(y)\}$$

with ϕ that is a convex and decreasing function defined in $[0,1]$ with $\phi(1)=0$.
Set $U=\frac{\phi(X)}{\phi(X)+\phi(Y)}$, $V=C(X,Y)$.
Then:

- *U is uniformly distributed on $[0,1]$,*
- *V is distributed on $[0,1]$ as its Kendall Distribution Function $K(v)$ where:*

$$K(v)=v-\frac{\phi(v)}{\phi'(v)}$$

- *U and V are independent random variables.*

The properties stated above imply that the Copula function C can be written as $C(x,y)=\phi^{-1}\{\phi(x)+\phi(y)\}$.

We assume that this properties hold even for our inner processes in order to employ the Archimedean family. This allows us to know analytical formulas of each single Copula class which are shown in Table 2.1. The Copula selection method will be undertaken in the empirical part.

Chapter 3

Empirical Framework

The following chapter opens with the electricity and EU Allowances pricing models calibrations in sections 3.1 and 3.2. This is presented starting from a brief introduction on the utilized market data and the statistical estimation techniques here employed. The consequent results are analyzed both from a statistical and theoretical point of view with the aim to assess their validity. In the case of EUAs, this leads to the introduction of a scenario-based transformation of the deterministic part of its stochastic model in order to assess the swing contract effect in different possible scenarios.
Furthermore, to construct a sound and reliable Monte Carlo simulation, in section 3.3 a copula function calibration is carried out utilizing the theory presented in the corrisponding subsection of the theoretical part.
Consequently, in section 3.4, all the previous estimated parameters are utilized to employ the Least Squares Monte Carlo method, whose statistical features are assessed looking at their consequent results. Then, comparisons are taken between results obtained from different parameters setting.
Lastly, a practical scenario-based case is constructed in 3.5 to show the importance of the swing contract based on a quanto option for companies under the ETS mechanism. This analysis is done under different scenarios looking at three different hedging strategies that reveal to be optimal in different situations.

3.1 Electricity Calibration

3.1.1 Data Presentation

The aim of this section is to calibrate the continuous models presented in the last chapter to historical data. The starting point is the data selection that is strictly linked to the choice of the possible swing contract's counterparts. As already stated before, the buyer has to be under the ETS mechanism framework to have interest in this type of contract, and its business should be affected even by electricity price fluctuations. Focusing on energy market, while the EUAs market is unique, the first isn't a broad and unique market for the entire European Union due to its regionality feature. Based on proximity and curiosity, we decide to select the Italian market where the reference national price is the "PUN", acronym of "Prezzo Unitario Nazionale" that means it is the result of an aggregation at the national level of prices of sub-regional markets, which are scattered in all the country.
The selected data provider is the GME S.p.A. that means "Gestore dei Mercati Energetici" and which is a company totally owned by the Italian government under the ARERA[1] rules. It was established during the liberalization of electricity sector, and it operates in power, gas and environmental markets . Within the electricity framework, it manages and controls different markets stated below:

- A Forward physical market (MTE), where contracts are exchanged until two days before the start of the delivery period and with different maturities equal to: the three months after the current one and the corresponding next four quarters (the quarter after the current one and the next three quarters) both for a base-load and peak-load perspective[2].

- A market for the trading of daily products (MPEG) in continuous trading mode.

- The day ahead auction market (MGP), where contracts for the day after are signed. We can consider it as the spot market reference even though in traditional financial markets the lag between sign and settlement is of two days instead of one.

- An intra-day auction market (MI), consisting of three auction sessions (MI-A) and one continuous trading session (MI-XBID). As MPEG market, it is used to cover unexpected energy needs of last time that are crucial for the well functioning of the electrical supply.

For the first estimation phase we should look at the GME market that we call "spot" from now on. The GME makes available MGP hourly data every month on its website, therefore the first task was their aggregation into daily average spot prices. The data goes from 2011 to the last traded month, allowing us to have a long time series whose path and statistics are showed in Figure 3.1 and Table 3.1 starting from year 2016. The summary statistics show

[1] ARERA states for " Autorità di Regolazione per Energia Rete e Ambiente".

[2] The difference among peak and base-load contract is the moment of day time when they are settled. In particular base-load refers to a price that is the result of the average among every hourly price in a day, while the peak price refers only to prices from 8 a.m. to 8 p.m., which is when the demand and price are usually higher due to energy consumption in factories and offices during the working hours on week-days.

Date	N.Obs	Mean	Std	Skewness	Kurtosis	Min	25Th Perc	Median	75Th Perc	Max
2016	366	42.78	10.33	0.97	0.53	24.99	35.03	40.1	47.84	80.48
2017	365	53.95	12.8	1.44	2.45	29.74	45.25	50.68	59.06	110.54
2018	365	61.31	11.41	0.48	0.29	31.53	52.37	60.82	68.69	107.17
2019	365	52.33	8.79	0.04	0.81	21.26	46.88	51.78	57.81	83.24
2020	366	38.91	11.89	0.08	-0.3	10.66	29.99	39.78	46.96	72.63
2021	365	125.45	78.23	1.26	1.05	37.0	65.43	96.38	181.18	437.06
2022	243	311.16	126.63	1.26	0.82	150.69	220.86	251.75	380.44	740.09

Table 3.1: Energy Spot Prices summary statistics

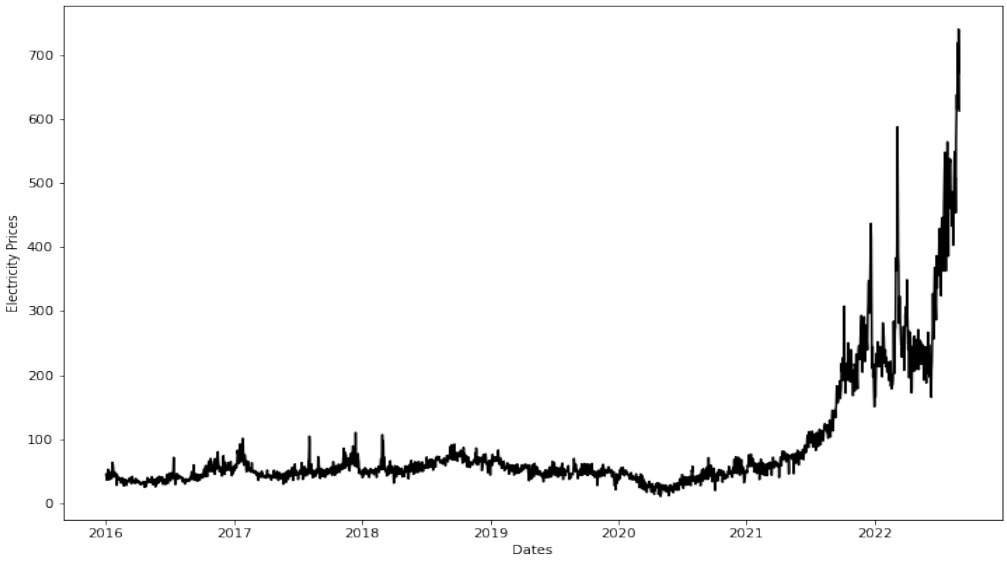

Figure 3.1: Energy Spot Prices from Jan 2016 to Aug 2022

the electricity price's volatility exploded in 2021 while in the previous years it was relatively low. It is remarkable notice that the price was never negative in the last years, meaning that the choice of an exponential stochastic process is realistic. The PUN process looked like to be stationary before 2021, feature that will be checked in the following pages.

Coming back to parameters estimation, we select the interval that goes from January 2016 to December 2019, before the Covid-19 crisis to exclude not ordinary periods which could heavily affect the calibration. In this way the Ornstein-Uhlenbeck process results stationary and normal as assumed in his theoretical part. We prefer prioritize the fulfilment of these basic properties rather than select another interval that incorporates year 2021 since the latter brings difficulties in data modeling due to the fall of historical theory on energy prices. This doesn't mean that it cannot be assumed to be valid again after these months of market turmoil, nevertheless we strive to strictly follow the historical literature on the most common model to utilize (OU Process) which will be taken into account after the following subsection on the seasonality estimation.

3.1.2 Seasonality Estimation

The seasonality term is applied to the natural log transformation of electricity prices, following the formula (2.17). With the aim of a good coefficients estimation, we decide to utilize the method employed in [24] where it is argued that the estimation methods for the seasonal pattern are usually sensitive to outliers. For example in [44], as in our case, it is utilized a multiple linear regression that is quite unstable in case of significant outliers. Their presence is realistic since upward and downward spikes are usual here, even though their identification isn't straightforward and unique. For this reason [24] proposes different methods for their detection like: Fixed price threshold (prices exceeding a fixed value are considered outliers), variable price threshold (prices that exceed certain percentiles) and many others. After that, we should replace outliers with a list of possible values like: a chosen threshold, the mean of the two neighboring prices or even an average value (i.e. the median of prices with same weekday and month within the series) [24]. It is important to note that the literature isn't concordant on the choice to replace or not these outliers from the parameter estimation, but we utilize this procedure since in this way we clean the seasonal pattern from the greatest volatility part, that could be significant in the following section during the calibration of the stochastic part.

In our case the treatment of extreme observations is conducted utilizing a variable threshold fixed to the 2.5 and 97.5 percentile values that are utilized as replacement terms for observations exceeding them respectively downward and upward. We remark that the final aim is obtain a more 'normal' and less spiky distribution which could lead to a better linear estimation of monthly and weekly seasonality terms.
The utilized method is structured as follow:

- Alongside to the log prices time series, two additional series are created representing the year fraction t and the indicator function $\mathbb{1}_{WD}$ that distinguishes weekends and Target-calendar holidays.
- A first linear regression is applied to log prices following formula (2.17);
- The estimated time series is subtracted from log prices;
- It is conducted the outliers detection and substitution with threshold values in 2.5% and 97.5% positions;
- The seasonality part is re-added;
- A second linear regression is applied to the new modified log-prices time series;
- The deseasonalized time series is derived subtracting the new estimated values to the initial/market log prices.

The significance of the method can be seen in Figure 3.2, where some upside jumps were detected by the algorithm and then substituted with limit values. For what concerns lowest outliers, instead, they occurred at the end of December 2019, when we expect an higher price due to cold temperatures, therefore these values could have been affected the linear regression bringing a lower level for the seasonality in those days. Due to their detection

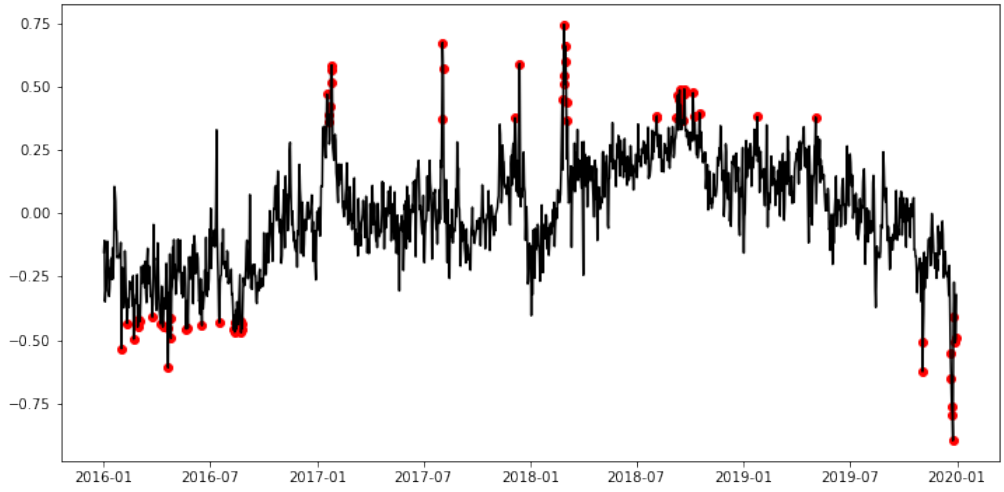

Figure 3.2: Outliers in the deseasonalized Log Price Time Series

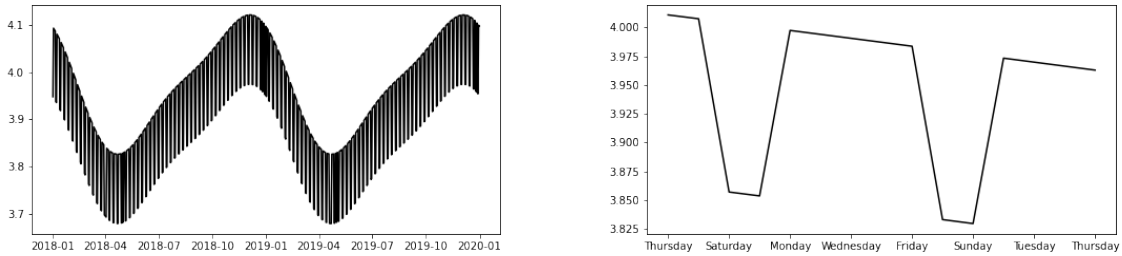

Figure 3.3: Monthly and Weekly Seasonal Component

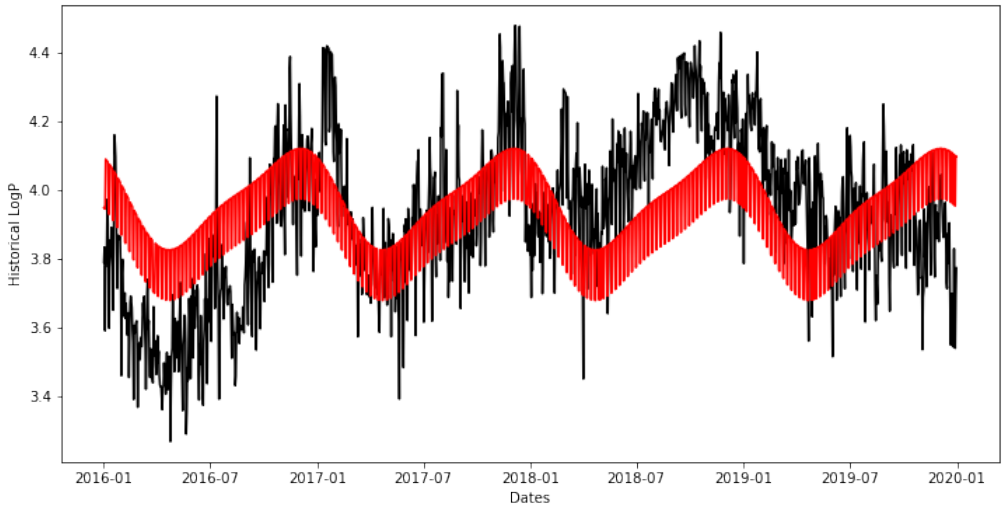

Figure 3.4: Comparison between Seasonality and PUN Log Prices (2016-19)

and substitution, that downside effect is avoided as it can be seen in Figure 3.3, where the highest level is placed at the end of the year and the comb shape is due to the presence of weekends when the price falls sharply. Lastly, is significant investigate the goodness of fit

	Mean	Std	Skewness	Kurtosis	Min	25th Perc	Median	75th Perc	Max
Seasonal Log Prices	3.93	0.24	-0.09	-0.01	3.06	3.78	3.94	4.1	4.71
De-seasonalized Log Prices	0.00	0.21	-0.15	0.14	-0.90	-0.14	0.01	0.16	0.75

Table 3.2: Seasonal and deseasonalized Energy Log Prices summary statistics for (2016-19)

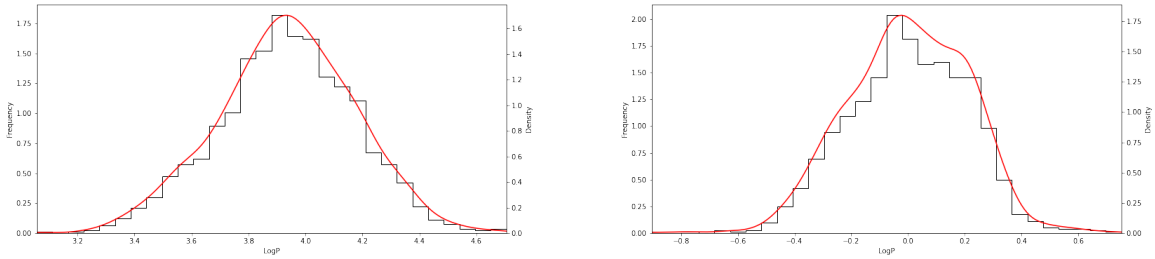

Figure 3.5: Energy Log Prices Histogram and Kde plots pre (left) and post (right) deseasonalization

starting from the comparison between seasonality and log prices: in Figure 3.4 it is clear the presence of an yearly component linked probably to winter season rather than summer. A possible explanation is the heterogeneity of temperatures in Italy during summer as well as the production of more solar energy at a lower cost; the investigation of the real motivation goes beyond the scope of this work.
If we focus on the linear regression, the applied method leads to a decrease in the Root Mean Squares Error (RMSE) and rise of R^2 in the estimation with outliers replacement; in particular they pass respectively from 0.211 and 0.242 values to 0.198 and 0.264, proving the the goodness of fit and increase in predictability.
Looking at the statistics in Table 3.2, it is worth notice that the log prices mean passes from 3.93 to 0, the standard deviation slightly decreases while Minimum, Median and Maximum value are simply scaled to a lower level without a change in the distance among them, suggesting that the seasonality effect doesn't affect the volatility of the model as it was desirable.
The main downside is the change in Skewness and Kurtosis measures that present worse results even though they both remain near zero, which is our preferable case since it is the level addressed to normal distributions[3]. This decline of Gaussian property is visible looking to two plots, in particular the histogram of deseasonalized data doesn't seem too symmetric and its *Kernel Distribution Estimation Plot*[4] doesn't look clearly normal as can be seen in Figure 3.5. Further analyses are conducted in the following subsection.

3.1.3 Stochastic Calibration

We introduce the calibration for the Exponential Ornstein-Uhlenbeck process first, before moving to the one with the addition of the jump part. The starting point is the deseasonalized

[3]In statistics the Skewness measures the level of asymmetry of a distribution (if it is symmetric it has value zero), while Kurtosis is an indication of the size of the distribution's tails. A zero level is linked to normality since the employed Python's library Numpy delivers the Fisher definition of Kurtosis, where a value of 3 is subtracted from the result in order to gives zero in case of the data distribute as a Gaussian.

[4]It is a plot that depicts the shape of the probability density function assuming the inner variable is continuous. It is very useful to assess the presence of normality property.

	ADF Test (i=0)	Arranz ADF Test (i=2)	Arranz ADF Test (i=3)
p-value	0.2	0.08	0.05

Table 3.3: ADF Test on $X_t^{*(i)}$ for different level of lag "i"

time series for the electricity log prices, obtained from the last subsection.

Since we utilize the Ornstein-Uhlenbeck model which dynamic is given by Formula 2.18, we should assume that the process is log-normal and stationary. The distribution of the electricity log-prices during $2016 - 2019$ period can be assumed normal for a significance level of 1%, since the p-value of the known *D'Agostino and Pearson's Test*[5] is equal to 0.35 before the deseasonalization and to 0.03 after.

For what concerns the stationarity, its assumption is based on the significance intervals of the k parameter but more importantly by an effective Unit Root Test. To conduct the latter test, we follow the work in [17] where, at first, the famous *Augmented Dickey-Fuller Test* is employed. It utilizes the null hypothesis of unit root presence $H_0 : \ (k-1) = 0$ for the equation:

$$\Delta X_t = c + (k-1)X_{t-1} + \sum_{n=1}^{r} k_n \Delta X_{t-j} + \epsilon_t \tag{3.1}$$

In the already cited work it is cited how the ADF test can be biased in presence of outliers like jumps and spikes. Therefore it is utilized an approach proposed by [2] where the process X_t is modified by a filter of order i defined as:

$$X_t^{*(i)} = Median(X_{t-i}, ..., X_t, ..., X_{t+k})$$

The latter resulting series substitutes X_t in the regression (3.1). The work [2] utilizes $i = 2$ while we find an acceptable result for $i = 3$ displayed in the Table 3.3, for which we can refuse the H_0 for a 5% level. The following step is the estimation of the Ornstein-Uhlenbeck process's parameters on the spot time series through its discretization to a daily frequency. The estimation method deployed is the *Maximum Likelihood Estimation* (MLE) which permits to find the best result maximizing the Likelihood function. The latter is a measure of "how likely" the data sample is generated by the selected distribution and the estimation tries to reach the best parameters to increase the likelihood. This method is widely utilized since it is usually consistent[6] and efficient. The general formula, applied for a set of parameters α and sample $x_1, ..x_n$ and known probability density f, is the following:

$$L(\alpha|x_1, ..., x_n) \ = \ \prod_{i=1}^{n} f(x_i|\alpha)$$

As can be guess from past lines, the method relies on two main assumptions:

- The observed data are generated independently and they are identically distributed;

[5]The D'Agostino and Pearson's Test combines properties of the normal distribution on Skewness and Kurtosis creating a unique test with a null hypothesis that regards normality. Therefore, when the p-value is lower than a certain significance level (i.e. 5% or 1%) we can refuse the null hypothesis, while on the contrary we cannot.

[6]When the sample size increases, the estimator'sdistribution converges to the true value.

- The parametric form, and so the probability density function of the inner process is known.

In the case of an Ornstein-Uhlenbeck process, its dynamic can be assumed to be normal due to the presence of the Brownian term. Based on that we can utilize its well know conditional PDF defined as:

$$f(x_t|x_{t-1}) = \frac{1}{\sqrt{2\pi\sigma^2}} \exp\Big(\frac{-(x_t - \alpha\kappa - (1-\kappa)x_{t-1})^2}{2\sigma^2}\Big) \tag{3.2}$$

We estimate parameter both through MLE and Least Squares observing that the long-mean term α looses its statistical significance when seasonality is subtracted (like in our case), meaning that, escluding seasonality, we are assuming a flat long trend for electricity. It is a strong but quite possible assumption for the future since the increase in energy demand could be off set by the entrance in the market of players with lower marginal costs due to renewable sources. Moreover all the other long term effects (i.e. inflation) can be included in the seasonal part.

Coming back to the MLE estimation, for its discrete approximation process it is utilized the homonymous Matlab's algorithm that minimizes the inverse of the maximum likelihood function utilizing the *Hybrid-simulated annealing algorithm* [52]. It is hybrid since firstly it is applied the *simulated annealing algorithm*, which is quite insensitive to user-generated parameters and perturbs initial guesses testing the goodness of fit until an approximated location for the global minimum is reached; then the process switches to a *direct search algorithm* (whose the one of default is the *GPS algorithm*) to resolve precisely the minimization problem.

During the estimation initialization, in addition to starting values definition, it is necessary to set parameters boundaries that are based on their theoretical assumptions. Volatility σ couldn't be negative since it is the square root of the variance multiplied by dt, therefore its domain is $[0\ ;\infty]$, whereas κ should assure stationarity lying in the range $[[0\ ;\infty]]$. We assess the validity of results looking at the estimators confidence intervals showed in Table 3.4 that presents good values for both parameters.

An analogous method can be utilized for the parameter estimation for the OU process with the additional jump component that introduces three new estimator parameters: σ_j, μ_j and θ. The first one has the same boundaries of σ since it is a volatility measure, whereas θ presents a tighter domain, $[0\ ;1]$, because it is the Poisson process parameter and represents the probability to incur in a jump. This time the probability density function can be approximated, as done by [17], recurring to the formula:

$$\begin{aligned} f(x_t|x_{t-1}) = (1-\theta)\Big[\frac{1}{\sqrt{2\pi\sigma^2}} \exp\Big(\frac{(x_t - (1-\kappa)x_{t-1})^2}{2\sigma^2}\Big)\Big] + \\ \theta\Big[\frac{1}{\sqrt{2\pi(\sigma^2+\sigma_j^2)}} \exp\Big(\frac{(x_t - (1-\kappa)x_{t-1} - \mu_j)^2}{2(\sigma^2+\sigma_j^2)}\Big)\Big] \end{aligned} \tag{3.3}$$

It's worth notice that α isn't included this time due to its non significance in the last estimation, while the PDF formula can be seen as an average between the density of plain OU process (as previous case) and the one of a Gaussian PDF with additional mean term μ_j and

	No-Jump Estimation			Jump Estimation			Seasonality	
	Estimate	2.5% CI	97.5% CI	Estimate	2.5% CI	97.5% CI		
κ	0.1169	0.0928	0.1411	0.1052	0.0812	0.1292	β_1	-0.10213
σ	0.0991	0.0955	0.1027	0.0816	0.0695	0.0921	β_2	0.08690
θ				0.1764	-0.0239	0.3768	β_3	-0.00051
μ_j				-0.0066	-0.0313	0.0181	β_4	0.03342
σ_j				0.1339	0.0783	0.1724	β_5	3.83025
RMSE		0.0991			0.0992		β_6	0.14685

Table 3.4: Energy parameters estimations

volatility σ_j, weighted for the probability of spikes occurrence θ. Then, it is applied the same MLE algorithm seen before, which reaches a convergence to an higher Maximum Likelihood but leading to a slightly worse RMSE (see Table 3.4). In addition, the confidence intervals aren't so good for θ meaning that it could be possible that the complete Jump term isn't significant, even though the σ_j and μ_j show acceptable results.

For what concerns Market Risk Premium (MRP) considerations, we already state its importance since the aim is to forecast future electricity prices to analyze the swing contract. The calibration of MRPs parameters should be undertaken starting from spot prices and then passing towards future ones observed in the market. The literature isn't concordant on assumptions upon MRP for energy matket: [43] and [50] assume it constant in time, [44] considers a time varying market price of risk, and [49] assesses the presence of MRP only in summer months. The evaluation process is, instead, concordant to utilize market forward and futures prices set in a given interval of time as dependent variable in a Least Squares method on risk-neutral estimation. In terms of formula, the procedure can be formalized starting from Formula 2.23 and applying:

$$min_\lambda \sum_{i=1}^{N} \Big(f_M(t,T) - E^{\mathbb{Q}}[f(t,T)|x_t] \Big)^2 \tag{3.4}$$

Where N represents the total number of observations composed by a spot and a future price.
We assume a constant market risk premium for energy prices to be estimated on a data interval of at least one year to avoid seasonal effects. In addition, due to recent market turmoil, we consider significant to assess its validity on latest data, incurring in a out-of-sample post spot calibration as done in [49] and [33]. In this way we can take into account the current situation in the λ term without affecting the inner stochastic path, representation of the energy market theory. Therefore, market data from January 2021 to September 2022 are taken into consideration considering quarterly and yearly maturities that goes from the end of 2022 to 2025. Coming back to the estimation process, following the literature, MRPs are calibrated keeping all other parameters constant and equal to their spot estimation values, then the RMSE is computed and it is compared to the base case where we assume a zero valued market risk premiums. The results are showed in Table 3.5 both for the two theoretical processes. It is important notice that, in the case of Jump Process, it is conducted a non

	No-Jump Estimation			Jump Estimation		
	Estimate	2.5% CI	97.5% CI	Estimate	2.5% CI	97.5% CI
λ	-0.0103	-0.0135	-0.0071	-0.0447		
ν_j				-0.0024		
RMSE $\lambda \neq 0$		0.7329			0.8929	
RMSE $\lambda = 0$		0.7224			0.7064	

Table 3.5: Energy Market Risk Premium parameters estimations

linear least squares estimation that applies a *direct search algorithm*[7] on the equation 2.25. It is worth remember that in this case the market risk premiums are two: the classical one linked to the OU process and a second one concerning the jump-size risk ν_j.

The Table 3.5 shows a quite small improvement in the RMSE when we pass from a zero to positive MRP in the no-jump model estimation. This is confirmed by the value which is very near zero even though significant (-0.0103). In the case of the Jump model, the RMSE decrease more than 20%, this brings us to be confident on the significance of at least λ while for ν_j the situation is more obscure since it has a value near zero and we don't have confidence intervals for such parameters estimation. Focusing on the sign of these three parameters, they are all negative, which imply the assumption of a positive forward premium (the forward price is greater than the future spot price estimated under the objective probability measure $\mathbb{P}$), meaning that, from a theoretical perspective, contract's buyers are willing to pay an higher price to be covered by future uncertainty (Contango market).

[7]Direct search algorithm are methods that don't utilize gradient information or derivatives during the research of the optimal point, but directly look at the points near the starting one trying to minimize the objective function. An example is the already cited GPS algorithm. Further information can be found in Matlab's documentation.

3.2 EU Emission Allowances Calibration

3.2.1 Data Presentation

The data selected for the EUAs price calibration regards spot and future prices provided by the European Energy Exchange (EEX) which is a German energy-related commodities exchange. It is the main player in the auction and management of emission certificates under ETS and it trades EUAs and its derivatives. The exchange is open only on weekdays following the European "Target" calendar, therefore, given a constant period, EUAs data presents a lower number rather than Energy prices data. Furthermore, it is open only in working hours, meaning that we couldn't have a reference price for every hour of the day as can be done for electricity. These are the main differences between EUAs and energy prices that could lead complexity during the Monte Carlo method; therefore, for sake of simplicity we will assume an ongoing price for EUAs during the simulation. This decision shouldn't affect severely the price determination since allowances are utilized as multiplicative factor of the quanto option payoff and, more importantly, the model parameters are re-scaled to a 365 days base during the final step of Scenario Based adjustment.
From Table 3.6 and Figure 3.6 it is clear the price dynamic of our asset is totally changed from year 2013 to now. In particular, the almost flat dynamic stops after 2018 when the spot price increases three times (maybe due to the "Market Stability Reserve" mechanism) and then it raises sharply again in the 4^{th} phase to the maximum level in September 2022. This analysis makes clear that the ETS is divided in phases different from each others.

Nevertheless this feature, the interval employed in the parameters estimation is the same of electricity spot prices(2016-2019). The differences in the inner process dynamics given by the different ETS phase will be incorporated in the market risk premium term which will be estimated through an out-of-sample method for the same interval of dates of energy calibration.

3.2.2 Parameters Estimation

As stated in the Theoretical part, there are no clear evidences on the best stochastic model to fit the emission allowances due to phase differences and the feature to be a niche market. For this reason, following the work of [13], we tried different processes in order to find the

Date	Obs	Mean	Std	Skewness	Kurtosis	Min	25Th Perc	Median	75Th Perc	Max
2013	250	4.47	0.67	0.09	0.61	2.72	4.14	4.46	4.86	6.52
2014	251	5.94	0.67	-0.16	-0.72	4.35	5.48	6.01	6.38	7.24
2015	253	7.68	0.59	-0.09	-1.19	6.42	7.18	7.61	8.19	8.65
2016	257	5.35	0.78	0.63	0.43	3.91	4.73	5.26	5.90	8.05
2017	255	5.83	1.10	0.65	-1.13	4.35	4.97	5.31	6.98	8.17
2018	246	15.67	4.42	-0.09	-0.90	7.62	12.93	15.86	19.55	25.19
2019	250	24.83	2.16	-0.36	0.03	18.72	23.41	25.06	26.25	29.76
2020	258	24.79	3.64	-0.30	-0.15	15.23	22.74	25.04	27.02	33.28
2021	261	53.43	12.67	0.41	-0.15	31.53	42.77	53.32	59.88	88.88
2022	169	83.44	6.04	-0.57	1.87	57.92	79.73	83.60	87.72	97.58

Table 3.6: EUAs Spot Price summary statistics

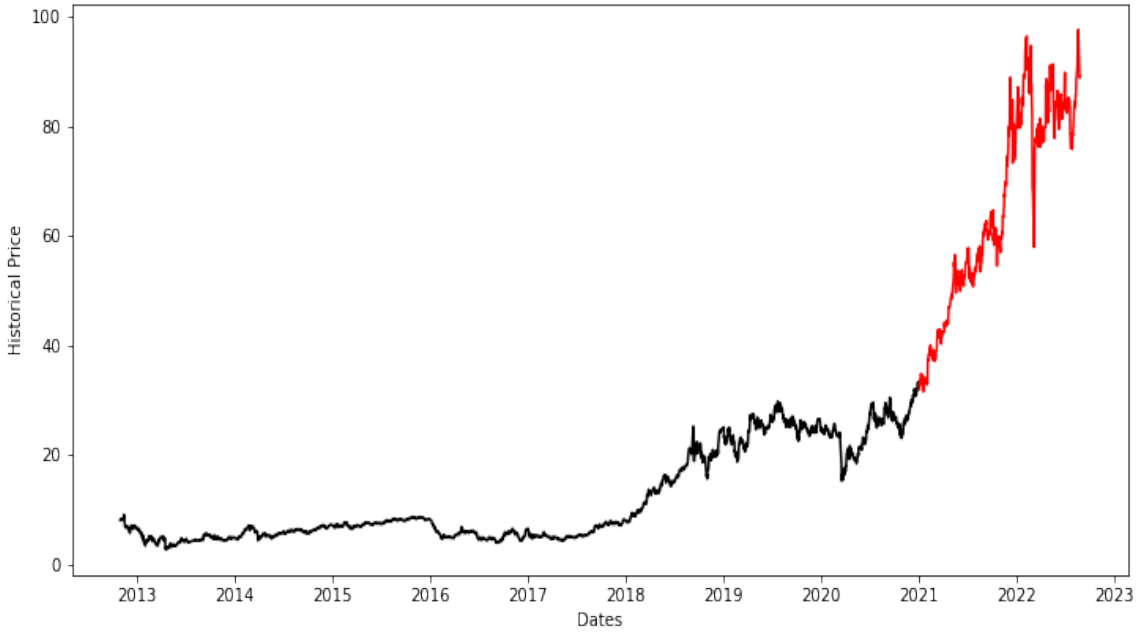

Figure 3.6: EUAs Spot Prices in phase 3^{th} (black) and 4^{th} (red) phase

one that fits better to our sample data, relying on t-statistics and Bayesian Information Criterion (BIC). The latter is a criterion to compare models during a calibration process which assesses the goodness of fit incorporating a penalty linked to the number of utilized parameters. The BIC value is computed as follow and the model with the lower result is considered the best in terms of fit and parsimony.

$$BIC = k \ \ln(N) - 2\ln(\hat{\mathbb{L}})$$

Where k represents the number of estimated parameters, n the number of observation utilized during estimation, and $\hat{\mathbb{L}}$ is the resulting Log-Likelihood value.

The analyzed models are four: the Ornstein-Uhlenbeck process, the exponential Ornstein-Uhlenbeck process, the Geometric Brownian Motion and the Square Root process. They are calibrated on previous presented spot data through the Maximum Likelihood Estimation on software "Matlab", exploiting their intrinsic properties and dynamic.
The MLE for the Square Root process deserves a particular mention since it is applied to the log prices, and the conditional density function has a closed form that is possible derive following the work of [28] whose method is utilized. Its transition density has a formula stated below:

$$f(X_{t+\Delta t}|X_t, \theta, \Delta t) = c\ e^{-u-v}(\frac{v}{u})^{\frac{q}{2}} I_q(2\sqrt{u\ v})$$

For:

$$c \ = \ \frac{2\alpha}{\sigma^2(1-e^{-\alpha\Delta t})}; \ u \ = \ c\ X_t\ e^{-\alpha\Delta t}\ ;$$

$$v \ = \ c\ X_{t+\Delta t}\ ; \ q \ = \ \frac{2\alpha\mu}{\sigma^2} - 1$$

	Exponential OU Process			GMB Process			Square Root Process		
	Estimation	**5% CI**	**95% CI**	**Estimation**	**5% CI**	**95% CI**	**Estimation**	**5% CI**	**95% CI**
mu				0.0016	0.0000	0.0035			
sigma	0.0307	0.0293	0.032	0.0307	0.0293	0.0320	2.076	-	-
alpha	4.38	-	-				0.032	-	-
kappa	0.0002	-0.0026	0.003				-0.015	-	-
RMSE	0.0307			0.0307			0.0432		
BIC	-4139.3			-4146.2			-6375.1		

Table 3.7: Model parameter values (2016-2019)

Where $I_q(2\sqrt{u\ v})$ is the modified Bessel Function of the first kind and of order q. This formula is utilized in the MLE reaching the equation to be maximized:

$$L(\theta) \ = \ (N-1)\ln(c) + \sum_{i=1}^{N-1}\Big(-u_{t_i} - v_{t_{i+1}} + 0.5\ q\ ln\Big(\frac{v_{t_{i+1}}}{u_{t_i}}\Big) + \ln(I_q(2\sqrt{u_{t_i}\ v_{t_{i+1}}})\Big)$$

Coming back to the calibrated parameters, it worth notice that the (non-exponential) Ornstein-Uhlenbeck process estimation is quite sensitive to initial values x_0 and it reaches a final result but not a good Maximum Likelihood value (-1897.3) and for this reason isn't showed in Table 3.7; this result is probably due to its arithmetic form rather than geometric as the other models.

The Square Root process seems to fit data well if we look at its BIC value (the highest), nevertheless the plot that compares historical and estimated values shows a visible difference between them; moreover, the parameter k is lower than zero, which represents not only the failure of the stationarity property, but also, in conjunction with other coefficients, they doesn't fulfil the base condition to have $\sigma^2 \leq 2 \cdot \kappa \cdot \alpha$. Therefore, it couldn't be ensured that the price is always positive, which it is a fundamental condition for a Monte Carlo simulation since if the price that goes inside the square root is negative the algorithm will stop. Stated these reasons, the direct consequence is to discard the model and select the final one between the two remaining geometric models.

From Table 3.7 it isn't immediately clear which one of the remained two models is the best since they are quite similar in term of RMSE and BIC values. We select the Geometric Brownian Motion (GBM) firstly because it is the one with better BIC (probably because it has 2 parameters instead of 3) and quite good t-statistics (both coefficients are significant at 5% level). In addition, in the Theoretical Part we state that for electricity prices it isn't possible consider the existence of a cost-of-carry relationship, and there the Ornstein-Uhlenbeck process is employed. In the case of EUAs it can be assumed the presence of a convenience yield in holding the asset since market players have to surrender a part of them to European controllers once a year. From this point of view it could be unsuitable consider the same underlying process to explain both.

Considering the Geometric Brownian Motion process, its price dynamic allows us to assume the log normality of EUAs prices given continuously compounded normally returns whose histogram and dynamic are showed in Table 3.7. As can be seen from the Kernel Distribution Estimation (KDE) Plot, the distribution presents an high number of extreme outliers in its tails (Kurtosis of 3.91); this leads to the rejection of the null hypothesis of

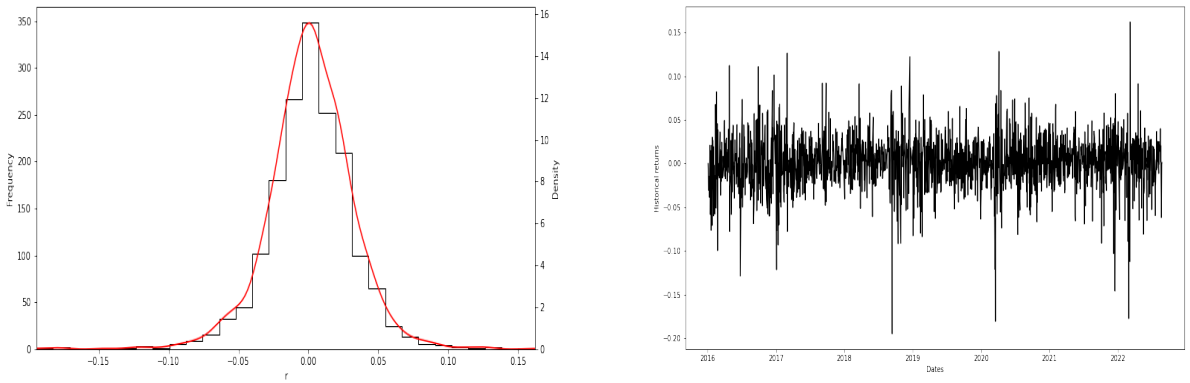

Figure 3.7: Histogram and Time Series of the EUA spot price returns (2016-19)

normality in the D'Agostino and Pearson's Test for any significance level. The price dynamic stated in Formula 2.26 can be re-written as:

$$S_{t+dt} = S_t \ \exp\Big((\mu - \frac{\sigma^2}{2})\ dt + \sigma\ dW_{dt}\Big) \tag{3.5}$$

While the pricing formula under the $\mathbb{P}$-measure for future prices is:

$$F(t,T) = E_t^{\mathbb{P}}[S_T] = S_t \ \exp(\mu) \tag{3.6}$$

The market risk premium has to be taken into account as done for the electricity model, since its future values will be simulated through Monte Carlo. The latter factor should be added to the exponential part of Equation 3.6 in order to pass from $\mathbb{P}$-measure to the risk-neutral one. Therefore the formula becomes:

$$F(t,T) = E_t^{\mathbb{Q}}[S_T] = S_t \ \exp(\mu - \lambda\sigma) \tag{3.7}$$

Its value is considered constant as in the case of electricity prices for sake of simplicity. To derive it, the Least Squares method is employed on a new sample of 3003 future prices whose maturity go from April 2021 to August 2025 provided by EEX. We employ an out-of-sample estimation in order to take into consideration the current state of the market as done for the electrcity calibration.

The obtained result presents a significant positive value for the Market Risk Premium which strongly decreases the RMSE of the same estimation where zero market premium is assumed as can be seen in Table 3.8. The difference in RMSE could be due to the inadequate selection of the model, situation that is far different from the energy future prices calibration. Despite this, the insertion of MRP helps us to improve the future price fitting, leading to more realistic simulations. Lastly, the MRP is positive, which could means the market is in "Backwardation", but due to the uncertainty in the model selection we ignore this possible property.

	Estimate	2.5% CI	97.5% CI
λ	0.06	0.06	0.06
RMSE $\lambda \neq 0$	1.692		
RMSE $\lambda = 0$	0.023		

Table 3.8: Market-Risk-Premium Model parameter values

3.2.3 Scenario Based Transformation

The aim of this subsection is to identify different scenario based EUAs price levels and utilize them to modify consequently the deterministic term μ of the Geometric Brownian Motion process employed to run the MC simulation. Our method relies on strong assumptions reported hereafter with the addition of two:

1. The EUAs price path is linearly dependent from the European level of CO_2 emissions (CO_2e) based on the formula:

$$E[EUA_T|\mathscr{F}_T] = \beta_0 + \beta_1 \; CO_2e_T \tag{3.8}$$

2. The relation stated above holds true regardless the ETS phase where we are.

3. It is possible apply IPCC forecasts to the European CO_2e framework.

4. The CO_2e levels for year 2022 - 2024 are based both on future worldwide IPCC-derived data and EEA historical data. We are assuming that past CO_2e data provided to the EEA by the 27 member states during 2021 are true.

The starting point of our method is the EEA European data which are necessary for the first steps. We collect EEA data on EU27 emissions from 2012 to 2020 and we employ one of them to scale the worldwide IPCC scenario-based to new European emission forecasts $EU\ CO_2e(T)$ (following Hp n.3) utilizing the formula:

$$EU\ CO_2e(T)\ :\ EEA\ CO_2e(t)\ =\ IPCC\ CO_2e(T)\ :\ IPCC\ CO_2e(t)$$

Where $T = 2050$ and $t = 2015$ since they are the years for which values can be derived from IPCC forecasts and it's present a correspondent EEA value. We apply the formula to every of the five worldwide scenarios and we obtain five different new europena forecasts. Once this step is completed, we derive European CO_2e values for years 2022 - 2024 utilizing an interpolating method between $EU\ CO_2e(2050)$ and $EEA\ CO_2e(t)$ for $t = (2015, 2019, 2020, 2021)$.

The interpolation method employed is the *Monotonic Cubic Splines*, whose algorithm was implemented by professor Marco Bianchetti in Visual Basic code for application on Microsoft Excel . In particular Ametrano and Bianchetti (2013) discovered that the so called "Hyman monotonic cubic filter" applied to natural splines not only ensures monotonicity but avoid some other problems linked to other methods like "Linear" and "Natural Cubic Spline" interpolations. They refer to the presence of spurious inflection points and in some cases extreme convexity. In any case, we tested both these three methods reaching quite identical paths meaning that in our case they are all adequate to the purpose. In fact, the emission dynamic doesn't require monotonocity, anyway it was selected a cubic interpolation instead a linear one since the use of lower order polynomials (as the cubic ones) brings a reduction in computational efforts and instabilities, together with the insured smoothness property given by cubic functions which have continuous first and second derivatives [51].

Dates	SSP5-8.5	SSP3-7.0	SSP2-4.5	SSP1-2.6	SSP1-1.9	EEA WEM	EEA WAM
2022-12-31	3,698,451	3,623,772	3,519,656	3,490,096	3,487,807	3,493,404	3,393,398
2023-12-31	3,897,295	3,749,060	3,544,711	3,480,622	3,471,572	3,478,371	3,344,879
2024-12-31	4,090,581	3,869,675	3,568,578	3,465,054	3,444,895	3,460,712	3,293,996
2025-12-31	4,277,477	3,985,144	3,591,175	3,443,702	3,408,306	3,434,909	3,233,373

Table 3.9: EEA and IPCC-derived Scenarios for GHG Emissions (ktCO2e)

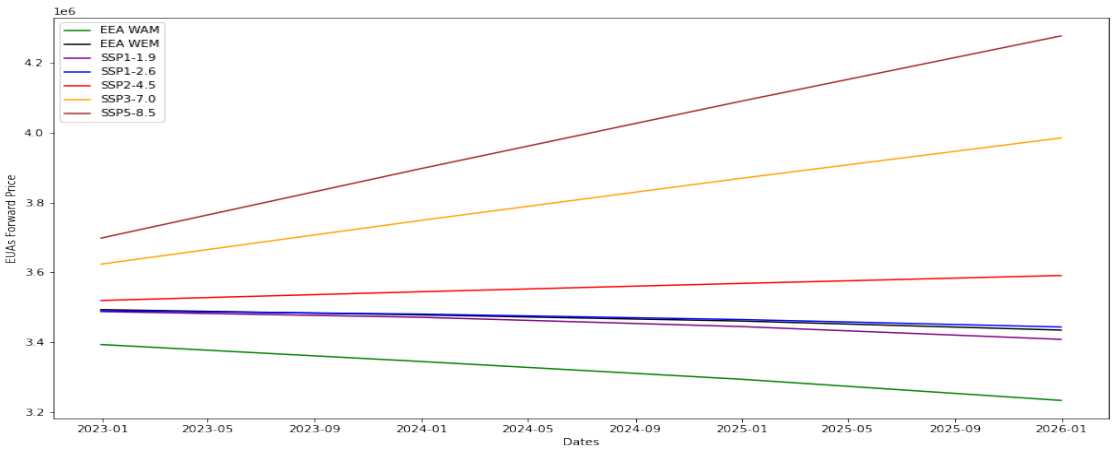

Figure 3.8: EEA and IPCC-derived Scenarios for GHG Emissions (ktCO2e)

The interpolation results are showed in Table 3.9 and, for a better visualization, in Figure 3.8. To seek of comparison, we report also the ones provided directly by EEA, which are based on EU member states' reporting in 2021 that we consider still valid. It is curious notice that the two IPCC best scenarios in terms of CO_2e reduction (SPP1-1.9 and SPP1-2.6), are almost identical. This is because their different behavior is assumed to start in the second half of the $21th$ century but we have utilized data in 2050 for the interpolation. The latter two paths are quite equal to the CO_2e of the WEM scenario provided by EEA, where the acronym states for "with existing measures", meaning it is the emission level that is assumed to be reached if no additional measure are implemented after 2021. In the case both IPCC and EEA scenarios are assumed true, our results are an indication that, on one hand, the best worldwide scenario could be assumed to be reached if every country commit itself to the cause as the same level done in past years by the European Union; on the other hand it means that the best European Scenario, named WAM which states for "with-additional-measures", couldn't be reached worldwide since the SPP1-1.9 CO_2e are far higher than the ones assumed by EEA. To summarize, the comparison among these different scenarios suggests us a low likelihood to reach European CO_2e levels for the rest of the world in the near decades.

The next step regards the computation and application of linear regression scaled coefficients that permit to obtain the final EUAs scenario-based forecasts starting from *EU* CO_2e of Table 3.9. The utilized data are the previous presented daily EUAs spot prices, provided by EEX, for the period 2012-2020 and the corresponding EEA emissions data for the European Union which are interpolated with the previous method to pass from yearly to daily

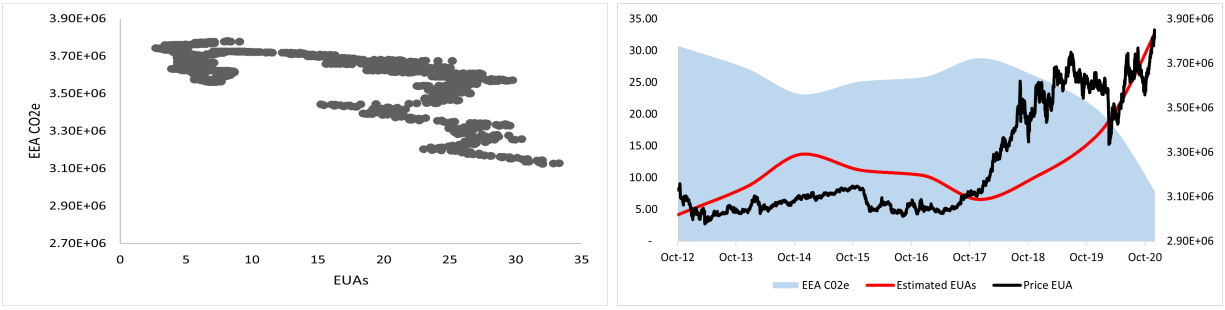

Figure 3.9: Historical vs Estimated EUA prices Historical interpolated CO2 emissions

data points, obtaining a better linear regression. This feature heavily affects the estimation due to its less precision but we consider it still significant since our interest is in the long mean pattern which can be identified through yearly data. For the sake of completeness we present in Figure 3.9 both the scatter plot between EUAs price and interpolated CO_2e together with their historical paths and estimated values. It is worth notice that the the estimation doesn't seem to be heavily affected by low precision since the estimated path dynamic looks like following the EUAs spot prices and it is diametrically opposite to the CO_2e ones. Coming to the goodness of fit of the model, both parameters are 1% statistically significant and the R^2 is quite high for a sole estimator (0.65).
The results are presented in Table 3.10 together with the graphical plots showed in Figure 3.10 which are quite identical to CO_2e ones.

Dates	SSP5-8.5	SSP3-7.0	SSP2-4.5	SSP1-2.6	SSP1-1.9	EEA WEM	EEA WAM
2022-12-31	88.75	92.03	96.59	97.88	97.99	97.74	102.12
2023-12-31	80.04	86.54	95.49	98.30	98.70	98.40	104.25
2024-12-31	71.57	81.25	94.45	98.98	99.87	99.17	106.48
2025-12-31	63.38	76.19	93.46	99.92	101.47	100.30	109.13

Table 3.10: EEA and IPCC-derived Scenarios for EUAs prices

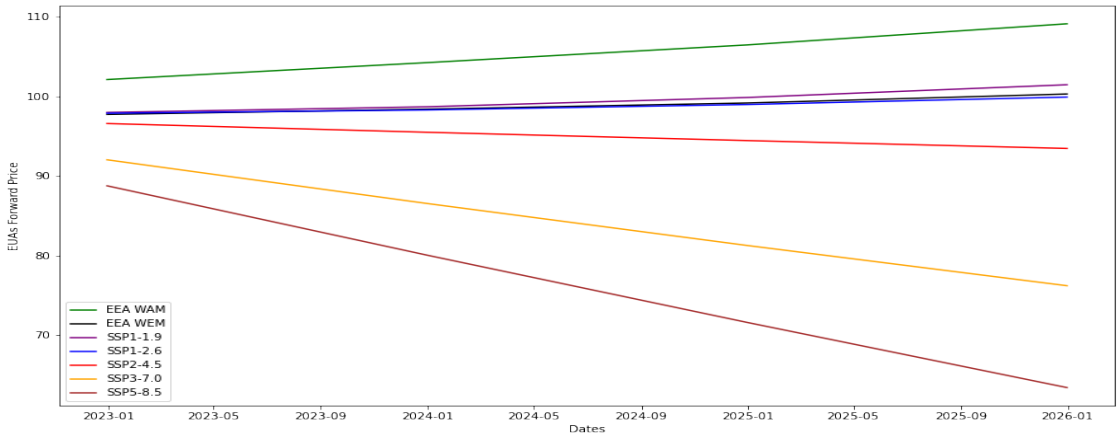

Figure 3.10: EEA and IPCC-derived Scenarios for EUAs prices

Scenario	Mean Term
SSP5-8.5	0.001696
SSP3-7.0	0.001916
SSP2-4.5	0.002191
SSP1-2.6	0.002272
SSP1-1.9	0.002283
EEA WEM	0.002270
EEA WAM	0.002462

Table 3.11: New deterministic term for different EUAs Scenarios

The final step is the transformation of the mean term μ for every different scenario presented above. The method utilize as input values the previously estimated parameters for the GBM and the EUAs forecast-ed values in dates 2022/12/31, 2023/12/31, 2024/12/31, 2025/12/31. Taking every EUA price at a certain maturity we can solve the Formula 3.7 for the expected EUA future price in terms of μ and then compute the mean among results from the same scenario. The final formula is presented below:

$$\mu_j = \frac{1}{n} \sum_{i=2022}^{2025} \Big[\Big(\frac{1}{\Delta t_i} \Big) \Big(\ln \Big(\frac{EUA(j)_{t+\Delta t_i}}{EUA_t} \Big) - (\sigma\lambda)\Delta t_i \Big) \Big] \quad \forall j \in Scenarios \tag{3.9}$$

Where Δt is the difference in terms of year fraction between the day t, equal to 2022/10/01, and the maturity dates listed before, n is the total number of future data. The formula inside the summation is the inverse of 3.7 where the unknown variable is μ and not $f(EUA_{t+\Delta t})$. The final outputs are showed in Table 3.11.
We won't bring μ for the case of the EEA WEM scenario to the Monte Carlo simulation phase since it is identical to the best twos of IPCC forecast but we keep the EEA WAM μ in order to see what could happen to the value of the contract if the market goes to EUAs values similar to the ones assumed in case of the best CO_2 emissions scenario for European Union.

3.3 Copula Calibration

As already stated in the Theoretical part, Copula functions are employed to model the dependence structure between electricity and EU allowances prices, since the plain bivariate normal distribution couldn't be assumed to fit the processes. In particular, the Henze-Zirkler multivariate normality test is deeply refused for different periods (2016-19, 2016-22, 2021-22) and frequency data (daily and weekly). The decision is to assess the fit of Archemedean copulas, under the hypothesis that our data fulfill properties of that family.

The sample selected to calibrate Copulas and analyze their goodness of fit goes from January 2021 to September 2022 since is the nearest period of time and we can assume a similar future dependence between the two underlyings. Given that, we estimate the distribution parameter θ for Frank, Clayton and Gumbel copulas relying on the sample Kendall Tau. This is possible due to the analytical formulas extracted from the result of the following Theorem cited by [38] and presented below.

Theorem 3.3.1 *Let X, Y be random variables with joint distribution of the form:*

$$C(x, y) = \phi^{-1}\{\phi(x) + \phi(y)\}$$

Then:

$$\tau = 4 \int_0^1 \frac{\phi(t)}{\phi'(t)} dt + 1 \tag{3.10}$$

From equation 3.10 and through integration integration by parts, it is possible recall the Kendall Distribution Function for the given copula; it incorporates the parameter θ that is derived from it.

The Kendal Tau (τ) is a dependence measure that forms the "Rank Correlations" familiy together with the Spearman ρ. They are computed on ranks and so depict monotonic relationships, differentiating them from the linear relation incorporated in the Pearson p. The latter is more influenced by observations in distribution tails, since they affect the shape of its linear trend, meanwhile the Kendall τ measures the monotonic trend, and considers every observation with the same relative weight in the definition of its value. The definition is the following:

Proposition 3.3.1 *Consider a pair of the two random variables for a given index as a single observation (x_i, y_i). Then consider two pairs defined as (x_i, y_i) and (x_j, y_j). Their relation can be identified in three cases:*

- *Concordant: when $x_i > x_j$ and $y_i > y_j$;*
- *Discordant: when either ($x_i > x_j$ and $y_i < y_j$) or ($x_i < x_j$ and $y_i > y_j$;);*
- *Nothing: when one of the two random variables presents equal values ($x_i = x_j$ or $y_i = y_J$).*

Then the Kendall τ values is defined looking at the relation among all observed pairs and computing:

$$\tau = \frac{(\#\ of\ Concordant\ pairs) - (\#\ of\ Discordant\ pairs)}{\#\ of\ total\ pairs} \tag{3.11}$$

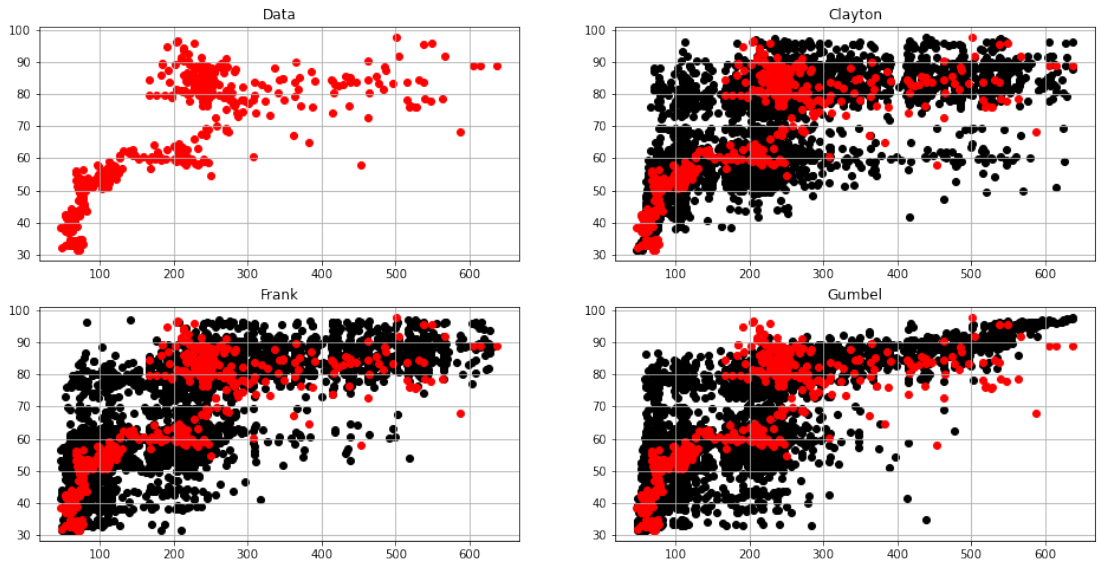

Figure 3.11: Sample Data (red) and simulated observations from the Copula Functions (2021-22)

It takes values between $[-1, 1]$ and it results equal to 0 in the case of independent random variables, -1 in case of countermonotonic and 1 for comonotonic ones.

Coming back to our estimation, from equation 3.10, utilizing Kendall Tau Distribution and analytical formulas in Proposition 2.5.2 and Table 2.1, it is possible derive equations in Table 3.13, which we utilized recursively to estimate θ starting from sample statics of Table 3.12.

The methods employed to assess which is the best Copula class to fit our data are two, either non and pseudo-parametric:

- Graphical analysis
- Root Mean Square Error Measure

The first graphical method, given the parameters θ for each single class given in Table 3.13, consists in the simulation of a random sample formed by bivariate observations generated from the estimated Copula parameter, and then, it is compared graphically with our real sample (2021-22). This permits to assess which plot has the better shapes and overlap as shown in Figure 3.11.

Pearson ρ	0.76
Kendal τ	0.64
Spearman ρ	0.83

Table 3.12: Dependence Statistics for Energy and EUAs daily spot prices (2021-22)

	τ	$\hat{\theta}$
Clayton	$\frac{\theta}{\theta+2}$	3.56
Frank	$1-\frac{4}{\theta}[1-D_1(\theta)]$	9.13
Gumbel	$\frac{\theta-1}{\theta}$	2.78

Where D is the Debye function of the form: $D_1(\theta) = \int_0^\theta \frac{t}{\theta(e^t-1)}dt$

Table 3.13: τ Formulas and Theta Estimation for Copula functions (2021-22)

	Clayton	Gumbel	Frank
RMSE	0.021	0.041	0.032

Table 3.14: Estimation RMSE for Archimedean Copula functions (2021-22)

The pseudo parametric method is linked to the computation of Root Mean Squares Error Measure between the historical empirical Copula function and the parametric one. In details, we compute a Copula estimation based on parameter θ on our sample data trasformed from X and Y to their empirical CDF $U1 = F_1(X)$ and $U2 = F_2(Y)$. The latters, of which we don't know the exact distribution family of belonging, are derived in the most general way, following empirical formula [25]:

$$F(t) = \frac{\sum_{j=1}^{N} 1_{\{x_j \leq t\}}}{N+1}$$

Then $U1$ and $U2$ time series are inserted in the copula distribution to derive its value for each sample pair $u1, u2$:

$$C(u1, u2) = C(F_1(x_j), F_2(y_j)) \quad for j \ = 1, ...n \tag{3.12}$$

In such way, it is possible reach the parametric estimation that should be compared with an empirical one explained hereafter.

The empirical join probability distribution, for a general pair observation x_i, y_i, is derived in the most general way, for the same reason cited before. The formula is presented below considering N as the number of total pair observations.

$$F(x_i,\ y_i) = \frac{\sum_{j=1}^{N} 1_{\{x_j \leq x_i\ ,\ y_j \leq y_i\}}}{N+1} \tag{3.13}$$

Lastly we are ready to compare the estimations and assess the goodness of fit, applying equations 3.12 and 3.13 to historical observation $\{x_i, y_i\}$ for $i = 0, ..., N$, and computing the RMSE measure.

Looking at Figure 3.11 and Table 3.14 , both methods show evidently that the best model is the Clayton family for its tiny lower-left tail. The plots and RMSE are showed above.

3.4 Least Squares Monte Carlo Method

In this section we apply the Monte Carlo simulation utilizing the model parameters estimated in the past sections to forecast possible EUAs and energy price paths. Then the Least Squares method of [32] is applied to the simulated paths to extract a unique price for our swing contract utilizing as final payoff the Formula 2.27. As represented below, the price is dependent from many parameters like the number of exercise options, the EUAs denominator D_{EUA} and the delivery period T. All these different factors will be analyzed to assess if the method is consistent with theory or not.

Monte Carlo Simulation

The first step, the MC simulation, is constructed starting from the date of 1^{st} October 2022 to the 31^{th} October 2024. We decide to take more than two years to permit to EUAs scenario-based forecasts to differentiate from each others since at the beginning they are tight because they starts from the same value. The starting EUAs price A_0 is fixed at 88 € and the PUN electricity price to 250 €, while the starting IPCC-derived scenario is the SSP2-4.5 since it is the medium one.

For sake of robustness we utilize 10000 different random paths for which we can assume independence one from the other as requested in these cases. The generation of the two $[0, 1]$ uniform numbers utilized for the derivation of the two Brownian Motion terms is undertaken employing the Clayton Copula formulas and the previously estimated θ parameter. For what concerns the Poisson process and the Gaussian one that form the Jump part, following the work of [49], we assume them independent from both the previously presented processes, meaning we can generate their uniform numbers in different moment. For sake of comparison we utilize the same Copulas random numbers to construct no-jump and jump energy price simulations.

The two different results are presented in the Appendix through Figures 5.1,5.2,5.3 and 5.4, where the total interval is showed together with a narrow one that concerns the last month, since we consider it the default delivery period for the options' exercise. The showed plots refer to the average path and for this reason jumps and other irregularities aren't visible for the energy price. In their comparison we should focus only on deseasonalized electricity part since EUAs and seasonal parts are equal. In particular the Ornstein-Uhlenbeck part fluctuates around zero as expected since the long term average κ was discovered to be insignificant in the calibration procedure. As can be seen, the seasonal part is heavily significant here, impacting the final swing price due to its weekly trend, and it may affect also the following estimation. This couldn't be already excluded since it is the first time that in literature seasonality is incorporated in the swing option price determination.
Lastly, the deseasonalized part is lower in the jump case rather than the other, this is mainly due to the negative Gaussian parameter μ_j that means the jumps are slightly more frequent downwards then upwards. The jump incorporation consequences couldn't be investigated here but only at the end of the already mentioned Least Squares method presented below.

Least Squares Estimation Method

The LS estimation method has its direct origin from the method utilized in [32]. To summarize the procedure, starting from the V-number of simulations regarding the two underlying assets for delivery period days T, we consider every time step going backward from the last day of the contract. At each step i we compute V different payoffs given by the formula $\max(S_i - K)$ for strike price K and forward energy price S_i, and by the EUAs multiplication factor A_i/D_{EUA}. We set D_{EUA} equal to 88 € by default since is also the starting EUAs price while the strike varies among our main estimations to permit us to assess the price monotonicity in terms of K. The default delivery period goes from 01/10/2024 to 31/10/2024 since a month is considered statistically significant and in line with the usual energy forward contracts.

In case of swing option with no dependent relation between the number of option rights exercised and the recovery period to wait until be allowed to exercise a new option, the number of options rights per date is inelastic to other parameters, meaning that if the quanto option is in-the-money the number of exercised options will be always the maximum allowed. For this reason, since we aren't interested in the number of exercises-time to recovery relation, we set the maximum number equal to 1 and minimum recovery time of one day.

Starting from the final time step $i = T$, the continuation value, stated in Formula 2.7, is equal to zero since its value is utilized as dependent variable for every Least Squares estimation. We have as many LS procedures as total exercise options N across the delivery period since every value function defined for a certain number of exercise options n depends by the continuation values Q_t^n and Q_t^{n-1} following the Formula 2.6. The LS estimation is implemented through OLS and GLS utilizing a family of basis function on the state variable as regressors, $F(x)$, where the family of polynomials should be orthogonal to fulfill the convergence of LS method. For this reason the two family employed are the Laugerre and Hermite functions presented below.

$$\text{Laguerre polynomial of } m \text{ degree: } \; L_m(x) = \frac{e^x}{m!}\frac{d^m}{dx^m}(X^m e^{-x}) \tag{3.14}$$

Where m represents the number of polynomials taken as basis function for which we approximate the series $\sum_{i=0}^{\infty}$. In [26] it is utilized a weighted term to be multiplied to each L_m of the form $e^{\frac{x}{2}}$ but we prove it isn't significant for the fit to our data and so it is discarded. On the other hand we multiply it for the similar weight function e^{-x} which permits us to assume its orthogonality over the interval $[0, \infty]$ as stated in [1].
The same analysis can be done for the Hermite family stated below.

$$\text{Hermite polynomial of order } m\text{: } \; L_m(x) = (-1)^m e^{x^2}\frac{d^m}{dx^m}e^{-x^2} \tag{3.15}$$

Here we multiply every polynomial by the weight function e^{-x^2} to assume orthogonality on the interval $[-\infty, \infty]$ as reported by [1].

The LS estimation can be conducted for a given state variable x_t and basis function family as independent variables $F(x_t)$ and dependent one Q_t^n. Then, the resulting coefficients are employed to fit the same dependent variables on all the sample path leading to a different $E^v[V_t^{n*}|x_t]$ for every path $v = \{1, ..., V\}$. Once this is completed, the Formula 2.6 is applied

to find the current value function V_i^{n*} for every $n = \{1, ...N\}$.
In order to pass to the next step we discount the value function for a discounting factor of the form $e^{-DF \cdot \Delta t}$ where DF is assumed to be the overnight interest rate named Ester, kept fixed for the entire estimation to a value of 0.015 based on ECB forecasts[8]; while Δt is equal to 1 when passing from a time step to another. Once we pass to next lower step, the discounted V_i^{n*} are utilized as new dependent variable for the next LS and so on.

We apply this method to a first MC simulation outcomes saving total RMSE, final swing price and estimation coefficients, then these latters are utilized in a second procedure where instead of estimating again the coefficients we utilize the ones already present on different regressors. In this way we find a new RMSE and swing price results that we called "robust" since it is a proof of the method convergence to a similar results.

Passing to the analysis of the estimation parameters, a central point is the selection of the state variable on which apply the polynomial family. [32] states how the presence in this estimation of exponential terms could lead to computational underflow for state values higher than 30, and recommends to normalize data to avoid numerical errors given by scaling problems. This is exactly what happens if the payoff Z_t or the price S_t are employed as state variable, resulting in high RMSE and the necessity to put non-negativity bounds to the continuation values to reach a sufficient but not always respected convergence. On the other hand, the result is quite good if the state variable Z_t is normalized dividing it for the strike price K as advised by [32]. Another important decision is the paths selection to estimate LS coefficients, since the literature suggests to consider only in-the-money paths in order to gain a better estimation. However, in our case the procedure results in a worse goodness of fit represented by the higher Robust RMSE, and a break in the monotonicity behavior of the swing price related to the strike one, as showed in Table 5.1 values against the ones of the Table 5.2, where all the paths were employed. For these reasons we decide to utilize all the paths in the following estimations.

Once that the state variable is agreed, the analysis passes to the correct selection of estimation method (OLS,GLS), polynomial family regressors (Laguerre, Hermite) and their corrisponding degree (3,4,5,6). Starting from the first couple of options, the results of the two LS methods are showed in Tables 5.3 and 5.2 that present almost equal values. Therefore, since the OLS estimation takes less time, the decision falls to utilize the latter one.

For what concerns the choice of the basis function family and its degree, [32] states how the number of independent variables should be proportional to the complexity of the problem, setting m to 3, while [26] sets it to 5 to ensure a better estimation. We assess all the possible outcomes (Tables 5.2, 5.4, 5.5, 5.6, 5.7, 5.8, 5.9 and 5.10) finding results quite similar where the swing price slightly increases with the number m. Since on one hand a degree of 3 seems a too low value for this problem, but, on the other hand, increasing m increases also the RMSE, we select $m = 4$ which is also the medium value between the ones

[8]The selection of a value of 0.015 for the Ester IR is roughly approximated utilizing ECB actual levels and forecast for Ester and Euribor 3 months IRs. In particular, in 2022 they are equal on average to 0.65% (Ester) and to 1.1% (Euribor 3M), while the forecast of the latter in 2024 amounts to 2.1%. We decide to apply the same delta to the Ester value going from 0.65% to almost 1.5%.

of papers utilized as reference literature.

Lastly, the polynomial family identified for the following analysis is the Laguerre since it is the one with lower RMSE values for equal m.

The next phase regards the assessment of the method's goodness of fit through the investigation of the swing price relation with the remaining parameters. We investigate if the price fluctuates with the changes in:

- EUAs multiplication factor D_{EUA},
- total number of exercise options N,
- length of the delivery period T.

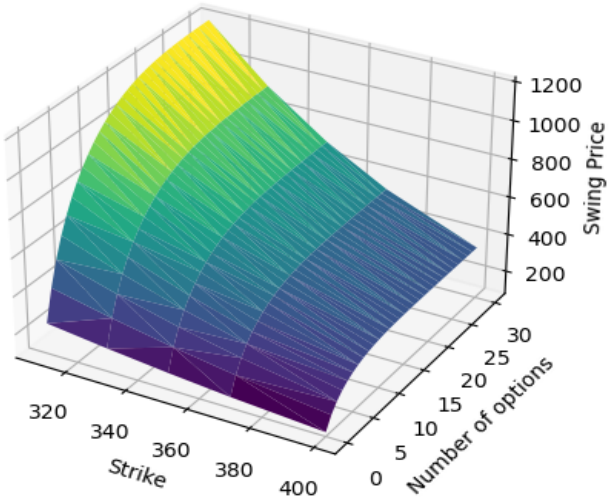

Figure 3.12: Swing Price in function of N_{ex} and Strike K

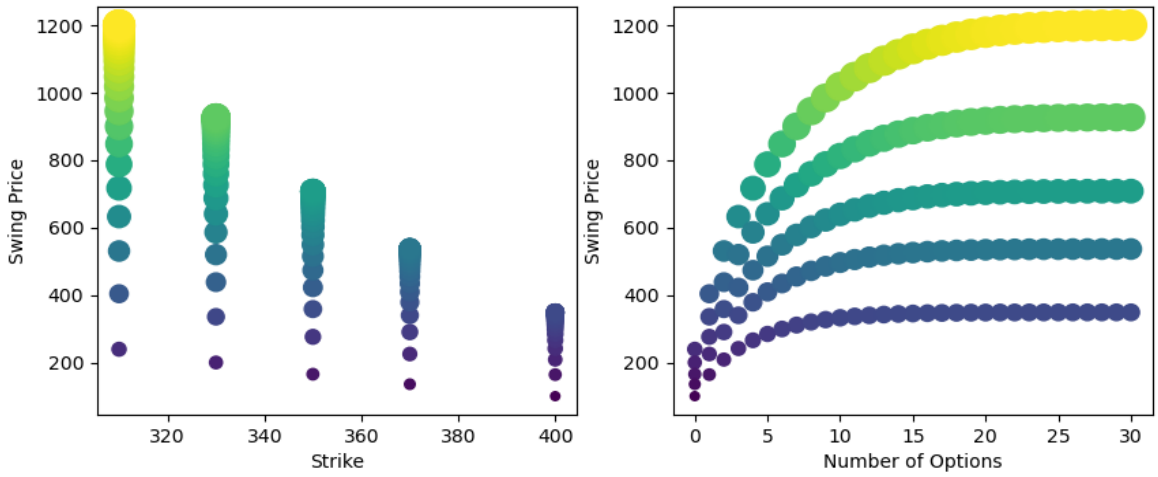

Figure 3.13: Swing Price in function of N_{ex} and Strike K respectively

The corresponding results are reported in Tables 5.12, 5.13 and 5.14 in Appendix with the expected monotonic path that can be verified for every relationship.

In particular,in Figure 3.12 the price of the contract is presented in function of strike and total number of exercise options N_{ex}. If we focus on the swing price-strike relation, as suggested by past presented tables, it could be assumed quite linear since the range bounds of the price looks linearly proportional to the strike price, as shown in Figure 3.13. For what concerns N_{ex}, the relation with price isn't linear but convex meaning the the price increases at an higher slope in the first options while it becomes almost flat in the last ones. This can be mainly due to the time value of money which permits to the contract holder to decide when exercise its options during all the default delivery period of 31 days. Higher is the option's in-the-moneyness, higher is its value due to the fact that there will be more opportunities to exercise the right. The curve is almost flat at the end mainly because the presence of weekends make the last options quite useless since in those days it is very unlikely to exercise due to the far lower energy value. As expected, the monotonicity condition is always fulfilled since the swing price for a given strike is always distinguishable from the ones with higher and lower strike.

For what concerns the total number of days T that forms the delivery period, the previous analysis is applied again. In Figures 3.14 and 3.15 can be seen the relation between the swing price, strike and T, where in the two dimensions plots it is possible notice a more linear trend for the T-swing price relation, even though it remains convex. This property could be caused by the first 5 time steps where T affects heavily the price since the number of available options diminishes consequently in any case since the maximum number of exercise at each step is equal to one. Lastly, a curious characteristic of the 2D plot of price against T shows us a lost in monotonicity within the same strike estimations. This should not happen since an additional day is always a benefit for the contract buyer, this unusual behaviour could be due to the presence of weekends. When the weekend coincides with the last day of delivery, the continuation values at time $T-1$ will be lower than usual and if the days remained are quite limited the final price could be affected by it resulting in a lower value.

Another indicator of the presence of the time value of money is evident in the same plot: the difference between two points for a different strike price increases with the increase of the delivery period[9]. Indeed we must remember the definition of time value, which is basically the premium the buyer is willing to pay for the probability that the option(s) will increase its value before the final expiry date.
It is worth notice that the swing price for a single option with a $T = 31$ is much more higher than the price for $T = 1$ and $N_{ex} = 5$, this is the clear evidence of the importance of the available time since in both cases we can exercise only one option but in the first we have 31 days to select the time while in the other only one.

[9]The visual proof is weakened by the fact that the points' size increases with the increase of the swing price.

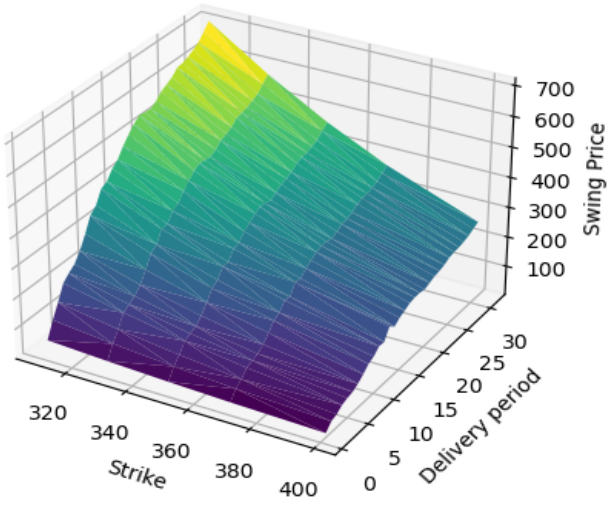

Figure 3.14: Swing Price in function of T and Strike K

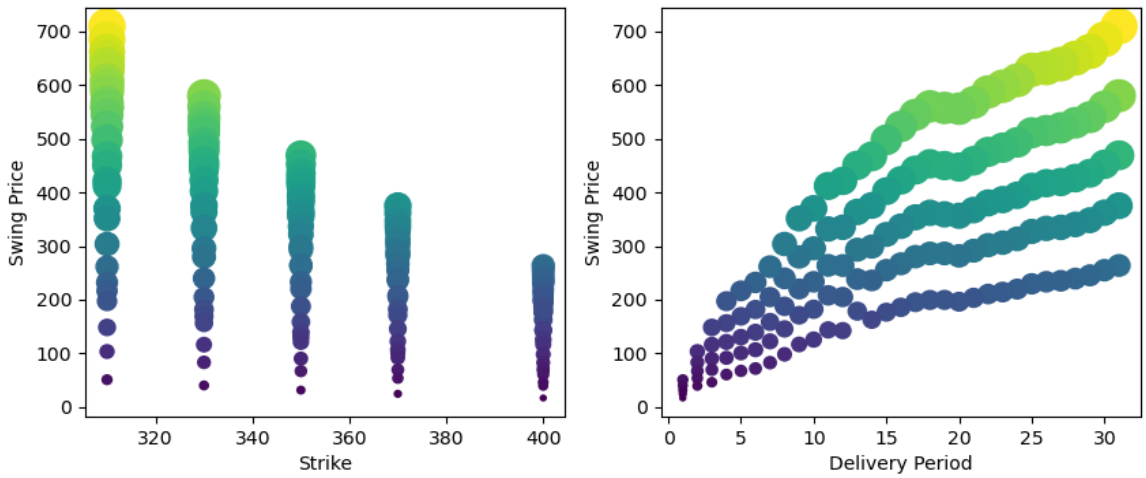

Figure 3.15: Swing Price in function of T and Strike K respectively

The next analysis regards the presence of differences in the swing contract price with and without Jump part incorporated in the energy price dynamic. In Table 5.11 are present results that can be compared with Table 5.4. As expected, (normal and robust) swing prices are much higher for the Jump-based estimation together with the RMSE values. This is probably due to the higher volatility of the random simulations which leads more paths to reach higher values that increase the swing price. The presence of a negative mean term μ for the size of the jump term doesn't nullify this characteristic, while certainly the jump part brings higher differences in lower and greater energy prices leading to an increase in RMSE. To conclude, it is a interesting finding since none of the papers in the literature apply the Monte Carlo Least Squares estimation of the swing price to a jump-based energy model. The result proves what it is deducible by theory: an additional randomness source brings

higher premiums due to higher uncertainty that makes the hedging contract more valuable compared to the plain vanilla one. Moreover, we should ask our-selves which price is the correct one since the nature and history of energy price suggest us that jumps are present and quite frequent in periods of market turmoil.

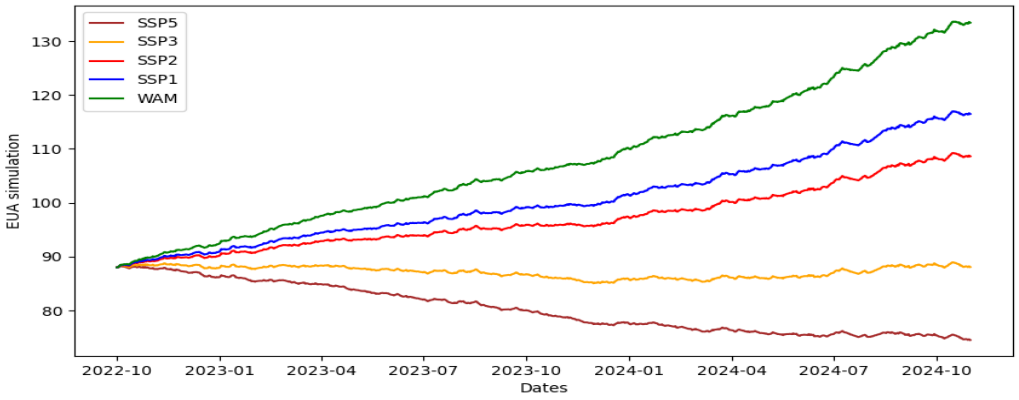

Figure 3.16: Scenario-based EUAs average price (2022-24)

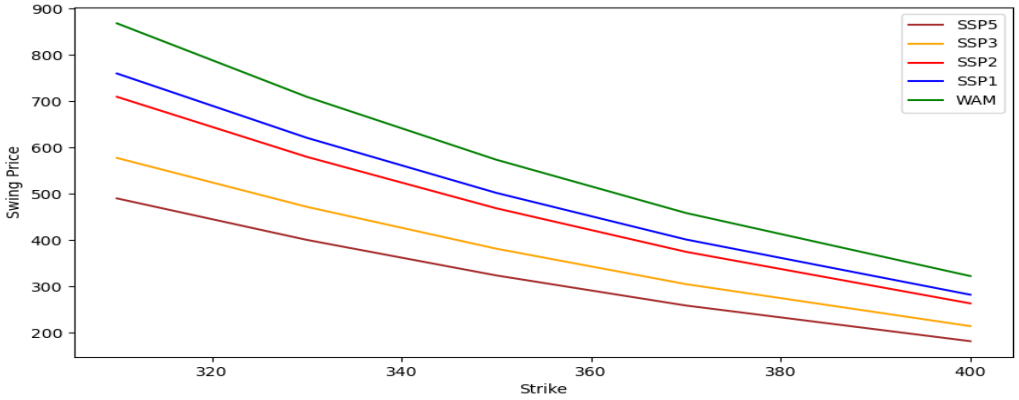

Figure 3.17: Swing Price in function of K and Scenario-based EUAs simulation

The last point to be assessed is the swing price sensitivity to the EU Allowances scenarios constructed in the last section. To compare them in the most reliable way, we utilize the same copula function uniform numbers changing only the mean term μ inside the Monte Carlo simulation. The resulting average EUAs and swing prices are shown in Figures 3.16 and 3.17. In the first one it could be noticed that paths are far from the others with the passing of time, while in the 3.17 it is worth see that the distance between swing prices decreases with the increase of the strike price, meaning that, as expected, the multiplicative term become less significant along with the size decrease of the energy payoff.
These final results permit us to assume a certain price movement in case of different future scenarios, leaving the door open to investigate the impact that this instrument can have on a company subject to ETS in different scenario-based cases. This analysis will be undertaken in the next section.

3.5 Practical scenario-based case

In this section it is illustrated a practical example to show how and under which conditions the swing contract on a Quanto option is useful for a company under the European Trading Scheme.
The decision was to select a real company in order to give more reality to the implementation. For this reason we consider one of the most famous and controversial polluters in Italy that ranks at the second place for the number of CO^2 emissions actioned to EU in 2021 with a total amount of $6,429,669$ [40]. This data regards the factory conglomerate named "Ilva" in Taranto that belongs to the firm Arcelor Mittal Italia S.p.A., and it is specialized in the steel refinering and production.

From past data on energy consumption and CO^2 emissions, we could roughly estimate the energy utilization in October 2024 for a total of 324.85 MWh [41]. To do so, we assume that only the 50% of costs linked to the required demand is affected by the prices fluctuations since it is impossible assume that a company of that size hasn't fixed-price contracts in place for the energy supply. Additional assumptions to run this analysis are many, both for PUN and EUAs prices: the retention of a constant daily energy price for the entire 24 hours, the decision to consider the EU emission certificates required in 2024 equal to the number auctioned in 2021, and the equal split of EUAs demand in the 12 months setting the number to be bought in October equal to 437,199.17 €. Since their emission auctions are reported by European Union we could assume the Ilva isn't exempted to pay this certificates amount but we could assume that a 30% will be provided by Italian government for free due to its central role in that region and its financial issues of past years. Furthermore, for sake of simplicity, we assume the company to be and operates 24/24 hours because it is simple but also realistic since costs could be high to stop and re-start its processes. Another parameter to be set is the contract size in term of MWh, for which we select a size of 324.85 MWh, instead of 1 MWh as of the previous section, to be in line with the required hourly demand. Passing to the strike selection we set it to 350 € since higher strikes could be quite unusual given that in the past six years only around 10% of prices were higher than the 16% of the mean of 15^{th}-days neighbour prices, therefore 350 € is a realistic price since it is higher only 16% of the weekly mean price.

Passing to the possible scenarios taken into consideration, we compare the Quanto-based swing contract hedging strategy with other two. The first concerns the possibility to not sign any swing contract, keeping a zero hedge position, while the second one is linked to the plain vanilla swing contract on a single call option on energy price, without take into consideration the EUAs behavior. Together with that, we consider three different EUAs scenarios presented in last chapter: the worst-in-case for the CO^2e increase (SSP5-8.5), the one in the middle for which we utilize the swing contracts prices (SSP2-4.5) and the best in case one linked to the increase of EUAs prices (WAM). The third scenario dimension is linked to energy prices on which is based the exercise decision and option payoff. In particular, we identify three different scenarios which can show a clear image on the possible outcomes:

- Energy Price Scenario 1: it is linked to the situation where none of the prices in the

delivery period (October 2024) permits to the options holder to exercise them. We assume a constant price equal to the PUN average price within our simulations of last section. It is equal to 294 € on which is considered the constant value for all days on which the Ilva energy costs are computed.

- Energy Price Scenario 2: it regards the intermediate situation where only 3 days present a energy price higher than the strike of 350€. The average price in those days is assumed to be 375 € on which payoff and energy costs are computed.

- Energy Price Scenario 3: it is the best in case scenario for our swing contract holder since all 5 options can be exercised during the 31 days of delivery. The average price in those days is assumed to be equal to 420 €.

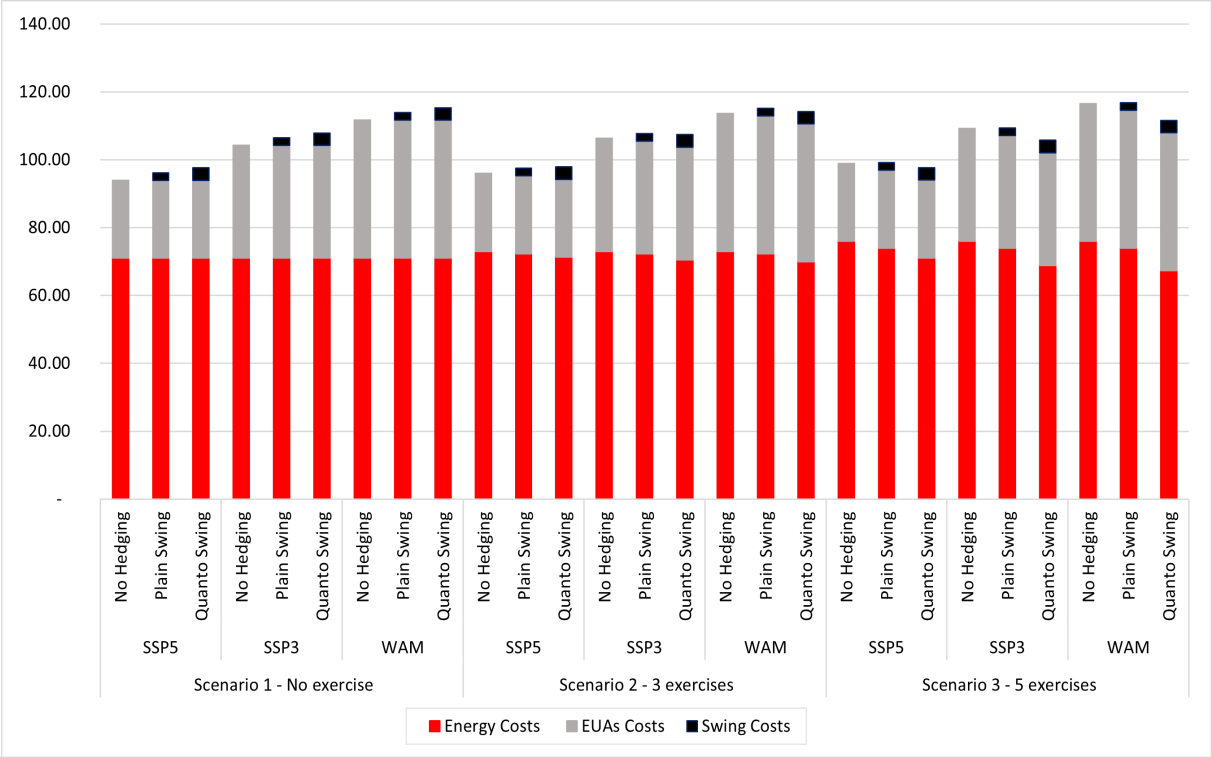

Figure 3.18: Ilva-based October-2024 Costs divided by cost type for different EUAs, Energy and Hedging Strategy Scenarios

From the Figure 3.18 we can derive many insights on the functioning of our swing contract. For sake of clarity we attach also the final Table 3.15, based on which the plot is constructed.
The first case to analyze is the Scenario 1, where no options can be exercised and of course the total costs are higher in cases when we subscribe contracts with a counter-party to hedge that risk. To summarize, in this scenario the passing from the worst EUAs scenario for our option payoff (SSP5) to the best one (WAM), turns things worse since costs levitate, due to higher EUAs price, without changing energy related and swing contract costs. In this situation the best strategy shouldn't be subscribe the contract in order to not incur in additional costs.

In the second energy scenario instead, three options of the swing contract are exercised against a total of five. This didn't permits our swing contract strategy to a cost decrease in case of the SSP5 EUAs scenario but in the SSP3 and WAM cases yes. The quanto based strategy permits to have a lower total cost with respect the strategy with only a plain swing contract even though the "No hedging" strategy remains the best.

In the last scenario (number 3) the energy prices during the month of October 2024 permits to the company to exercise five options with an higher payoff given also by the multiplicative factor. Here, the best strategy is to subscribe the swing contract on quanto option since the price became lower from the the previous EUAs scenario for every EUAs scenario as expected in situation of extreme upwards spikes.

The example gives us the possibility to look at the utility of our derivative instrument in different situations. The results are in line with our expectations since in case of lower energy and EUAs prices the contract isn't powerful, leading only to higher costs, while for higher price levels it raises in importance since we can mitigate both the increases in terms of cost reduction. In Table 3.15 the contract payoff isn't showed since it is subtracted only to the Energy costs during its construction even it is in the middle between energy and EUAs hedging. To conclude, we didn't provide insights on the probability of occurrence of this set of scenarios since it goes beyond the scope of this work and it can be an open point for further analysis.

Energy Scenarios	EUAs Scenarios	Hedging Strategy	Energy Cost	EUAs Cost	Swing Costs	Total Costs
Scenario 1 - No exercise	SSP5	No Hedging	71.06	22.96	0.00	94.02
		Plain Swing	71.06	22.96	2.18	96.20
		Quanto Swing	71.06	22.96	3.66	97.67
	SSP3	No Hedging	71.06	33.22	0.00	104.28
		Plain Swing	71.06	33.22	2.18	106.46
		Quanto Swing	71.06	33.22	3.66	107.94
	WAM	No Hedging	71.06	40.64	0.00	111.70
		Plain Swing	71.06	40.64	2.18	113.88
		Quanto Swing	71.06	40.64	3.66	115.36
Scenario 2 - 3 exercises	SSP5	No Hedging	73.07	22.96	0.00	96.03
		Plain Swing	72.37	22.96	2.18	97.51
		Quanto Swing	71.31	22.96	3.66	97.93
	SSP3	No Hedging	73.07	33.22	0.00	106.29
		Plain Swing	72.37	33.22	2.18	107.77
		Quanto Swing	70.53	33.22	3.66	107.41
	WAM	No Hedging	73.07	40.64	0.00	113.71
		Plain Swing	72.37	40.64	2.18	115.19
		Quanto Swing	69.96	40.64	3.66	114.26
Scenario 3 - 5 exercises	SSP5	No Hedging	75.97	22.96	0.00	98.93
		Plain Swing	74.02	22.96	2.18	99.16
		Quanto Swing	71.09	22.96	3.66	97.71
	SSP3	No Hedging	75.97	33.22	0.00	109.19
		Plain Swing	74.02	33.22	2.18	109.42
		Quanto Swing	68.91	33.22	3.66	105.80
	WAM	No Hedging	75.97	40.64	0.00	116.61
		Plain Swing	74.02	40.64	2.18	116.84
		Quanto Swing	67.34	40.64	3.66	111.64

Table 3.15: Ilva-based October-2024 Costs divided by cost type for different EUAs, Energy and Hedging Strategy Scenarios

Chapter 4

Conclusion

This thesis attempted to analyze from different points of view a swing contract on a Quanto option for two different underlying assets: energy and EU CO^2 emission allowances. To do so, we firstly identified the best stochastic models for the two assets, calibrating the model on historical data from 2016 to 2019 and adding the market-risk-premium term in order to stay under the risk-neutral measure and be allowed to simulate forward prices without loss of consistency. After that the best copula function class is identified (the Clayton copula) and its parameter is estimated in order to employ it for the dependent simulation of energy and EUAs price paths. Then, the Monte Carlo simulation was undertaken to be able to apply the Longstaff and Schwartz estimation method for the determination of the swing contract initial price. Lastly the different parameters-based results are analyzed and a final scenario-based practical example is conducted to assess the contract's goodness of utilization in different possible situations.

With respect the utilized literature, the thesis presents some new additional features like the employment of a energy model that considers a yearly and weekly pattern, and the incorporation of a jump-based part. The latter isn't so significant probably because the historical data don't present a huge amount of spikes. Coming back to the insertion of weekly seasonality, it affects the final estimation since the property of monotonicity isn't always respected with the change of the delivery period T. In every other estimation the monotonicity is respected leaving the space to identify a powerful time value of money. For istance, the latter is verified clearly in the price difference between the swing option in the case of a delivery period of 31 days and only one possible exercise option and the lower price given by the swing characterized by 5 different options to be exercised in the delivery period of one day.

The final practical example allowed us to gain some insights on when and under which assumptions the swing contract on Quanto options is valuable for a company under ETS. As expected, it gains utility in case of high energy and EUAs prices, while it is useless if the energy doesn't present upper spikes and the transition risk (accounted by allowances price) doesn't increase in the next years. To summarized, every company should assess the cost-benefit trade-off, which could result even in the discard of the swing contract strategy due to the presence of costs not considered in this thesis or due to complexity that an instrument of this type can bring for a firm of the manufacturing industry.

The possible downsides of the approach utilized in this thesis are many. Firstly, the fall of the set of assumptions needed to utilized the LS method, as well as the not perfect goodness of fit of stochastic processes selected for the two underlying assets. Then, once that more suitable models are identified, even the Copula estimation can be conducted with a higher statistical level employing a pseudo-parametric estimation. Furthermore, the scenarios building procedure is based on a single linear regression between CO^2 emissions and the cubic spline interpolation of EUAs prices, which can be considered a quite weak method to validate it.

In the light of the last rows, additional researches on this theme would be beneficial. Firstly the same procedure can be applied to more recent data considering also the Covid-19 crisis or at least the last ETS 4^{th} phase finding a way to deal with the break of stationarity and normality for the energy dynamic. In that case the jump component should be more significant but it could lead to the fall of other assumptions.

Another possible starting point could be the investigation of the likelihood of occurrence of EUAs scenarios together with the ones presented in the final practical example, in order to assess the validity of this customized financial instrument.

The last interesting further research could be the incorporation of the EUAs value inside the OLS estimation employed for the derivation of the swing price. This will bring more complexity and its coherence should be previously assessed deeply, since we should remember that allowances price affects the quanto option payoff only in its multiplicative term, while the moneyness is linked only to the energy price.

Chapter 5

Appendix

MC Simulation Results

Figure 5.1: No-Jump full simulation

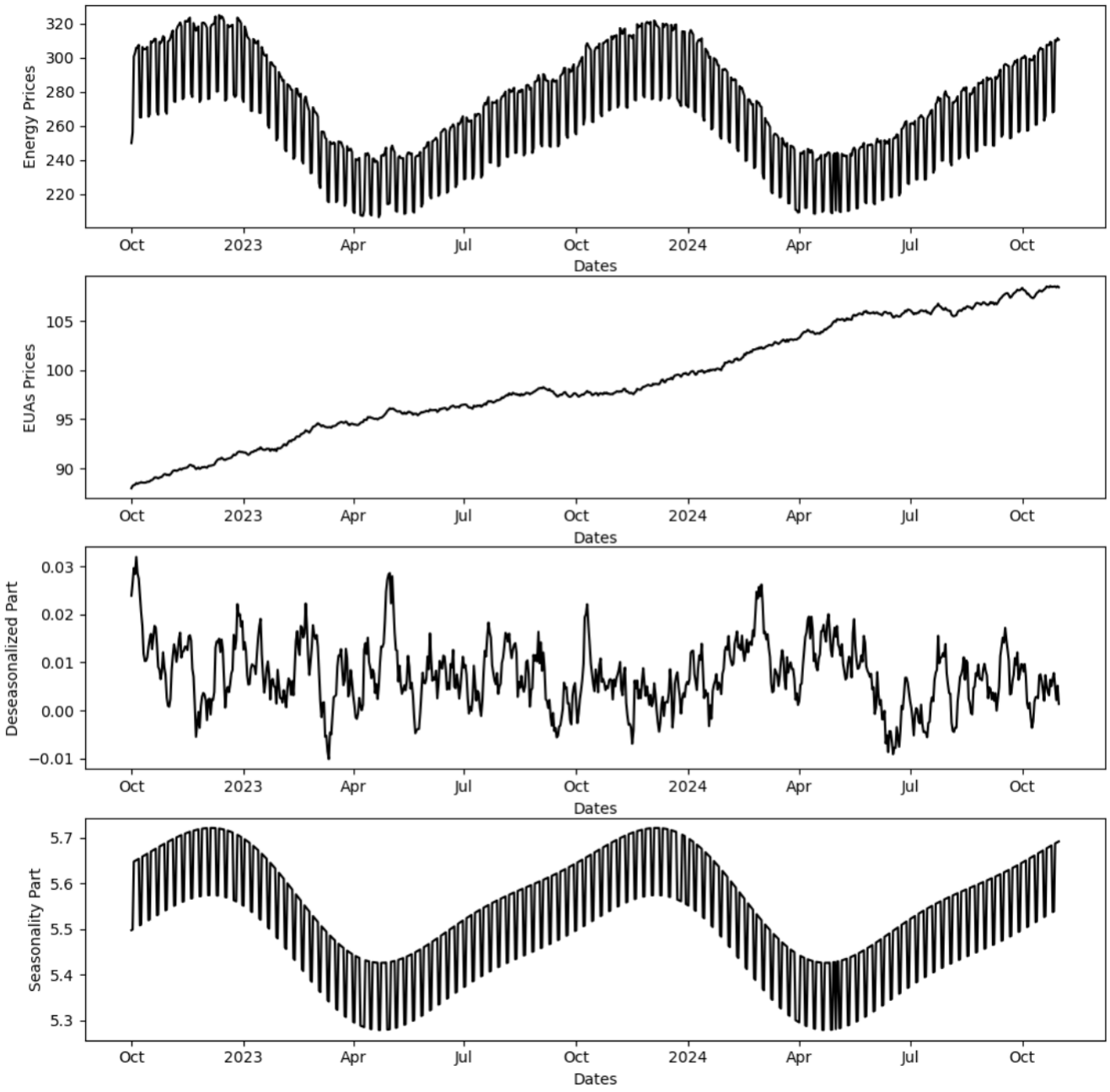

Figure 5.2: No-Jump delivery period simulation

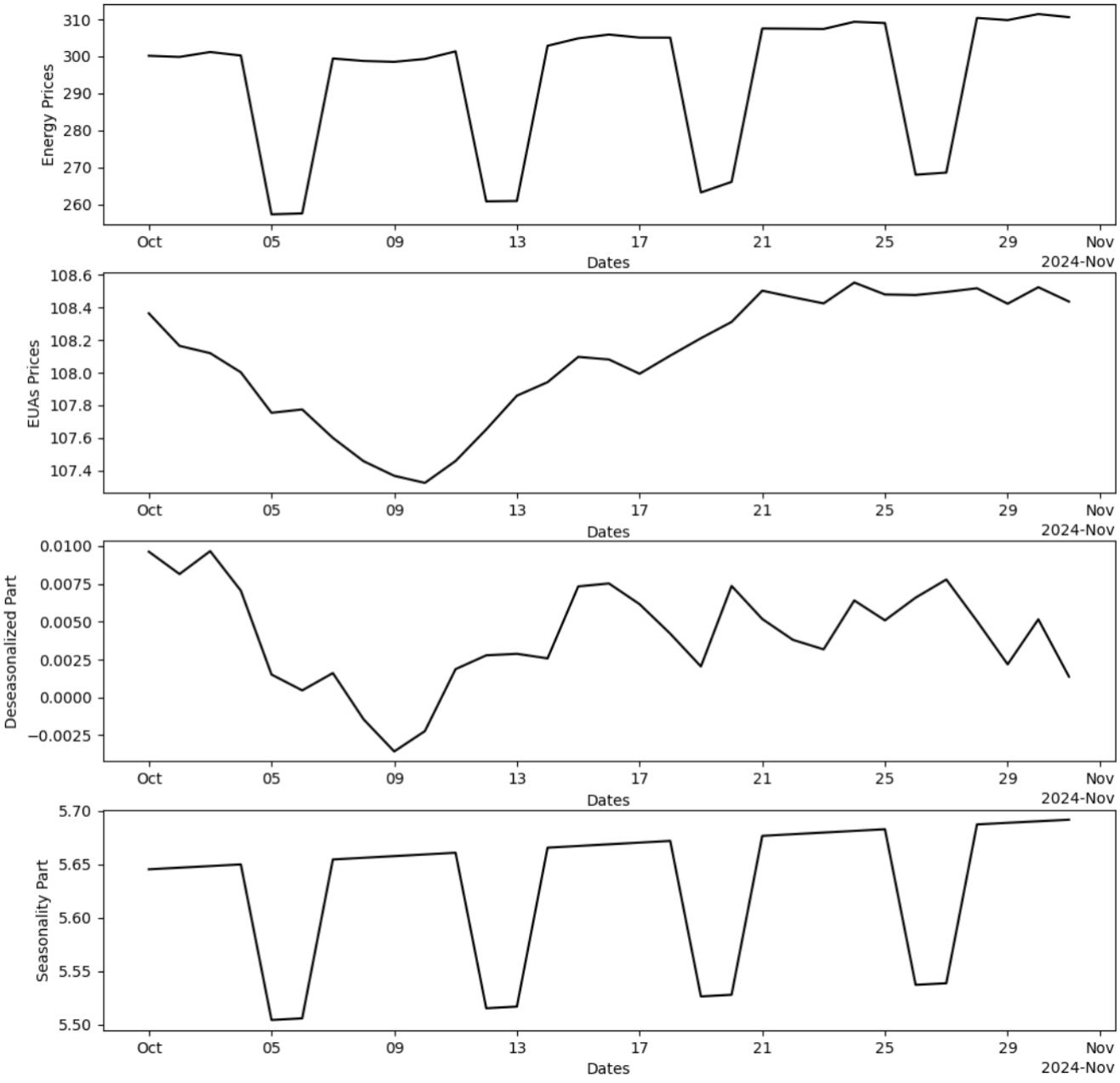

Figure 5.3: Jump full simulation

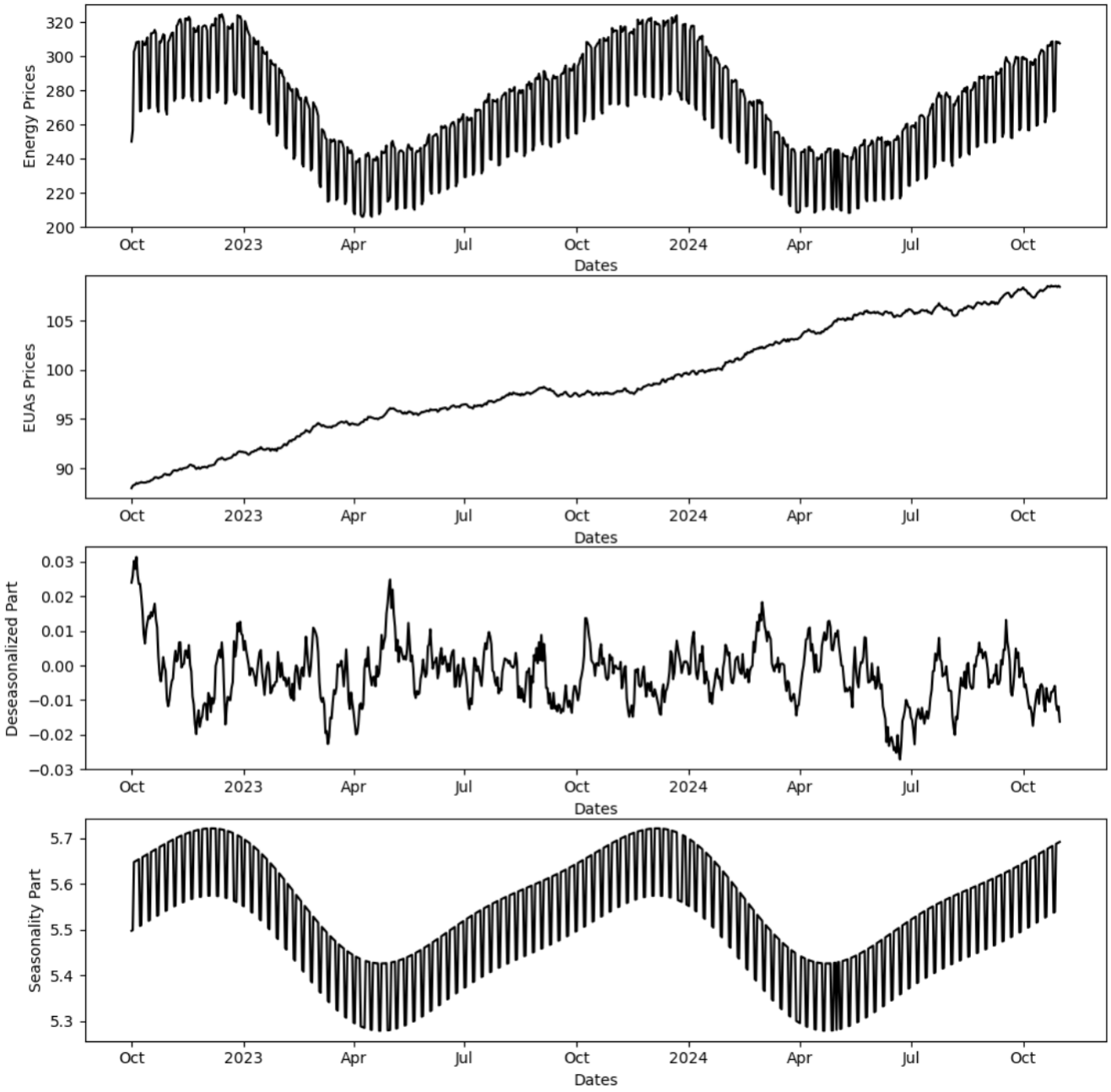

Figure 5.4: Jump delivery period simulation

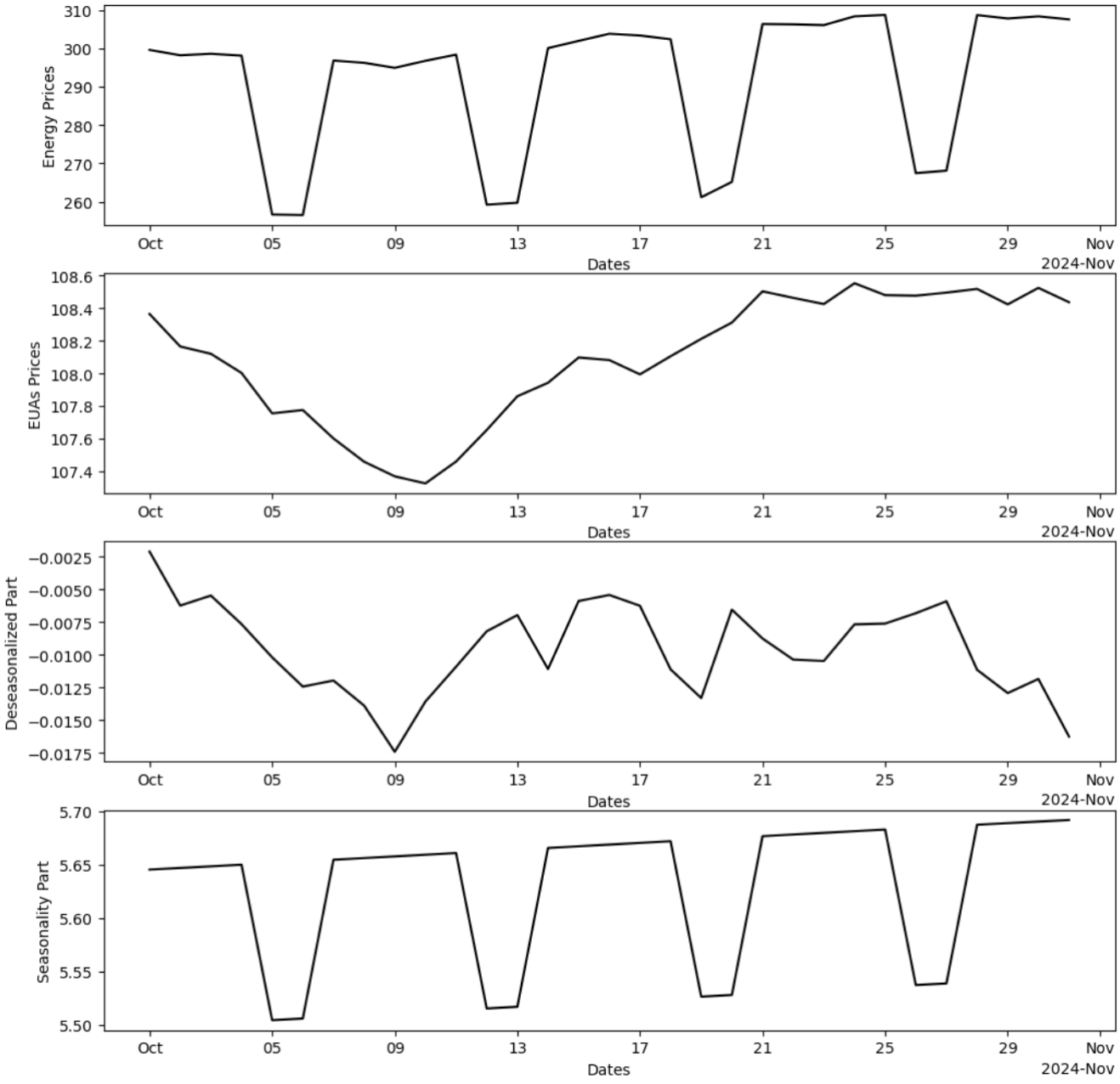

Least Squares Results

We group here the summary tables on the different Least Squares procedures applied to the same EUAs and electricity price simulations. The delivery period is 31 days. We change estimation parameters whose legend is stated below.

- D_{EUA}: EUAs price denominator to compute the multiplicator factor.
- LS: least squares method applied (i.e. OLS,GLS).
- $F(x)$: Basis function family applied to construct LS regressors (i.e Hermite, Laguerre).
- n: Degree of the polynomial utilized as basis function ($F(x)$).
- N_{EX}: number of exercise options.

- Scenario: title of the EUAs scenario which determines the deterministic μ term of its dynamic.
- S: strike price utilized during LS.

As mentioned in section 3.4, every table presents the total $RMSE$ and final swing price values for the two different estimation procedures. In the first one the parameters coefficients are estimated through the LS method while in the second the same coefficients are utilized to estimate the dependent variable variable at every step. Since this second procedure is utilized to assess the goodness of results, we call it "Robust".

Result for LS estimation on In-the-Money paths:

Table 5.1: $D_{\text{EUA}} = 88,\ LS = \text{GLS},\ F(x) = \text{Laguerre},\ n = 5,\ N_{ex} = 5,\ Scenario = \text{SSP2}$

Strike	310	330	350	370	400
Swing Price	1,341.47	1,278.55	1,210.42	1,247.69	1,334.66
RMSE	24,275.12	23,869.73	23,259.46	21,747.17	20,661.93
Robust Swing Price	1,334.21	1,270.48	1,201.84	1,238.90	1,326.55
Robust RMSE	19,425.78	18,866.07	18,646.96	19,592.74	23,275.87

Results for LS estimation on all paths:

Table 5.2: $D_{\text{EUA}} = 88,\ LS = \text{GLS},\ F(x) = \text{Laguerre},\ n = 5,\ N_{ex} = 5,\ Scenario = \text{SSP2}$

Strike	310	330	350	370	400
Swing Price	715.90	586.97	476.76	383.67	272.88
RMSE	18,996.03	17,124.32	15,326.19	13,597.95	11,206.83
Robust Swing Price	709.17	579.24	467.86	374.21	263.04
Robust RMSE	22,186.49	21,423.60	20,816.47	21,751.17	22,894.25

Table 5.3: $D_{\text{EUA}} = 88,\ LS = \text{OLS},\ F(x) = \text{Laguerre},\ n = 5,\ N_{ex} = 5,\ Scenario = \text{SSP2}$

Strike	310	330	350	370	400
Swing Price	715.90	586.97	476.76	383.67	272.88
RMSE	18,996.03	17,124.32	15,326.19	13,597.95	11,206.83
Robust Swing Price	709.17	579.24	467.86	374.21	263.04
Robust RMSE	22,186.49	21,423.60	20,816.47	21,751.17	22,894.25

Table 5.4: $D_{\text{EUA}} = 88,\ LS = \text{OLS},\ F(x) = \text{Laguerre},\ n = 3,\ N_{ex} = 3,\ Scenario = \text{SSP2}$

Strike	310	330	350	370	400
Swing Price	715.96	588.36	478.44	385.35	274.80
RMSE	19,054.36	17,138.28	15,310.55	13,571.23	11,166.67
Robust Swing Price	712.52	582.48	470.96	376.70	265.40
Robust RMSE	20,584.93	18,637.06	16,757.11	14,960.88	12,540.16

Table 5.7: $D_{\text{EUA}} = 88,\ LS = \text{OLS},\ F(x) = \text{Hermite},\ n = 3,\ N_{ex} = 5,\ Scenario = \text{SSP2}$

Strike	310	330	350	370	400
Swing Price	723.39	593.15	481.76	387.70	276.40
RMSE	18,912.08	17,056.31	15,259.54	13,540.64	11,146.76
Robust Swing Price	717.90	585.57	472.81	378.29	266.98
Robust RMSE	20,555.72	18,640.56	16,807.76	15,089.84	12,921.48

Table 5.8: $D_{\text{EUA}} = 88,\ LS = \text{OLS},\ F(x) = \text{Hermite},\ n = 4,\ N_{ex} = 5,\ Scenario = \text{SSP2}$

Strike	310	330	350	370	400
Swing Price	714.93	587.56	477.63	384.12	273.15
RMSE	19,050.36	17,148.39	15,329.66	13,594.05	11,192.32
Robust Swing Price	708.28	579.71	468.84	374.94	263.69
Robust RMSE	20,921.78	19,172.67	17,751.63	16,576.30	15,892.49

Table 5.5: $D_{\text{EUA}} = 88,\ LS = \text{OLS},\ F(x) = \text{Laguerre},\ n = 4,\ N_{ex} = 4,\ Scenario = \text{SSP2}$

Strike	310	330	350	370	400
Swing Price	716.62	587.99	477.64	384.11	273.06
RMSE	18,972.95	17,103.14	15,306.94	13,583.97	11,193.44
Robust Swing Price	709.75	580.31	469.20	375.24	263.87
Robust RMSE	20,756.54	18,976.29	17,459.11	16,142.51	15,134.94

Table 5.6: $D_{\text{EUA}} = 88,\ LS = \text{OLS},\ F(x) = \text{Laguerre},\ n = 6,\ N_{ex} = 5,\ Scenario = \text{SSP2}$

Strike	310	330	350	370	400
Swing Price	714.91	586.14	476.45	383.46	272.43
RMSE	19,026.39	17,149.44	15,350.15	13,625.81	11,248.77
Robust Swing Price	707.61	578.08	467.43	374.15	262.73
Robust RMSE	31,966.07	34,856.15	42,422.32	47,315.16	79,920.94

Table 5.9: $D_{\text{EUA}} = 88,\ LS = \text{OLS},\ F(x) = \text{Hermite},\ n = 5,\ N_{ex} = 5,\ Scenario = \text{SSP2}$

Strike	310	330	350	370	400
Swing Price	716.93	587.85	477.45	384.18	273.30
RMSE	19,016.71	17,129.94	15,325.30	13,595.83	11,204.37
Robust Swing Price	709.83	579.81	468.34	374.56	263.49
Robust RMSE	22,302.61	21,744.45	21,707.43	23,909.00	28,154.98

Table 5.10: $D_{\text{EUA}} = 88,\ LS = \text{OLS},\ F(x) = \text{Hermite},\ n = 6,\ N_{ex} = 5,\ Scenario = \text{SSP2}$

Strike	310	330	350	370	400
Swing Price	715.15	586.53	476.73	383.57	272.41
RMSE	19,030.35	17,153.47	15,353.51	13,626.66	11,245.54
Robust Swing Price	707.78	578.44	467.73	374.22	262.55
Robust RMSE	28,024.63	30,715.69	37,893.84	40,475.37	83,236.77

Results for LS estimation on all paths with JUMP part:

Table 5.11: $D_{\text{EUA}} = 88,\ LS = \text{OLS},\ F(x) = \text{Laguerre},\ n = 4,\ N_{ex} = 5,\ Scenario = \text{SSP2}$

Strike	310	330	350	370	400
Swing Price	796.61	671.77	562.35	467.91	351.97
RMSE	21,419.20	19,597.29	17,846.54	16,158.02	13,763.47
Robust Swing Price	789.59	664.08	553.28	457.71	341.78
Robust RMSE	23,917.65	22,072.95	20,360.44	18,773.84	16,594.69

Results for LS estimation on all paths with different D_{EUA}:

Table 5.12: $S = 350,\ LS = \text{OLS},\ F(x) = \text{Laguerre},\ n = 4,\ N_{ex} = 5,\ Scenario = \text{SSP2}$

D_{EUA}	90	95	120	150
Swing Price	467.03	442.45	350.27	280.22
RMSE	14,966.78	14,179.06	11,225.09	8,980.07
Robust Swing Price	458.77	434.63	344.08	275.26
Robust RMSE	17,071.13	16,172.65	12,803.34	10,242.68

Results for LS estimation on all paths for different N_{ex}:

Table 5.13: $D_{\text{EUA}} = 88,\ LS = \text{OLS},\ F(x) = \text{Laguerre},\ n = 4,\ Scenario = \text{SSP2}$

Strike	310	330	350	370	400
1	239.48	200.12	165.40	135.74	100.33
2	404.13	335.78	276.26	225.35	164.18
3	530.85	438.47	358.56	290.46	208.86
4	632.96	520.20	422.84	340.16	241.66
5	717.21	586.33	473.89	378.76	266.03
6	788.07	641.12	515.44	409.56	284.79
7	848.56	687.34	549.89	434.62	299.57
8	900.67	726.62	578.65	455.16	311.19
9	945.81	760.04	602.73	471.95	320.26
10	984.91	788.51	622.80	485.64	327.32
11	1018.84	812.73	639.49	496.71	332.78
12	1048.21	833.23	653.25	505.60	336.92
13	1073.55	850.56	664.60	512.68	340.04
14	1095.43	865.24	673.93	518.33	342.40
15	1114.29	877.61	681.57	522.80	344.17
16	1130.49	887.95	687.76	526.29	345.49
17	1144.27	896.49	692.71	528.99	346.45
18	1155.88	903.47	696.62	531.05	347.16
19	1165.51	909.08	699.65	532.58	347.66
20	1173.44	913.56	701.98	533.73	348.02
21	1179.94	917.11	703.77	534.60	348.28
22	1185.21	919.90	705.14	535.24	348.47
23	1189.40	922.04	706.16	535.71	348.60
24	1192.69	923.68	706.92	536.04	348.70
25	1195.22	924.89	707.46	536.28	348.76
26	1197.10	925.76	707.84	536.44	348.80
27	1198.48	926.38	708.09	536.54	348.82
28	1199.48	926.82	708.28	536.62	348.84
29	1200.18	927.12	708.40	536.66	348.85
30	1200.62	927.31	708.47	536.69	348.86
31	1200.87	927.41	708.51	536.71	348.86

Results for LS estimation on all paths for different T delivery days:

Table 5.14: $D_{\text{EUA}} = 88,\ LS = \text{OLS},\ F(x) = \text{Laguerre},\ n = 4,\ N_{ex} = 5,\ Scenario = \text{SSP2}$

Strike	310	330	350	370	400
31	709.75	580.31	469.20	375.24	263.87
30	685.48	559.81	452.48	362.24	255.05
29	662.85	540.33	435.78	348.23	245.50
28	650.40	529.90	426.78	340.42	239.40
27	639.32	520.49	419.48	334.85	235.29
26	631.84	515.47	417.27	333.02	233.48
25	628.69	511.22	410.64	327.30	229.66
24	609.00	493.40	394.71	313.53	219.80
23	598.01	483.48	386.66	306.36	214.35
22	587.47	475.62	380.48	301.79	210.63
21	567.75	459.00	367.20	291.40	203.52
20	556.12	447.36	356.47	281.81	196.31
19	557.62	450.12	359.19	286.31	199.72
18	560.47	453.43	362.05	286.32	199.57
17	544.81	441.78	353.65	280.28	195.44
16	523.15	422.57	337.02	266.97	185.84
15	498.03	402.39	321.74	255.11	176.79
14	467.23	375.77	299.09	236.01	162.69
13	450.58	363.71	293.28	238.40	178.69
12	421.58	335.01	263.74	205.05	142.40
11	412.11	331.88	264.05	208.20	143.75
10	370.25	295.90	233.41	182.27	125.71
9	351.52	279.72	220.05	171.05	116.64
8	303.90	239.85	187.66	145.59	98.19
7	261.61	204.88	158.67	122.44	82.68
6	232.28	181.79	139.36	106.77	71.73
5	216.54	169.07	130.25	100.69	67.32
4	197.32	156.34	121.27	91.70	60.51
3	148.42	116.28	90.21	69.44	46.16
2	103.45	83.18	66.97	53.61	39.35
1	50.88	40.19	31.54	24.59	16.78

Bibliography

[1] M. Abramowitz et al. *Handbook of Mathematical Functions with Formulas, Graphs, and Mathematical Tables*. New York: Dover, 1972.

[2] M. Arranz et al. *Effects of Applying Linear and Nonlinear Filters on Tests for Unit Roots with Additive Outliers*. Statistics and Econometrics Series. 2000.

[3] Benth et al. *Stochastic Modelling of Electricity and related markets*. Singapore: World Scientific, 2008.

[4] F. Benth et al. "On the optimal exercise of swing options on electricity markets". In: *The Journal of Energy Markets* (2012).

[5] F. Benth et al. *Quantitative Energy Finance*. New York: Springer, 2014. Chap. 2.

[6] W. Bühler et al. *Dynamic equilibrium valuation of electricity futures*. working paper. 2004.

[7] M. Caporin et al. "Model based Monte Carlo pricing of energy and temperature quanto options". In: *Munich Personal RePEc Archiv* (2001).

[8] *A European Union Carbon Border Adjustment Mechanism: Implications for developing countries*. 2021. URL: `https://unctad.org/system/files/official-document/osginf2021d2_en.pdf`.

[9] *Carbon Border Adjustment Mechanism: Questions and Answers*. 2021. URL: `https://ec.europa.eu/commission/presscorner/detail/en/qanda_21_3661`.

[10] *EU ETS Handbook*. 2015. URL: `https://www.sallan.org/pdf-docs/ets_handbook_en.pdf`.

[11] R. Carmona et al. "Optimal multiple stopping and valuation of swing options". In: *Mathematical Finance* (2008).

[12] J. Cox et al. "A Theory of the Term Structure of Interest Rates". In: *Econometrica* 53 (1985).

[13] G. Daskalakis et al. "Modeling CO2 emission allowance prices and derivatives: Evidence from the European trading scheme". In: *Journal of Banking and Finance* 33 (2009).

[14] D. Duffie et al. "Transform analysis and asset pricing for affine jump-diffusions". In: *Econometrica* 68(6) (2000).

[15] P. Duinker et al. "Scenario analysis in environmental impact assessment: Improving explorations of the future". In: *Environmental Impact Assessment Review* 27 (2007).

[16] EEA. *Projections in hindsight. An assessment of past emission projections reported by Member States under EU air pollution and GHG legislation*. Technical Report. Eurpoean Environmental Agency, 2015.

[17] A. Escribano et al. "Modelling Electricity Prices: International Evidence". In: *Oxford Bulletin of Economics and Statistics* 73.5 (2011), pp. 622–650.

[18] *The double materiality of climate physical and transition risks in the euro area*. 2022. URL: https://www.ecb.europa.eu/pub/pdf/scpwps/ecb.wp2665~622858d454.en.pdf.

[19] C. Genest et al. "Statistical Inference Procedures for Bivariate Archmedean Copulas". In: *Journal of the American Statistical Association* (1993).

[20] *GME's Profile*. 2022. URL: https://www.mercatoelettrico.org/En/GME/Info/ProfiloAziendale.aspx.

[21] M. Haugh. *An Introduction to Copulas*. Quantitative Risk Management course, IEOR Department at Columbia University. 2016.

[22] J. Hull. *Options, Futures , and Other Derivatives*. 9th ed. England: Pearson, 2015.

[23] IPCC et al. *Global warming of 1.5°C. An IPCC Special Report on the impacts of global warming of 1.5°C above pre-industrial levels and related global greenhouse gas emissions pathways, in the context of strewnghteniing the global response to the threat of climate change, sustainable development and effrt to eradicate poverty*. Special Report. Intergovernmental Panel on Climate Change, 2018.

[24] J. Janczura et al. "Identifying spikes and seasonal components in electricity spot price data: A guide to robust modeling". In: *MPRA: Munich Personal RePEc Archive* (2012).

[25] A. Karakas et al. *Archimedean Copula Parameter Estimation with Kendall Distribution Function*. 2017.

[26] R. Kiesel et al. "Valuation of commodity based swing options". In: *Journal of Energy Markets* 3 (2010).

[27] M. Kjaer. "Pricing of swing options in a mean reverting model with jumps". In: *Applied Mathematical Finance* 15 (2008).

[28] K. Kladivko. *Maximum likelihood estimation of the Cox-Ingersoll-Ross process: the Matlab implementation*. MATLAB Central File Exchange. 2022.

[29] A. Kolmogorov et al. *Introductory real analysis*. New York: Dover Publications, 2006.

[30] H. Kuo. *Introduction to stochastic integration*. New York: Springer, 2006.

[31] D. Lay et al. *Linear Algebra and Its Applications*. London: Pearson, 2016.

[32] F. Longstaff et al. "Valuing American options by simulation: A simple least-squares approach". In: *Review of Financial Studies* 14 (2001).

[33] J. Lucia et al. "Electricity Prices and Power Derivatives: Evidence from the Nordic Power Exchange". In: *Review of Derivatives Research* (2000).

[34] N. Meinshausen et al. "Monte-Carlo methods for the valuation of multipleexercise options". In: *Mathematical Finance* (2004).

[35] *Eni, Enel, Edison, A2a e non solo. Ecco la hit parade di chi produce più energia elettrica. Report Arera*. 2019. URL: https://www.startmag.it/energia/eni-enel-edison-a2a-e-non-solo-ecco-la-hit-parade-di-chi-produce-piu-energia-elettrica-report-arera/.

[36] *Quote di mercato per tipologia di cliente - ARERA*. 2022. URL: https://www.arera.it/it/dati/mr/mree_quote.htm.

[37] *MIT - Radiative Forcing*. 2022. URL: https://climate.mit.edu/explainers/radiative-forcing.

[38] N. Naifar. "Modelling dependence structure with Archimedean copulas and applications to the iTraxx CDS index". In: *Journal of Computational and Applied Mathematics* (2011).

[39] J. Pan. "The jump-risk premia implicit in options: evidence from an integrated time-series study". In: *Journal of Financial Economics* 63 (2002).

[40] *Union Registry, Verified Emissions for 2021*. 2022. URL: https://climate.ec.europa.eu/eu-action/eu-emissions-trading-system-eu-ets/union-registry_en.

[41] *Ministero dell'ambiente e della sicurezza energetica, Stabilimento di Taranto (ex ILVA)*. 2022. URL: https://va.mite.gov.it/it-IT/Oggetti/Documentazione/2038/4338?Testo=rapporto%5C%20anuale%5C%202020&x=0&y=0&pagina=3.

[42] R. Rubinstein et al. *Simulation and the Monte Carlo Method*. New Jersey: Wiley, 2017.

[43] E. Schwartz. "The stochastic behavior of commodity prices: implications for valuations and hedging". In: *Journal of Finance* 52(3) (1997).

[44] J. Seifert et al. "Modelling Jumps in Electricity Prices: Theory and Empirical Evidence". In: *Review of Derivatives Research* 10 (2007).

[45] R. Sidney. *A Probability Path*. Boston: Birkhauser, 2005.

[46] L. Teng et al. "The pricing of Quanto options under dynamic correlation". In: *Journal of Computational and Applied Mathematics* 275 (2015).

[47] *United Nations Climate Change - The Praris Agreement*. 2022. URL: https://unfccc.int/process-and-meetings/the-paris-agreement/the-paris-agreement.

[48] T. Vargiolu. *Advanced Topics in Quantitative Methods in Finance*. M.Sc. in Quantitative Finance, University of Bologna. 2022.

[49] P. Villaplana. *Pricing Power Derivatives: A Two-Factor Jump-Diffusion Approach*. Working paper. 2003.

[50] S. Wilkens et al. "The pricing of electricity futures: Evidence from the European energy exchange". In: *Journal of Futures Markets 27/4* (2007).

[51] G. Wolberg et al. "An energy-minimization framework for monotonic cubic spline interpolation". In: *Journal of Computational and Applied Mathematics* (2002).

[52] M. Woody et al. ". MEMLET: An Easy-to-Use Tool for Data Fitting and Model Comparison Using Maximum-Likelihood Estimation". In: *Biophysical Journal* (2016).

[53] N. Young. *Introductory real analysis*. Cambridge: Cambridge University Press, 1988.